Universidade Nova de Lisboa
Faculdade de Ciências e Tecnologia
Departamento de Química

Imperial College London
Chemical Engineering Department

Polyimide and Polyetherimide Organic Solvent Nanofiltration Membranes

Por: Marta Sofia Fragoso da Silva

Dissertação apresentada na Faculdade de Ciências e Tecnologia da Universidade Nova de Lisboa para obtenção do grau de Mestre em Engenharia Química e Bioquímica

Orientadores: Andrew G. Livingston e João Paulo G. Crespo
Supervisor Diário: Yoong Hsiang See Toh

Lisboa
2007

Abstract

Integrally asymmetric skinned Lenzing P84 and Matrimid 5218 polymide membranes and Ultem 1000 polyetherimide membranes were prepared. Crosslinking of membranes using aliphatic diamines resulted in marked improvement in chemical stability. This however resulted in a decline in flux with only Lenzing P84 demonstrating good flux in DMF. Further variation of membrane dope parameters and operating conditions allowed for good control of the MWCO of membranes made from Lenzing P84. SEM pictures of Lenzing P84 membranes revealed a significant difference in membranes morphology. The presence of macrovoids increased when using more DMF in the dope solution. These studies demonstrate the possibility of developing OSN membranes using different polyimides and opens up future possibilities for controlling the MWCO of these membranes. Preliminary modelling demonstrates that good control of the MWCO could extend the application of OSN membranes to allow the fraction of molecules in the NF range.

Acknoledgements

I would like to thank and express my sincere gratitude to my daily supervisor Yoong Hsiang See Toh and my supervisor Prof. Andrew Livingston. Their support was precious to finish this work.

Contents

List of Tables

List of Figures

List of Symbols

A	Area of membrane
c_i	Mole concentration of component i
$C_{feed,i}$, $C_{F,i}$	Concentration of feed of compound i
$C_{permeate,i}$, $C_{P,i}$	Concentration of permeate of compound i
$C_{retentate,i}$, $C_{R,i}$	Concentration of retentate of compound i
D_i	Fick's Law Coefficient
ε	Porosity
J_i	Membrane flux of component i
K	Kozeny constant
K_i	Sorption coefficient
p_0	Pressure in the fluid at the feed interface
p_i	Pressure in the fluid at the permeate interface
R	gas constant
r	pore radius
S	Surface area per unit volume
T	Absolute temperature K
t	time
τ	Tortuosity
μ	Liquid viscosity
μ_0	Standard chemical potencial of component i
μ_i	Chemical potencial of component i
V	Volume of permeate
$V_{P,i}, V_{R,i}, V_{F,i}$	Volume of permeate, retentate and feed of compound i
υ_i	Molar volume
ϕ	Association parameter (-)
μ_0	Viscosity of bulk solution (Pa.s)
$\Delta\pi$	Osmotic pressure difference
ΔP	Pressure difference
$\Delta x \text{ or } l$	Membrane thickness
γ_i	Activity coefficient of component i

Nomenclature

DDA	1,12 - dodecyldiamine
DMF	*N,N*-Dimethylformamide
EDA	Ethylene diamine
HDA	1,6 – hexanediamine
MEK	Methyl Ethyl Ketone
MF	Microfiltration
MWCO	Molecular Weight Cut Off
NF	Nanofiltration
NMP	N - Methylpirrolidone
ODA	1,8 – octadiamine
OSN	Organic solvent nanofiltration
PDA	1,3 – propylenediamine
PEG	Poly(ethylene glycol)
RO	Reverse osmosis
THF	Tetrahydrofuran
UF	Ultrafiltration

1 Literature Review

1.1 Introduction

Membrane filtration was not considered a technically important separation process until 25 years ago and today, membranes have gained an important place in chemical technology and are used in a broad range of applications due to its multidisciplinary character. [1]

A promising market for membranes is environmental applications where membrane technology can be applied in clean technology [2,3] and biological processes where compatible membranes are vital.

A membrane is a semi-permeable barrier that shows different selectivity between species. In separation applications, the goal is to selectivily allow a specie to permeate through the membrane freely whilst hindering the permeation of other components.

Nanofiltration membranes are membranes that are used in the separation of molecules in the range of 200-1000 $g.mol^{-1}$. Research on nanofiltration membranes has thus far been focused on aqueous systems due to the unavailability of suitable solvent stable membranes. However the recent development of new membranes [4,5] and materials has resulted in membranes suitable for use in solvent environments. Due to these advances, some OSN membranes are commercially available and some work has been published on the transport properties [6-8] and the application in non-aqueous environments [9-14]. This has not been fully explored and there is still much room for development both in the field of application as well as membrane stability.

Crosslinking of polymeric membranes has been shown to increase the chemical and thermal stability of membranes [15,16]. One of the aims of this project will be the development of different polyimide membranes and improving their stability by crosslinking and, secondly demonstrate the control over the MWCO of crosslinked and non-crosslinked membranes using a combination of membrane parameters and process conditions.

1.2 Membrane Separation Process

Membrane technology is an emerging technology and because of its multidisciplinary character it can be used in a large number of separation processes [1]. The membrane is the heart of every membrane process and can be considered as a semi-permeable barrier between two phases.

The objectives of separation may be described by the following [1]:

Concentration:	The desired component is present in low concentration and solvent has to be removed.
Purification:	Undesirable impurities are to be removed.
Fractionation:	A mixture must be separated into two or more desired components.
Reaction Mediation:	Combination of chemical/biochemical reaction with a continuous removal of products that will increase the reaction rate.

Membrane processes are characterized by the fact that the feed steam is divided into two steam, i.e. an influent steam is separated into two effluent steams known as the permeate steam and the retentate (concentrate) steam. The permeate steam is the portion of the fluid that has passed thought the membrane and the retentate contains the constituents that have been rejected by the membrane. A schematic representation of steams associated with a typical membrane separation system is given in Figure 1.1.

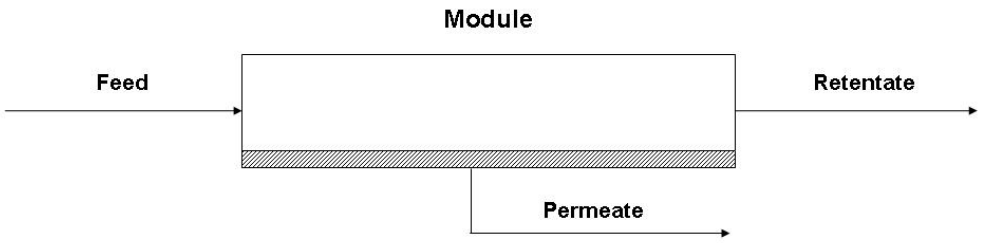

Figure 1.1 Schematic representation of a membrane process where the feed stream has been separated into a retentate and a permeate stream. [1]

Transport thought the membrane takes place because of differences in physical and/or chemical properties between the membrane and the permeating components. Therefore a driving force for the transport of species across the membrane is required and is usually of the form of a potential gradient, pressure gradient, electric potential gradient or temperature gradient (ΔP, ΔC, ΔT, ΔE) (Figure 1.2). However such driving forces rarely occur alone and it is often the result of a combination of the above mentioned effects that result in separation.

Other than the driving force, the membrane itself is the principle factor determining the selectivity and flux. In fact, the nature of the membrane, ie. structure and material, determines the type of application, ranging from the separation of macroscopic particles to the separation of molecules of an identical size and shape.

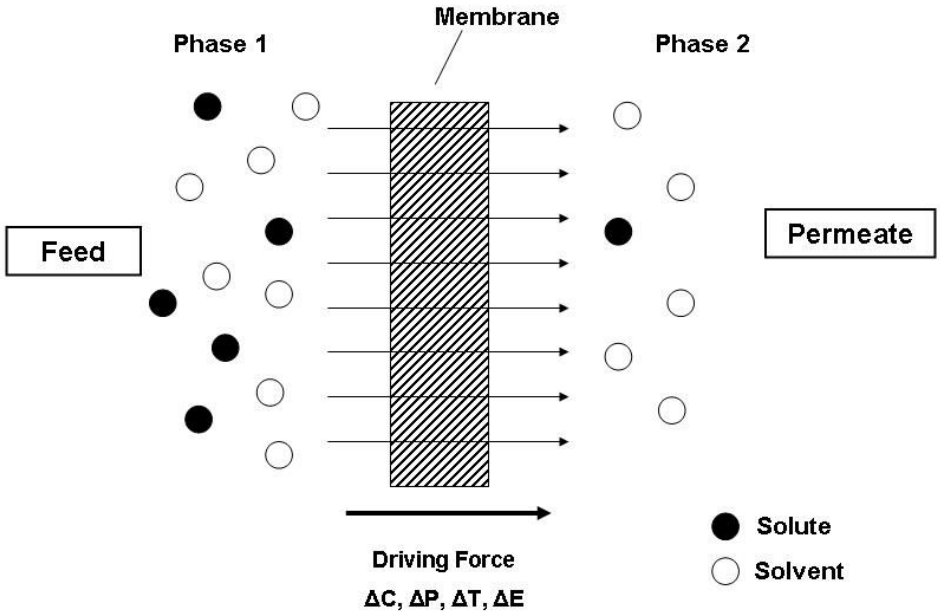

Figure 1.2 Schematic representation of a two-phase system separated by a membrane. Phase 1 is usually considered as the feed while the phase 2 is considered the permeate. [1]

Several types of membrane separation processes have been developed for specific industrial applications. Processes such as Reverse Osmosis (RO), Nanofiltration (NF), Ultrafiltration (UF) and Microfiltration (MF) involve positive pressure driving forces to effect separation. These processes are applicable to different sizes of molecules with MF differentiating the largest sizes (e.g. bacteria and particulates) and RO the smallest (e.g. salts). (Figure 1.3)

Reverse Osmosis (RO)

RO is able to eliminate all dissolved solids, bacteria, viruses and other germs contained in water. This process is normally used for desalting water using membranes that are permeable to water but essentially impermeable to salt. Brackish water desalination, seawater desalination, ultrapure water, wastewater treatment and organic solvent separation are also processes where RO is used. [17]

The flux through the membrane is approximately inversely proportional to the membrane separating layer and for this reason most RO membranes have an asymmetric structure with a dense toplayer (thickness ≤ 0.1 μm) supported by a porous sublayer (thickness ~ 50-150 μm), the resistance towards transport being determined mainly by the dense layer [1]. Almost all RO membranes are made from polymers (e.g. cellulose acetate and polyamide). They are generally composite or asymmetric membranes. In composite membranes, the support material is commonly polysulfone while the thin film is made from various types of polyamines.

RO membranes have the smallest pores with pore diameters ranging from approximately (0.5-1.5 nm) and the operating pressure for this kind of membranes is up to 200 bar. [18]

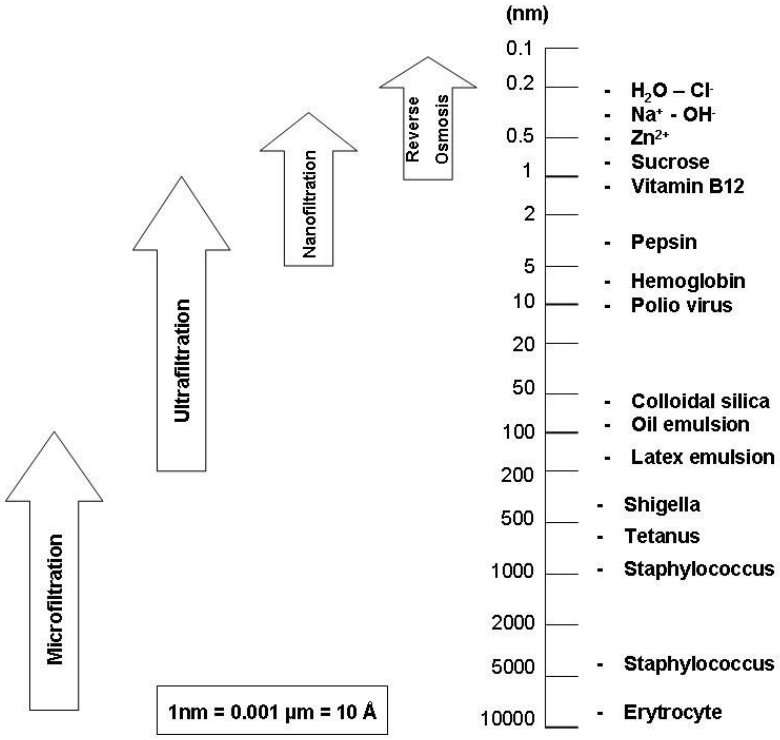

Figure 1.3 Reverse osmosis, ultrafiltration, microfiltration and conventional filtration are related processes differing principally in the average pore diameter of the membrane filter. [1]

Nanofiltration (NF)

As with reverse osmosis, nanofiltration is used when low molecular weight solutes, such as inorganic salts or small organic molecules (eg. glucose), have to be separated from a solvent.

The main field of application from this kind of membranes is the removal of low levels of contaminants from already relatively clean water because nanofiltration membrane usually have high rejections to most dissolved organic solutes with molecular weights above 100-200 $g.mol^{-1}$ and good salt rejection at concentrations below 1000-2000 ppm salt. The operating pressure is not also not as high as RO allowing operation at 4-10 bar. [17]

Aqueous NF membranes usually have a composite structure with a dense toplayer (thickness ~ 1 µm) supported by a sublayer (thickness ~ 150 µm). [17] The basic principles of NF are similar to the ones of RO because the have the same range of pore size (0.2-4 nm) however they are very different from ultrafiltration since the size of the solute to separate is different.

Ultrafiltration (UF)

Ultrafiltration is a membrane process whose nature lies between nanofiltration and microfiltration. This process is primarily a size-exclusion based pressure driven membrane

separation process [19]. This process is typically used to retain macromolecules and colloids from a solution. The average pore diameter of the membrane is in the 1-200 nm range. UF membranes are usually anisotropic structures made by the Loeb-Sourirajan process. They have a finely porous surface layer or skin, which performs the separation, supported on a much more open microporous substrate that provides mechanical strength. [17]

These membranes are made from a limited number of materials such as primarily polyacrylonitrile, poly(vinyl chloride), polyacrylonitrile copolymers, polysulfone, poly(ether sulfone), poly(vinylidene fluoride), some aromatic polyamides and cellulose acetate [17]. Their MWCO range is from 1000 to 100 000 $g.mol^{-1}$. UF processes generally operate at 2-10 bar through in some cases up to 25-30 bar.

Ultrafiltration is used in environmental applications such as electrocoat paint, oil-water emulsions and product recycling; applications in food industry like cheese production [20], clarification of fruit juice, sugar refining vegetable protein processing; biotechnology applications, for example, bioreactor processes and tissue culture systems; preparation of ultra-pure water, hemofiltration and polymer industry. [17,19,21]

Microfiltration (MF)

Microfiltration refers to filtration processes that use porous membranes to separate suspended particles with diameters between 100-10000 nm. Thus, microfiltration membranes fall between UF membranes and conventional filters. Pore sizes of MF membranes are in the range of 0.05-3 µm. Thus, MF typically operates at low transmembrane pressures to minimize build-up of suspended solids at the membrane surface. Pressures of 0.3-3.3 bar and cross-flow velocities of 3-6 $m.s^{-1}$ in tubular modules are common. MF is the most open membrane and removes starch, bacteria, molds, yeast and emulsified oils.

This process is typically used in sterile filtration of pharmaceuticals, sterilization of wine and beer, microfiltration in the electronics industry and for drinking water treatment. [17,22]

In general, the applications fall into one of the following major categories: (i) Purification; (ii) Clarification; (iii) Sterilization; (iv) Concentration and (v) Analysis. [19]

1.3 Preparation of Synthetic Membranes

There are several techniques available to prepare polymeric membranes. The most important techniques are sintering, track etching, stretching and phase separation processes. The latter is the primary means of preparation of commercial polymeric membranes [1] and the final

morphology of the membranes depends greatly on the material properties and process conditions.

1.3.1 Phase Inversion

Phase inversion is a process whereby a polymer is transformed in a controlled manner from a liquid to a solid state. Solidification is initiated by transition in a process of liquid-liquid demixing. At a certain stage during demixing, the phase with the higher polymer concentration will eventually solidify forming the solid matrix. It is the control of the initial transition phase that determinates the membrane morphology. The phase separation of polymer solutions can be induced in several ways: [1]

Controlled solvent evaporation [23,24] is a process by which the polymer is dissolved in a mixture of volatile solvent and a less volatile non-solvent. As the solvent evaporates the concentration of polymer in the non-solvent increases and eventually leads to the precipitation of the polymer. The polymer solution might be cast in a suitable backing – a glass plate or another kind of support which may be porous or non-porous. In solvent evaporation, an important aspect is the temperature of the casting solution. This technique has been used for the preparation of UF and RO membranes. [25]

Precipitation from the vapour phase [26] involves casting the polymer solution, consisting of a polymer and a solvent, in an environment saturated with the non-solvent. His prevents evaporation of the solvent and precipitation takes place when the non-solvent vapour penetrates into the solution. [27] This leads to a porous membrane without toplayer. This technique was the basis of the original microporous membranes and is still used commercially by several companies as Millipore for example. [25]

In *thermal precipitation* the solvent quality usually decreases when the temperature is decreased. After demixing is induced, the solvent is removed by extraction, evaporation or freeze drying. [28]

In *immersion precipitation* the polymer is cast on a support. After that the system is immersed into a coagulation bath of the non-solvent. The solvent exchange leads to the precipitation of the polymer. The polymer precipitation by water is called the *Loeb-Sourirajan Process* and remains by far the most important membrane preparation technique. Most commercially available membranes in use today are prepared via this method.

In the following section, the phase behaviour of the ternary systems involving the polymer, solvent and non-solvent will be discussed as well as the implications of the phase transitions on the morphology of the membranes. More complex systems exist but the discussion will stick to a

ternary system for simplicity. In the phase diagrams (Figure 1.4), three types of phase separation behaviour can be identified: liquid-liquid demixing, solid-solid demixing and solid liquid demixing. However it is the liquid-liquid demixing that plays a central role in the generation of the required morphology. [28,29]

Asymmetric phase inversion membranes can be prepared from many polymers by the following procedure [30,31]:

1) The polymer is dissolved in an appropriate solvent to form a 10-30 wt% solution;
2) The solution is cast into a film 100-500 μm thick;
3) The film is quenched in a non-solvent, typically water or an aqueous solution.

1.3.1.1 Liquid-liquid Demixing

In general two mechanisms are well known for liquid-liquid demixing: nucleation and growth (NG) and spinodal decomposition (SD) [27]. While NG occurs when the polymer system departs from the homogeneous and stable region to the metastable region which is located in the spinodal and binodal lines in the phase diagram on the other hand SD occurs when the system enters an unstable region in the phase diagram. [32] The concentration fluctuates with time in this region and results in bicontinuous morphology.

The original approach of Strathmann et al. [30] was to present the process of membrane formation as a line through the phase diagram. However this theory assumes a precipitation path as a single line representing the average composition of the whole membrane which is not completely correct. Firstly because the rate of precipitation and the precipitation path represented through the phase diagram differ at different points in the membrane (top and bottom layer of the membrane) and secondly because the precipitation process does not follow a determinate path. A schematic phase diagram for an isothermal ternary polymeric mixture consisting of polymer/solvent/non-solvent is represented in Figure 1.4 which is able to demonstrate the dependence of the demixing on thermodynamics. During membrane formation the composition changes from composition A, which represents the initial casting solution composition, to a composition C, which represents the final membrane composition. The position of composition C on Polymer-Non-solvent axis determines the overall porosity of the membrane. At composition C the two phases are in equilibrium: a solid (polymer-rich) phase, which form the matrix of the final membrane, represented by point S, and a liquid (polymer-poor) phase, which constitutes the membrane pores filled with precipitant, represented by point L. The point B represents the concentration at which the polymer initially precipitates. [17] Recently much effort has been made to calculate the pathways through the phase diagram and to use them to predict the effect of membrane formation variables on the fine membrane structure. As quantitative predictors of membrane performance this approach has failed.

However, as a tool to qualitatively rationalize the complex interplay of factors determining membrane performance, the phase diagram approach has proved useful. [1,33,34]

The phase diagram is separated into a homogeneous phase (area between the polymer/solvent axis and the binodal line), and an area representing the demixing gap. This occurs when sufficient non-solvent is present in the system. The size and location of this demixing gap depends on the molar volumes of the components, the polymer-solvent interactions, the polymer non-solvent interactions and the solvent-non-solvent interactions. These interactions may be described by the Flory-Huggins description of polymer solutions. The influence of these variables on the phase diagrams have been discussed by Altena et al. [35] and Yilmaz et al. [36] and the influence of the parameters may be summarised as follows:

- Polymers and solvents with low mutual affinity increase the magnitude of the demixing gap.
- Low compatibility of solvent-nonsolvent mixtures result in large differences in solvent/nonsolvent ratio in the equilibrium phases.

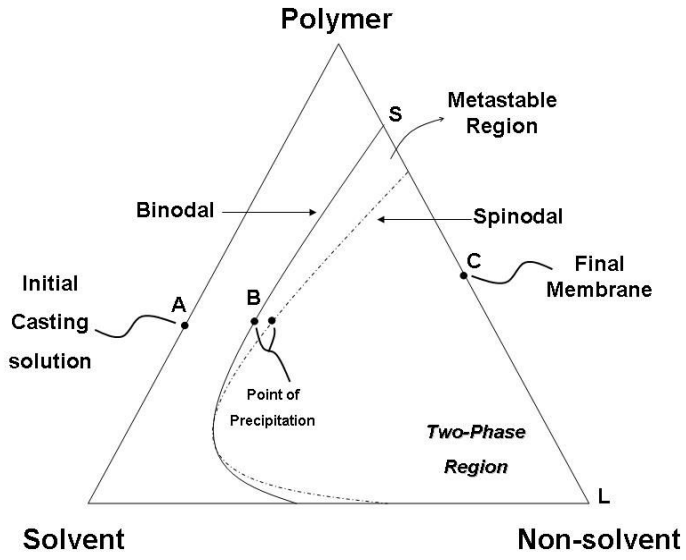

Figure 1.4 Membrane formation showing a path through the three-component phase diagram from the initial polymer casting solution (A) to the final membrane (C) *(Adapted from W. Baker, Richard)* [17]

Ternary phase diagrams are not widely reported in literature. However the interaction parameters already studied give us an indication of the size of the demixing gap. The polymer non-solvent interactions may be determined using swelling measurements [37]. The solvent non-solvent interactions can be calculated from the activities and the polymer solvent interaction can be determined from osmometry measurements. The Flory Huggins parameter may be estimated using the Hildebrand solubility parameter (by the Flory-Rehner theory using membrane swelling experiments [38]).

Mass Transfer

Liquid-liquid phase separation is induced by non-solvent diffusion which means that the kinetic information of the exchange process between the solvent and non-solvent as well as the thermodynamic information is required to predict the morphology of the resultant membrane.

Cohen et al. [39] proposed the first mass transfer model. Later another models were proposed by Reuvers et al. [29] and Cheng et al.[40]. The models start from using basic diffusion equations and the continuity equations for both the bath side and the film side. The most important aspect to consider when doing calculations is the boundary initial conditions and many assumptions are used to simplify such as [41]:

- No convection occurs on the film side or the bath side.
- Instantaneous equilibrium exists at the interface both on the bath and film sides.
- No polymer dissolves in the coagulation bath.
- Demixing and growth occurs by NG in the polymer poor phase.

The mass transfer models describe the composition of the solution as a function of the space coordinates. This has implications as to the delay time before the onset of demixing and hence the final morphology of the membrane. The majority of literature however fails to describe the surface morphology just at the onset of immersion precipitation. This and the subsequent coarsening might be critical in the prediction of the morphology of the separation layer in asymmetric membranes.

1.3.1.2 Membrane Morphology from Immersion Precipitation

Kimmerle and Strathmann [42] identified four structural elements in the morphology of membranes prepared by immersion precipitation: cellular structures, nodules, bicontinuos structures and macrovoids.

1.3.1.2.1 Cellular structures

Broens et al. [43] have shown that the formation of such structures is the result of the nucleation and growth of the polymer poor phase. Cellular structures are present in most membranes prepared by delayed precipitation so the delay time for demixing is an important parameter since under rapid demixing [28] (< 1 sec), the membranes formed will have a thin top layer and a sublayer with macrovoids. On the other hand if the delay time is slow (few seconds to minutes), the membranes will have a dense and thick top layer due to the high concentration of the polymer solution at the onset of demixing. The porosity and degree of interconnectivity between the pores will also be low [44]. The speed of demixing depends on the mass transfer in solution as well as the thermodynamics of the system as described by the phase diagrams [29].

1.3.1.2.2 Nodules

In literature the origin of the nodules has been ascribed to micelles [45], para-crystallites [24], aggregates [46], inhomogeneities in the polymer solution [47,48] or perturbations [49]. More recently Kimmerle et al. [42] proposed that the spheres are formed by nucleation of a polymer rich phase. Pinnau et al. [34] and Boom et al. [50] state that the diffusion processes during formation of the top layer are fast enough for the polymer solution to become highly instable and cross the spinodal curve. In this mechanism nodule formation is supposed to result from spinodal decomposition. Wienk et al. [51] proposed that a nodular structure is formed by spinodal demixing of the polymer solution, rapidly followed by vitrification of the polymer matrix. Nodules are formed in a phase-separation process under conditions or fast outdiffusion of solvent and fast indiffusion of nonsolvent and its formations are independent of the polymer concentration of the casting solution [51]. Later, the same author, proposed that nodules are partly fused spherical beads with a diameter of approximately 25-200 µm and results from a very rapid precipitation conditions during membrane formation [52]. They are frequently observed in the dense top layer of the membranes [28,53,54]. While the mechanism and origins of these nodules is disputed they have been attributed to (i) aggregates or micelles already present in the dope [24,45,55], (ii) formation via liquid-liquid demixing during phase inversion [50,51,56], (iii) artefacts of sample preparation [57,58].

1.3.1.2.3 Macrovoids

Macrovoids are large elongated pores that can stretch over the length of the membrane thickness. The presence of macrovoids is not generally favourable in NF because they may lead to structural weakness in the membrane when high pressures are applied [1]. Macrovoids are usually associated with systems those exhibiting instantaneous demixing, whereas when a delayed onset of demixing occurs macrovoids are absent. Strathmann and Kock [59] stated that this kind of structures take place with instantaneous precipitation with the non-solvent often being water. Most of the techniques that can be used to delay the onset of demixing will also result in the disappearance of macrovoids and includes increasing the viscosity of polymer solution. The walls of macrovoids are usually porous hence the coalescence of the macrovoids with the surrounding polymer poor droplets remains possible.

1.3.1.3 Influencing Parameters on the Membrane Morphology

Membrane morphology is influenced by several main parameters those will be discussed in this section. These variations are true for most polymers used to prepare membranes. The factors are: [1]

- Choice of solvent/non-solvent system

- Polymer concentration
- Composition of the coagulation bath
- Composition of the polymer solution

Secondary factors such as the use of additives, the temperature of casting solution and the evaporation time also change the morphology of the membranes and may indirectly change the separation performance of membranes.

1.3.1.3.1 Choice of solvent/non solvent system

In order to prepare membranes by immersion precipitation is necessary to take care while choosing the system solvent/non-solvent since the polymer must be soluble in the solvent and the solvent and the non-solvent must be completely miscible. [1] The miscibility of the components is described by the free energy of mixing. However the non-ideality of the solvent systems means that this has to be modified to include the activity coefficients for binary and ternary systems.

As the mutual affinity between the solvent and non-solvent decreases, this reduces the gradient of the tie lines in the two phase region in the ternary diagram. Mixtures that have high affinity as DMSO or DMF result in instantaneous demixing forming the morphology with a thin top layer with macrovoids [60,61]. Conversely if there is low affinity between the mixtures then this will delay the onset of demixing forming the dense and thick top layer. Ways to delay the onset of demixing includes the addition of solvent/additives to the coagulation bath [59] or the introduction of additives to the dope solution.

1.3.1.3.2 Polymer concentration

The polymer concentration in the casting solution has a significant effect on membrane structure and properties. A low polymer concentration in the casting solution tends to favour the formation of finger like structures implying that the volume fraction of polymer decreases and consequently a lower porosity is obtained. [1] However, if the initial polymer concentration in the casting solution is increased a much higher polymer concentration is observed at the interface favouring the sponge likes structures [26].

The polymer concentration can also alter the performance of the membranes. Mulder [1] demonstrated using a cellulose acetate/dioxane/water system that the flux of ultrafiltration membrane formed decreased with increasing polymer concentration. This is due to the higher initial polymer concentration at the film interface leading to a less porous top layer.

1.3.1.3.3 Composition of the coagulation bath

The solvent composition of the coagulation bath can influence the morphology of the membranes formed. It does this by delaying the onset of liquid-liquid demixing. At an extreme case the composition of solvent in the coagulation bath can be used to switch from a porous to a nonporous membrane [1]. Deshmukh and Li [62] showed this experimentally using a PVDF/DMAc/water system and changing the ethanol:water content in the coagulation bath. As the ethanol concentration in water bath was increased from 0% to 50%, the long finger like structure near the outer wall of the fibre slowly changed through a short finger-like structure to a sponge-like structure.

1.3.1.3.4 Composition of the casting solution

The non-solvent may also be added to the casting solution to affect the type of morphology produced. The maximum amount of non-solvent that may be added to the casting solution can be determined from the ternary diagram. The amount of non-solvent added must be in the homogeneous region such that demixing does not occur, which means that the composition must be in the one-phase region in the ternary diagram where all the components are completely miscible with each other. As with the case of changing the composition of the coagulation bath, changing the composition of the casting solution has a similar effect. The adding the non-solvent to the casting solution will decrease the demixing time hence altering the type of membrane morphology produced. Increasing the polymer composition in the casting solution has also been shown [63] to decrease the MWCO due to a more dense morphology in the top layer.

1.3.1.4 Formation of Composite Membranes

A development of composite membranes was a major breakthrough in the history of membrane technology. Composite membranes consist of two different materials, with a very selective membrane material being deposited as a thin layer (0.1 - 1μm) upon a more or less porous sublayer. The actual selectivity is determined by the thin top layer, whereas the porous sublayer merely severs as a support. Coating is used when there is a necessity to reduce the membrane thickness and to increase the flux of the membrane. [1] This kind of membranes are normally used for pervaporation [64] and gas separation [65]. Several procedures may be used to coat the membrane. The advantage of using a composite membrane (Figure 1.6) over a single material asymmetric membrane (Figure 1.5) is that each layers can be optimised independently to obtain the desired membrane selectivity, permeation rate, chemical, mechanical and thermal resistance [1,66].

The majority of membranes used in the manufacture of OSN membranes are composite membranes. The success of Koch membranes have stimulated much academic work in improving such membranes and in particular, membranes with a PDMS top layer on a PAN support are wide reported [5,67-69]. Whilst each layer of the composite membrane is chemically stable in a wide range of organic solvents, the rubbery separating layer of many of the membranes swells appreciably in many solvents resulting in diminished selectivity through convective transport across the membrane [68,70]. In addition, differential swelling in the layers could, in some instances, result in the de-lamination of the top layer and result in membrane failure. The active layers of such membranes are also usually applied as coatings, thus resulting in a layer often several microns thick. Compared to asymmetric membranes where the separation layer is often reported to be several nm, this presents a significant hindrance to mass transport. As such, membranes composed of a single material are preferred in the formation of OSN membranes.

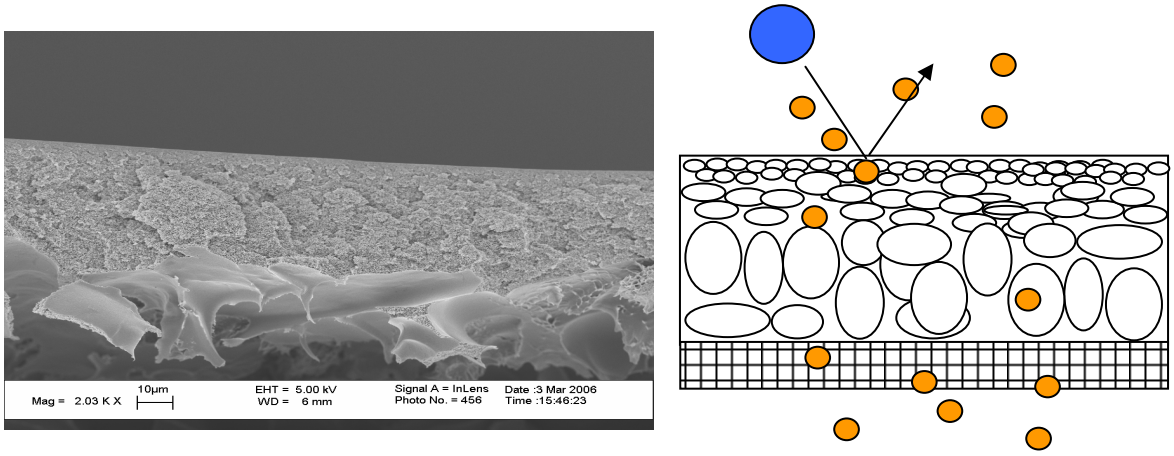

Figure 1.5 SEM picture of the cross-section of an asymmetric membrane on the left and schematic of integrally skinned asymmetric membranes on the right [71]

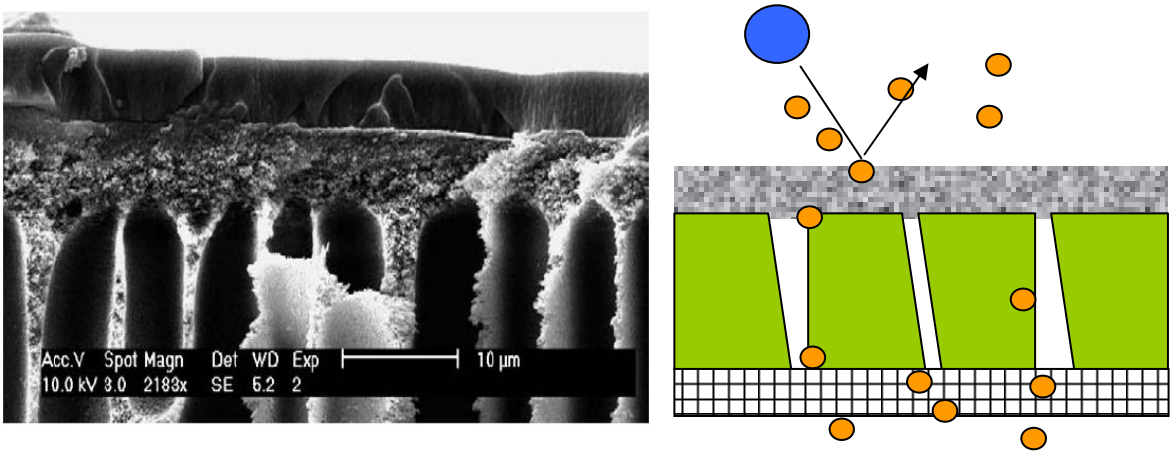

Figure 1.6 SEM picture of the cross-section of a PDMS membrane on a PI-support on the left [72] and schematic thin film composite on the right [71]

1.3.1.4.1 Interfacial polymerisation

In interfacial polymerisation, a polymerisation reaction takes place between two reactive monomers at the interface of two immiscible solvents. The support layer is first immersed in an aqueous solution containing the monomer and subsequently immersed in an organic layer containing the other reactive monomer. This results in a dense polymeric top layer, ie a thin film on the support [1]. Amines are often used in the aqueous phase and acid chlorides in the organic phase [66,73,74].

1.3.1.4.2 Dip coating

Dip-coating is a very simple and useful method capable to produce very thin membranes but with a dense top layer to use in reverse osmosis, gas separation and pervaporation [1]. Firstly the membrane is immersed into a bath, coating solution, containing a low concentration (< 1%) of solute. As the membrane is withdrawn from the solution, a thin film adheres to the surface of the membrane. The film is then put into an oven where crosslinking and solvent evaporation occurs [75-77]. Care should be taken while heating up the membrane for cross-linking because if the polymer is glassy and the glass transition temperature is exceeded, defects might occur in the membrane. In this process it is also important to characterise the performance of the asymmetric support layer. It should ideally have a narrow distribution for pore size and have a high surface porosity [78]. This is such that the effects of pore penetration by capillary forces can be offset by careful solvent selection or by pre-filling the pores. Failure to recognise the effects of pore penetration might result in poor mass transfer rates. [79]

1.3.1.4.3 Plasma polymerisation

Plasma polymerisation is a convenient way for the deposition of thin polymer films of the order of 100 nm or less [80]. The polymers produced in this way are different from those produced in normal synthesis in two ways: first because the material has a highly crosslinked structure and secondly the chemical structure of the monomer is not necessarily preserved through fragmentation and recombination [81]. The polymerisation is carried out in an evacuated reactor where the membrane support is placed. A gas (e.g. N_2) is ionised and passed into the reactor. The monomer is then fed separately into the reactor and this collision of ions with the substrate results in the formation of radicals. This will eventually result in the deposition when the molecular weight of the polymer gets too high [1]. Plasma polymerisation depends on many factors including reactor design, power level, substrate temperature, frequency, monomer structure, monomer pressure, and monomer flow rate [82]. Thus, for example, a very thin layer of thickness in the range of 50 nm can be obtained provided that the concentration of the monomer in the reactor (the partial pressure) is carefully monitored [1].

1.3.1.5 Effect on Molecular Weight Cut Off (MWCO)

Ohya et al. [83] showed that in the formation of a polyimide membrane, the increase of casting temperature led to an accelerated solvent evaporation thus increasing the polymer concentration at the surface. This led to both a decrease in flux and MWCO. The evaporation time also had similar effects with a decrease in flux and MWCO with increasing evaporation time. The MWCO could also be varied using various additives to the casting solution. Okazaki et al. [84] had used the additives phenanthrene, pyrene, triphenyl phosphate and polystyrene to change the MWCO in the formation of polyimide membranes. The MWCO increased with increasing molecular weight of the additives. However work by Sterescu et al. [85] show that unbounded additives in a polymer matrix tend to decrease the permeability and selectivity of membranes. Jimenez et al. [86] showed that the mean pore size and MWCO of the membranes also were decreased either by increasing the PES concentration in the casting solution or by increasing the solvent evaporation time. However, the effect of the PES concentration was more important than that of the evaporation time. MWCO of the surface modified membranes was smaller than that of their unmodified counterparts.

1.4 Organic Solvent Nanofiltration (OSN)

Nanofiltration is a pressure driven membrane process, situated between reverse osmosis and ultrafiltration that is in the separation of small molecules such as sugars. The membranes for NF usually have high rejections to most dissolved organic solutes [17] and may be composite membranes with the active layer formed by interfacial polymerisation or asymmetric membranes formed by phase inversion. The typical size of pores associated with NF is in the range of 0.2 - 4 nm. The pressures used are lower than that of RO and are in the region of 5 – 30 bar. At present NF can be divided into two different applications: those in aqueous systems and those in organic solvent systems. The former has been developed and researched in depth for a number of years but it is not until recently, with the development of solvent resistant NF membranes, that its application in solvent systems has become more prevalent. The proliferation of such technology represents new possibilities and applications of membranes within the fine chemicals industry in instances such as assisted organic synthesis [87] and applications in pure organic solvents.

A major issue on the selection of membranes for use in organic solvent nanofiltration is the chemical, mechanical and thermal stability of such membranes under filtration conditions. Polymeric membranes are less resistant to harsh chemical environments (e.g. strong acids and dipolar aprotic solvents), severe temperatures and oxidative conditions as compared to inorganic membranes [88,89]. However the advantages of selectivity and high chemical resistance of the type of polymers available today make polymeric (organic) membranes still

relevant. Several types of polymers exist which are used in the synthesis of membranes: homopolymers, copolymers, block copolymers and graft polymers. These may be either linear or branched polymers. The membranes may be formed by dissolving the polymer and casting them without any covalent bonds between the polymer chains.

1.4.1 Industrial Available Nanofiltration Membranes

Koch Membrane Systems [90] distributes a line of chemically stable NF membranes for caustic, acid, and solvent streams, which find many important and pioneering applications in food, pharmaceutical and chemical industries. Furthermore, the materials of construction of these membrane modules should consider the combined effects of aggressive acids, bases or solvents, pressure and temperature. The SelRO® [90] membranes modules and systems are supplied using special materials and element design, compared to the traditional RO and NF systems. SelRO® chemically stable flat sheet hydrophobic solvent stable NF membranes MPF-50 for industrial NF applications are supplied as 21.6 cm × 27.9 cm sheets soaked in their preserving solution (50% ethanol and water). The MPF-50 is a composite membrane consisting of three layers [91] with a non-woven backing. The top layer is made of polydimethylsiloxane (PDMS) [5] with a polyacrylonitrile (PAN) support. Machado et al. [92,93] have reported minimal swelling behaviour of the MPF-50 and MPF-60 (< 3 % in ethanol, methanol, N-propanol and acetone). However more rigorous membrane tests by Van der Bruggen et al. [91] found the membranes to be only semi-solvent stable with the membranes showing visible damage after ten days of exposure to methylene chloride, hexane, ethyl acetate, ethanol, and acetone.

The STARMEM™ [94] range of integrally skinned asymmetric OSN membranes manufactured from polyimides [95]. An active skin layer less than 0,2 mm in thickness with a pore sizes of $<50x10^{-10}$ m is reported. [96] They are supplied in sheets of 215 x 280 mm or in spiral wound elements. The maximum pressure that they can hold is 60 bar and a temperature of 50ºC. STARMEM™ is stable in a wide range of solvents such like alcohols, alkanes, aromatics, ethers and ketones. STARMEM™ has been used extensively in research due to their good resistance to organic solvents. [7,8,95,97-99]

1.4.2 Membrane Characterization

Membrane characterization is a very important part of membrane research and development because the design of membrane processes and systems depends on reliable data relating to membrane properties.

Membrane characterisation parameters may be described as either performance (functional properties such as flux and rejection) related or morphology (both physical and chemical

parameters) related [100]. The most common parameters used to characterize membranes are based in its performance because although much effort has been made to explain the relation between the morphology and the functional performance [101] until now no fundamental quantitative model is able to describe the phenomenon.

In the field of OSN membrane selection is often based upon the molecular weight cut off (MWCO) as specified by the manufacturer [102]. MWCO is defined by plotting the rejection of solutes versus their molecular weight, and interpolating this data to find the molecular weight corresponding to the 90% rejection. However, as techniques for obtaining MWCO values are often not disclosed, this leads to non-uniformity within the industry. A standardised method have been developed for aqueous NF systems using salts and sugars [103] (e.g. raffinose, maltose).

Many methods have been chosen in the literature by different authors to try and characterise the MWCO of OSN membranes.

The alkane system reported both branched and linear alkanes of increasing MW to determine the MWCO [54]. This method also allows the accurate determination of the MWCO at a low range of 100-400 $g.mol^{-1}$. However, drawbacks of using alkanes include the lack of commercially available pure species of molecular weight >400 $g.mol^{-1}$, and the difficulty of detecting these compounds. Limited solubility in many more polar organic solvents also makes it difficult to compare the MWCO of membranes across different solvents.

An alternative to alkane system is the use of different compounds with increasing MW covering the NF range (200–1000 $g.mol^{-1}$). Although the MW of the test compound gives an indication of the expected rejection, variability in the structure and functionalities of the compounds results in differing solute–membrane interactions and a non-linear increase in rejection with MW [104]. The use of different test compounds also precludes the possibility for the determination of the MWCO in a single filtration as the detection of multiple compounds in a single test solution is not easily feasible. Thus a series of filtrations, each with a single solute, may be necessary.

The use of dyes was also proposed by several authors [11,13,105] to determinate the MWCO of membranes. However dyes have a peak absorption wavelength, they absorb over a range of wavelengths which leads to prevent the use of a range of different sized dyes in a single test to determine the MWCO. Furthermore, many dyes are charged and could have interactions with the membrane, thus altering the observed rejection. The limited solubility of dyes in a broad range of solvents also limits their further application. Some dyes are also inorganic and usually charged. This might result in poor solubility in some organic solvents and possible interactions with the polymer.

Recently See Toh et al. [106] developed a simple and reliable method to characterise the MWCO of OSN membranes. This method uses styrene oligomers to determine the MWCO in several organic solvents. The oligostyrenes cover a large range and were able to provide many points to give a comprehensive description of the membrane performance in the nanofiltration range providing valuable information on membrane and equipment integrity.

1.4.3 Choice of Polymers and Membrane Preparation

The selection of suitable materials for use in OSN are based on several characteristics including film forming ability, commercial availability, cost, chemical and thermal stability.

Lenzing P84 (HP Polymer GmbH, Germany) is a co-polyimide of 3,3'4,4'-benzophenone tetracarboxylic dianhydride and 20% methylphenylenediamine and 80% toluenediamine (BTDA-TDI/MDI) with a Tg of 315°C. The polymer, developed by The Upjohn Company, is aromatic, fully imidized, highly polar and insoluble in most organic solvents. However it is soluble in polar aprotic solvents such as dimethyl formamide (DMF), dimethyl sulfoxide (DMSO), dimethyl acetamide (DMAc), n-methylpyrrolidone (NMP) [21] and in mixtures with dioxane [107]. It has been reported to show better chemical resistance than other PIs such as Matrimid and Sixef [21], making it a prime candidate for use in OSN. White [4] has previously demonstrated the use of this PI in the manufacture of an OSN membrane showing good chemical stability and separation performances. Qiao et al. [108] also used a P84 to develop a pervaporation membrane as they consider this material a potential candidate for developing high separation performance pervaporation membranes. P84 belongs to the aromatic polyimide family which possesses a number of attractive mechanical and physicochemical properties [109]. In addition, polyimides are reasonably stable in most organic solvents [21] and weak acids . Their selectivity towards water is attributed to the preferential interaction between water molecules and the imide groups through hydrogen bonding. Not only showing superior performance as membrane materials for gas separation [110], they are also promising for vapour permeation [111] and pervaporation for separation of water and organic mixtures [109,111-115]. A most recent commercially available polyimide, has received significant attention for applications as a novel membrane material in ultrafiltration [4], nanofiltration [54] or gas separation [116]. P84 has been shown to be stable in many organic solvents such as toluene, hydrocarbons, alcohols and ketones [4,54], and also exhibits high selectivity with superior anti-plasticization properties against CO_2 in gas separation [116].

In conclusion polyimides are a class of polymers with excellent chemical [21,117] and physical properties. Polyimides have high permeabilities and permselectivities making them prime candidates for use as precursors in the formation of OSN membranes. However most importantly, many polyimides are commercially available thus improving the reproducibility of membranes manufactured from such material.

Matrimid 5218 (Huntsman Advanced Materials GmbH, Switzerland) is a BTDA-DAPI formed from 3,3',4,4'-benzophenone tetracarboxylic dianhydride (BTDA) and 5(6)-amino-1-(4'-aminophenyl)-1,3-trimethylindane (DAPI) and it has a Tg of 302ºC [118]. In the last decade, Matrimid 5218 has been widely studied in the last decades as a material for gas separation membranes [119]. Nanofiltration membranes have been fabricated from different polyimides including Matrimid 5218 [4,120]. However its use in OSN applications has thus far been limited [120] due to its poorer stability in many organic solvents. It was discovered that this polyimide was good to form membranes for the low temperature separation of low molecular weight organic materials from solvents by hyperfiltration. Benefits are improved energy costs and throughput of product when the membrane separation technique is used in the solvent dewaxing process for lube oil. Matrimid 5218 is a polyimide so that it has an excellent chemical resistance and thermal stability [4].

Polyetherimide (PEI) is a versatile polymer already used in electrical engineering due to their thermal properties (Tg above 225ºC). Polyetherimides (PEIs) constitute a large thermoplastic polymer family [121] which have good mechanical, thermal and electrical properties [122]. They are moreover relatively stable to acids, weak bases, and hot water hydrolysis. They are also flame retardant, can withstand energetic radiation and usable for food contact. Ultem 1000 (General Electric Plastics Ltd., UK) grade PEI manufactured from the polycondensation of bisphthalic anhydride and 1,3-diaminobenzene is known to be totally amorphous [123]. Compared to other polyimides, the ester linkage between the chains has been reported [124] to offer better chain flexibility and hence improve processability of the membrane. Peinemann et al. [125] successfully demonstrated the preparation of asymmetric porous PEI membranes for gas separation [126]. PEI membranes have an unusually high He selectivity compared to other commercial polymers combined with a reasonable He permeability. As with most asymmetric membranes, they are prepared by phase inversion [1]. Peinemann et al. [125] prepared an integral asymmetric membranes for gas separation by casting a poly(ether imide) solution in tetrahydrofuran (THF) and gamma-butyrolactone (GBL) and coagulating in water. Tao et al. [127] and Kim et al. [128] also prepared polyetherimide membrane by phase inversion. In the first case the membrane showed a typically asymmetric structure consisting of a thin and dense skin layer, a sponge morphology and a porous bottom. The authors also showed the effect of 1,4-dioxane in the casting solution and it is relation with MWCO and the various effects of polymer concentration, evaporation time and coagulation bath temperature.

1.4.4 Effects of Experimental Conditions on Membranes Performance

The functional performance of a membrane can be defined by the: flux and rejection. The flux (J) is defined as the volumetric (mass or molar) flow though the membrane per unit area of the membrane per unit time:

$$J = \frac{V}{A \cdot t}$$ **Equation 1.1**

The rejection of a specie i, R_i is given by the following formula:

$$R_i = \left(1 - \frac{C_P}{C_R}\right) \times 100\%$$ **Equation 1.2**

The mass balance of a closed system also allows for the solute in the system to be accounted for. The mass balance (MB) is given by the following equation:

$$MB\ (\%) = \frac{C_P \times V_P + C_R \times V_R}{C_F \times V_F} \times 100\%$$ **Equation 1.3**

The effect of pressure, temperature and concentration on the rejection and flux has been documented by several authors [87,92,95]. Some pertinent results are summarised below.

Pressure

Scarpello et al. [95] performed experiments with STARMEM™ 122, STARMEM™ 240 and MPF-50 in dead end filtration. The results show that firstly, the flux increases with increasing pressure. The range of pressures tested was between 0,5 – 60 bar. This phenomenon was also reported by Whu et al. [70]. However was not linear due to the compaction of the membrane resulting in the sealing of some pores in the membrane and hence the rate of increase of flux declined [87,97]. Machado et al. [92] also reported linear and non-linear flux as result of different pressures applied to the system. Scarpello et al. [95] also reports an increase in rejection of solutes with pressure. Whilst this is desirable for the retained species a compromise has to be reached between maintaining a high solvent flux and to allow separating of a partially rejected solute.

Temperature

Machado et al. [92] reported that it is usually hypothesized that a rise in temperature increases permeation flux through either a reduction in solvent viscosity or an increase in solvent diffusion coefficient [129] or by an increase in polymer chain mobility [130]. However more research would have to be done to determine the contributions of each factor. A general trend of decreasing rejection is observed with increasing temperature. For polymeric membranes, this might be the result of a transition from the glassy state to the rubbery state [1]. An increased in free volume in the rubbery state might also be a reason for the observed increase in flux. However rejection could suffer as the membrane starts to swell.

Concentration

The flux decreased with increasing solute concentration. This is explained by an increase in osmotic pressure and an increase in the effects of concentration polarisation (see section 1.4.5), hence a decrease in flux [17]. However pore/membrane fouling, the extreme case of concentration polarisation, might also be important in explaining the decrease in fluxes and increase in rejections for certain results.

Conditioning

Inconsistencies in the literature data on OSN flux and rejection data prompted a study on conditioning by Gibbins et al. [97]. The study compared data from Whu et al. [87] and Machado et. al. [92] and theorised that the discrepancy might be due to the pre-conditioning of the membranes. The study showed that compaction under pressure reached a maximum after which the flux remains constant. The membranes should hence be conditioned in pure solvent until after the initial decline. Only after this initial decline can the membrane performance be considered reproducible. Membrane conditioning is therefore important in maintaining reliable data on the flux and rejection.

1.4.5 Membrane Limitations

Concentration Polarization

Concentration polarization occurs in the majority of separation processes but its consequences are especially severe in membrane processes. When a molecular mixture is brought to a membrane surface with a certain concentration $C_{i,bulk}$, (Figure 1.7) some components permeate the membrane under a given driving force while others are retained. This leads to accumulation of retained material ($C_{i,m}$) and to depletion of the permeating components in the boundary layer adjacent to the membrane surface. This causes a concentration gradient to build up in the layer ($C_{i,bl}$) and causes a diminishing driving force for the more permeable component whilst increasing that for the less permeable component. In the worst case scenario, concentration polarisation might also result in the formation of a cake (Figure 1.7) on the surface of the membrane. The build up of concentration in the layer also causes a flux in the direction opposite to that of the flux, ie diffusive flux (represented as J_{diff} in Figure 1.7).

The causes and consequences of concentration polarization may differ in the different membrane processes. One of the main consequences is phenomenon know as membrane fouling [25] due to precipitation if the concentration of the less permeable component becomes significant.

The effect of concentration polarisation might be reduced by the reduction of the boundary layer. This may be accomplished by improving the hydrodynamic conditions on the feed side of the membrane. This might be physically done using feed spacers or turbulence promoters

within the flow channels of the membrane. The effects of concentration polarisation may sometimes counteract intuitive behaviour. Reddy et al. [131] experienced a decrease in rejection with increasing pressure and had attributed this drop to concentration polarisation. An extreme case of concentration polarization is membrane fouling (Figure 1.8).

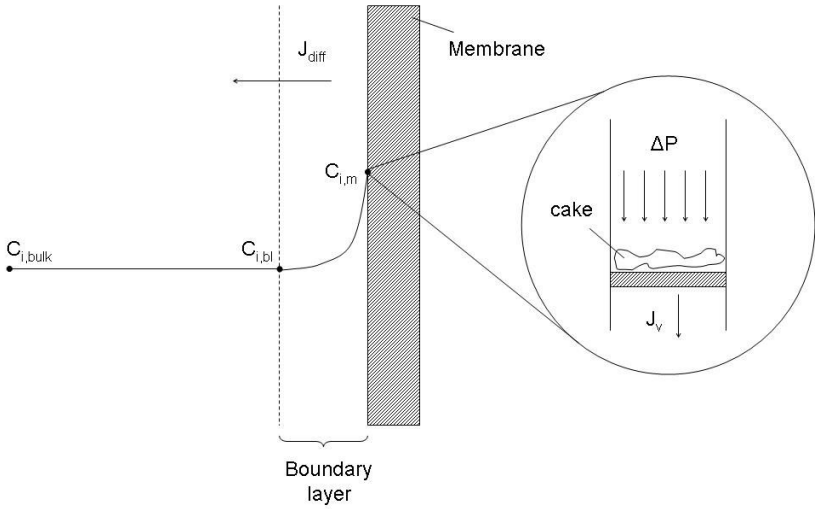

Figure 1.7 Concentration profile in pressure driven processes like MF, UF, NF and RO

Compaction

Compaction is the mechanical deformation of a polymeric membrane matrix which occurs in pressure-driven membrane processes. During compaction, the porous structure densifies and as a result the flux declines. Compaction produces a dense and compact structure of the membrane thus reducing the effective pore size of the membrane. This also increases the charge density of charged membranes. [132] After relaxation, the flux will generally not return to its original value since the deformation process is often irreversible. The extent to which compaction occurs is dependent on the pressure applied to the membrane and the morphology of the membrane.

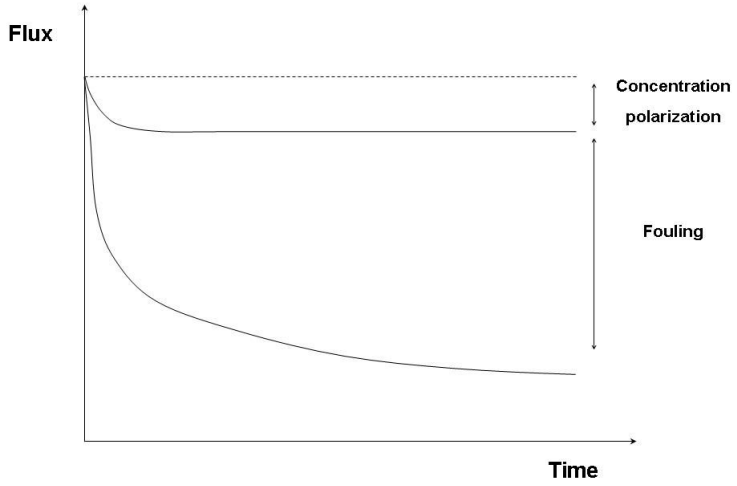

Figure 1.8 Flux as a function of time showing both concentration polarisation and fouling effects [133]

1.4.6 Crosslinking of Membranes

Crosslinking of the polymer chains might also be induced using either a chemical reaction or through radiation. Crosslinking has a huge effect on the physical, mechanical and thermal properties of the membranes. Most significantly, this causes the polymers to become insoluble [1]. This gives the membranes the solvent resistant characteristics.

Commercial polyimide (PI) OSN membranes have been show to give good performances in several organic solvents (e.g. toluene, methanol, ethyl acetate etc. [14]) but are however unstable in amines [21] and have generally poor stability and performance in polar aprotic solvents such as methylene chloride (DCM), tetrahydrofuran (THF), dimethyl formamide (DMF) and n-methyl pyrrolidone (NMP) in which most of these membranes are soluble. Inorganic membranes [134] have been developed which offer good stability in most organic solvents but they are often more expensive and difficult to handle. In order to solve that problem crosslinking of polymeric membranes has been studied and shown to increase the chemical and thermal stability of membranes [15,16] However, this is often at the expense of a decrease in permeability of membranes [135-137].

Several crosslinking strategies for polyimides have been proposed including the use of radical initiated (thermally or via the use of UV) and chemical crosslinks [136,138-140]. However post casting modification of polymer films presents the easiest method of manipulation as this allows the desired morphology of the membranes to be attained via phase inversion followed by further crosslinking on the pre-formed membrane to maintain this morphology in aggressive conditions. [12]

As for OSN the membrane stability of the underlayer is as critical as the separating layer due to solvent permeation, effective crosslinking of the whole membrane must be achieved. Several chemical crosslinking strategies for use in membranes have been proposed and includes the introduction of condensable crosslinking sites during polymer preparation [141,142] and the use of di/poly-amines in a ring opening reaction [139].

1.5 Transport Mechanism

The most important property of membranes is their ability to control the rate of permeation of different species. [17] The transport of the material across the membrane is principally controlled by the driving force and whether the membrane exhibits active or passive transport properties [1]. Two different mass transfer models [143] are used frequently to describe this permeation process and provide the basis for which various models reported in literature

[7,13,54,144,145]. A graphical representation of the pressure and chemical potential profiles of the two models is given in Figure 1.9.

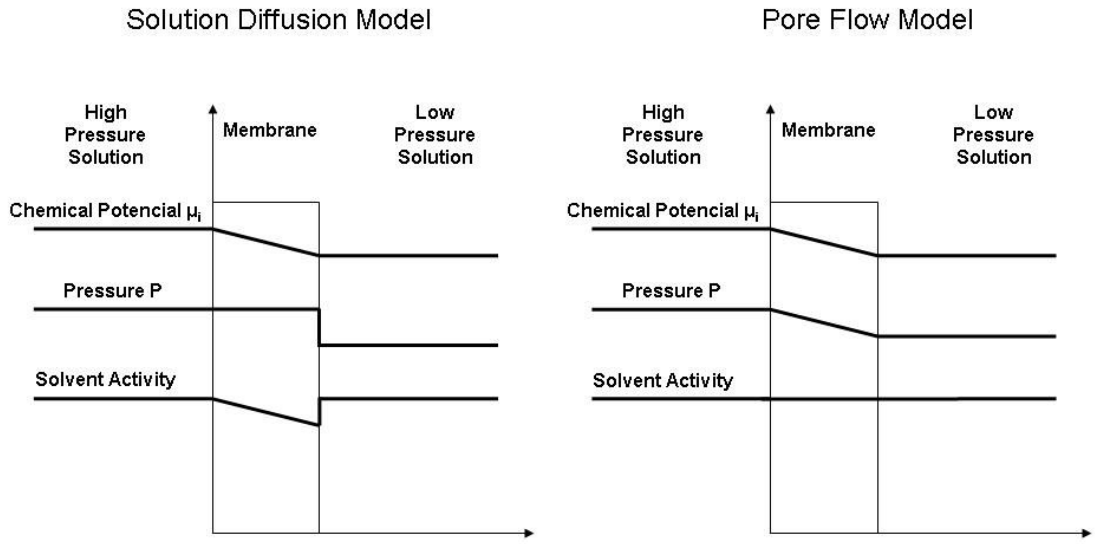

Figure 1.9 Comparison between the pressure driven permeation of one component solution through a membrane according to the Solution Diffusion and Pore Flow models. [143]

Both models were proposed in the nineteenth century, but the pore flow model, because it was closer to normal physical experience, was more popular until the mid-1940s. Although solution diffusion model was uncontroversial it was used to explain transport of gases through polymeric films. By 1980 the solution diffusion model became the more applied model to describe the membrane transport theory especially in RO, pervaporation and gas permeation in polymer films. [17]

1.5.1 Pore Flow Model

The pore flow model developed by Sourirajan and Matsuura [146], considers the process whereby the permeants are separated by pressure-driven convective flow through tiny pores. Separation is achieved between different permeants as one of the permeants is excluded (filtred) from some of the pores filled by other permeants. The pore flow model assumes a constant concentration gradient (Figure 1.9). This implies that the chemical potential gradient is now only expressed as a pressure gradient. The Hagen Poiseuille equation (Equation 1.4) gives a very good description of transport through membranes consisting of equal number of parallel pores. This equation can be used to describe the relationship between the solvent flux and applied pressure where J is the solvent flux, ε the porosity, r the average pore radius, ΔP the differential pressure across the membrane, μ the liquid viscosity, Δx the membrane thickness and τ the tortuosity factor [147] which is normally defined as the ratio of the true length of the

flow path and the straight-line distance between the beginning and end points [148]. However in reality very few membranes possess such structures.

$$J = \frac{\varepsilon \cdot r^2}{8 \cdot \mu \cdot \tau} \frac{\Delta P}{\Delta x}$$ **Equation 1.4 [149]**

Some membranes have a structure similar to a system of closely packed spheres. This might be found in membranes that have been prepared by sintering or membranes that have a nodular top layer prepared using phase inversion. In such cases the above equation might be modified for spheres to give the Carmen Kozeny [150-152] equation:

$$J = \frac{\varepsilon^3}{K \cdot \eta \cdot S^2 \cdot (1-\varepsilon)^2} \frac{\Delta P}{\Delta x}$$ **Equation 1.5**

In this equation J is the solvent flux, K the Kozeny constant, ε the porosity, S the surface area per unit volume, ΔP the differential pressure across the membrane, μ the liquid viscosity and Δx the membrane thickness.

1.5.2 Solution Diffusion Model

The solution diffusion model was developed by Lonsdale et al. [153], has been revisited by Wijmans and Baker [143] and has been adopted by White [54] and Peeva et al. [7] to describe membrane transport in systems using PI OSN membranes. Solution diffusion model has a basic principle: diffusion. Diffusion is the process by which matter is transported from one part of a system to another by a concentration gradient [17]. Thus, for solute transport, the traditional solution diffusion model uses a simple concentration gradient across the membrane thickness as the driving force. However most models developed in literature such as those from Williams et al. [154], were based on general systems with water as the primary solvent. Bhanushali et al. [13] describes the difference between aqueous and non-aqueous systems and describes special considerations with regards to the membrane swelling and various interaction parameters for non-aqueous systems. This is due to the vast differences in the structures and properties of the solvents.

Assumptions for the Solution Diffusion Model [17,143]:

- Fluids on either side of the membrane are in equilibrium with the membrane material in the interface;
- Rate of absorption and desorption at the membrane interface are much higher than the rate of diffusion through the membrane;
- The pressure within the membrane is uniform;

- Chemical potential gradient across the membrane is expressed only as concentration gradient;
- Solvents are independent of each other.

The basis of the model [143] is that driving forces (pressure, concentration, temperature and the electromotive force) can be expressed as a chemical potential gradient. The flux (Ji) of a single component solvent (i) may be given by:

$$J_i = -L_P \frac{d\mu_i}{dx} \qquad \textbf{Equation 1.6}$$

Restricting ourselves to driving forces generated by concentration and pressure gradients, the chemical potential may be expressed as flows:

$$d\mu_i = RT\, d\ln(\gamma_i c_i) + \upsilon_i\, dp \qquad \textbf{Equation 1.7}$$

where c_i is the molar concentration (mol/mol) of component i, γ_i is the activity coefficient linking concentration with activity, p is the pressure and υ_i is the molar volume of component i. This may be further simplified for an incompressible fluid or solid, ie when volume does not change with pressure:

$$\mu_i = \mu_i^{\,0} + RT\, d\ln(\gamma_i c_i) + \upsilon_i\,(p - p_i^{\,0}) \qquad \textbf{Equation 1.8}$$

where $\mu_i^{\,0}$ is the chemical potential of pure i at a reference pressure $p_i^{\,0}$. Equating the chemical potentials at the solvent/membrane interface and equating to the equation for the chemical potential in an incompressible fluid as in the case of reverse osmosis yields the follow:

$$c_{i0(m)} = K_i c_{i0} \qquad \textbf{Equation 1.9}$$

$$c_{i0(m)} = K_i\, c_{i0} \exp\left(\frac{-\upsilon_i\,(p_0 - p_i)}{RT}\right) \qquad \textbf{Equation 1.10}$$

The sorption coefficient K_i is assumed to be the same on both sides of the membrane and is independent of both the pressure and concentration. The expressions for the concentrations within the membrane at the interface in equations 1.9 and 1.10 can now be substituted into the Fick's law expression yields the following which is applicable both to the solute and solvent in terms of the pressure and concentration difference across the membrane:

$$J_i = \frac{D_i K_i}{l}\left[c_{i0} - c_{il} \exp\left(\frac{-\upsilon_i (p_0 - p_i)}{RT} \right) \right] \qquad \textbf{Equation 1.11}$$

1.6 Summary of Literature Review and Research Motivation

Nanofiltration (NF) is the most recently developed pressure-driven membrane separation process and has properties that lie between those of ultrafiltration (UF) and reverse osmosis (RO). The nominal molecular weight cut off (MWCO) of NF membranes is in the range of 200-1000 $gmol^{-1}$. With the recent advent of organic solvent nanofiltration (OSN), there has been an increased application in many areas including pharmaceutical, fine chemical and petrochemical industries [102].

Nanofiltration membranes have been fabricated from different polyimides including BTDA based Lenzing P84 and Matrimid 5218 and from Ultem 1000 polyetherimides. Polyimides have interesting mechanical, thermal and electrical properties making them interesting for many industrial applications. Developing these polyimides could see the extended range of application of OSN in the separation of high MW compounds enabling the fractionation of molecules in a membrane cascade type system [155].

P84 has been reported to confer good performance in OSN membranes [12] however these membranes still have MWCO in a small range thus limiting their further application. The control of MWCO is critical to the further development of these membranes. A good control using both membrane formation parameters and process conditions will allow the successful separation of species in OSN. Several authors [83,84,156] have previously attempted to change the MWCO of PI membranes by changing several formation parameters. However, the MWCO change reported and measured in these cases did not successfully report good control over the membrane separation performance. Yanagishita et al. [113] suggests that the MWCO of PI membranes made from PI-2080 can be varied by changing the DMF/dioxane ratio in the membranes.

Current challenges facing the application of OSN is the general lack of commercially available membranes with broad stability in a large range of solvents [9]. To address these challenges, a method of improving the chemical stability of Lenzing P84 polyimide membranes was described through chemical crosslinking for application in OSN [12].

The crosslinking strategy currently applied to Lenzing P84 could be extended to the other polyimides to improve solvent stability of these membranes. Tin et al. [136] proposed the same crosslinking reaction for matrimid 5218. Matrimid 5218 has been used in many instances for gas

separation applications [119]. Its use in the literature in OSN applications has thus far been confined to that of White et al. [120].

Recent investigations on polyetherimides (PEI) biocompatibility have shown that this polymer do not exert any significant level of cytotoxicity or hemolysis and allow the attachment and growth of cells [157,158]. Therefore, it was anticipated that PEI is a candidate for biomedical applications for parts of intraocular lenses, biosensors, oxygenators or neuroprostheses [159]. So that Ultem 1000 became an alternative polymer for nanofiltration membrane. It has been used in many instances in gas separation [160,161], ultra [162] and nanofiltration membranes [128,163]. The ester linkage between the chains have been quoted [124] to offer better chain flexibility and hence improve processibility of the membrane. Ultem has also been reported to have better resistance to hot water hydrolysis [123] than other PI. Thus far, there are no studies of applications of Ultem 1000 in OSN.

In this work we propose the use of the crosslinking strategy applied previously [12] in the fabrication of OSN membranes with controllable MWCO using Lenzing P84, Matrimid 5218 and Ultem 1000. The control of the separation performance and chemical stability will allow membranes to be tailored for specific applications.

2 Experimental Techniques and Process Validation

2.1 Introduction

A consistent and reliable method of measuring separation performance allows membrane manufacturers to both improve their membranes and provide information for end users to make a selection. [164] Membrane characterisation parameters may be described as either performance related or morphology related. [100] Morphological parameters include both physical (e.g. pore size, pore size distribution, pore shape, skin layer thickness or surface roughness) and chemical parameters (e.g. charge density, hydrophilicity or hydrophobicity), whilst permeation related parameters describe functional properties such as flux and rejection. Permeation parameters are often more practical for membrane selection due to the effect of different process conditions [165] on the performance of membrane systems, and the difficulty in relating morphological parameters to membrane performance.

In OSN membrane selection is often based upon the molecular weight cut off (MWCO) as specified by the manufacturer. [106] The MWCO is defined by plotting the rejection of solutes versus their molecular weight, and interpolating this data to find the molecular weight corresponding to the 90% rejection. See Toh et al. [106] proposed the use of homologous polymers with steadily increasing MW has several attractive characteristics. With uniformly increasing monomer units, oligomers are ideal for the characterisation of membranes relatively of their MWCO.

In order to characterise the membranes developed in this work, a consistent testing regime is set out in this chapter. A homologous series of styrene oligomers were used which allow us to obtain a rigorous and comprehensive understanding of the MWCO of OSN membranes [106] using dead end and cross flow filtration. Dead end filtration was initially used for quick membrane screening and characterisation. This is however not ideal as membrane compaction has been shown to occur over an extended period [97] and the hydrodynamics in dead end filtration is much poorer than that used in cross flow. As such the initial sloping work was done using dead end filtration to determine preliminary characteristics whilst a more detailed study will be done in the cross flow set up.

2.2 Experimental

2.2.1 Chemicals

The solute used includes a homologous series of styrene oligomers. The styrene oligomer mixture contained a mixture of PS580, PS1050 (purchased from Polymer Labs, UK) and α-methylstyrene dimer (purchased from Sigma–Aldrich,UK). The organic solvent used was toluene (AnalaR). One gram each of the oligostyrene standards and the dimer were dissolved in toluene to make up the oligostyrene test solution.

2.2.2 Membranes

The commercial membrane tested was STARMEM™ 122 [94]. The integrally skinned asymmetric polyimide membrane is quoted to have a MWCO of 220 $g.mol^{-1}$ and a hydrophobic active layer (manufacturer's data). [7,14,54,95]

The STARMEM™ range of integral asymmetric OSN membranes have an active surface manufactured from polyimides [95]. An active skin layer less than 0,2 mm in thickness with a pore sizes of $<50x10^{-10}$ m covers the polyimide membrane body. [96] They are supplied in sheets of 215 x 280 mm or in spiral wound elements. The maximum pressure that they can hold is 60 bar and a temperature of 50ºC. STARMEM™ is stable in a wide range of solvents such like alcohols, alkanes, aromatics, ethers and ketones. This type of membrane has been used extensively in research due to their good resistance to organic solvents. [7,14] The membrane was characterised according to its pure solvent flux and molecular weight cut off (MWCO). This was done by using a test solution of oligostyrene.

2.2.3 Molecular Weight Cut Off determination

Filtration experiments were conducted using membranes in a stainless steel, SEPA ST (Osmonics, USA) dead end nanofiltration apparatus (Figure 2.2) and in a cross flow cell (Figure 2.3 and Figure 2.4).

For dead end filtration, 1mL of feed, permeate and retentate samples were taken for analysis. In cross flow filtration, the feed and the retentate concentration were assumed identical and samples were taken only of each of the permeates and from the feed.

Care should be taken when using some solvents in the analysis as some of them have functional groups that would obscure the solute peaks during analysis. Samples in toluene,

ethyl acetate or hexane require the solvent evaporated and the solute re-dissolved in the mobile phase prior to analysis to facilitate peak clarity.

For the analysis of the styrene oligomers, an Aglient 1100 HPLC system was used. Separation of the oligomers was achieved using an ACE 5-C18-300 column (Advanced Chromatography Technologies, ACT, UK). A mobile phase of 35 vol% analytical grade water and 65 vol% tetrahydrofuran (AnalaR) was used with 0.1 vol% trifluoroacetic acid. The UV detector was set at a wavelength of 264 nm.

Figure 2.1 shows the chromatogram of the separation and detection of the styrene oligomers in a sample test solution. The individual species were identified by a comparison of peak retention times with the GPC curves provided by Polymer Labs for the SEC standards PS580 and PS1050. Good separation between each peak enabled the discrete determination of the rejection of each species. This avoids the need for the de-convolution of data often experienced when trying to determine the MWCO using SEC.

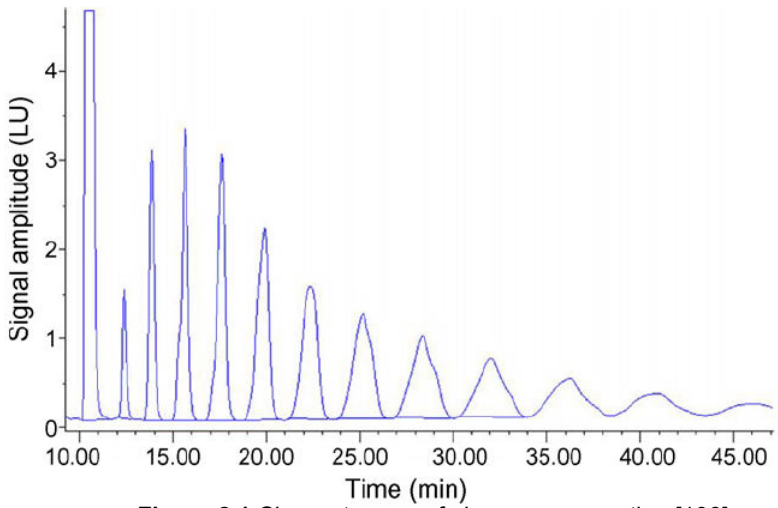

Figure 2.1 Chromatogram of olygomer separation [106]

The experimental rejection of solute i was calculated by the following equations in dead-end filtration and cross-flow filtration, respectively:

$$R_i\ (\%) = \left(1 - \frac{C_{permeate,i}}{C_{retentate,i}}\right) \times 100 \qquad \textbf{Equation 2.1}$$

$$R_i\ (\%) = \left(1 - \frac{C_{permeate,i}}{C_{feed,i}}\right) \times 100 \qquad \textbf{Equation 2.2}$$

A plot of the rejection of solute against the molecular weight allowed the MWCO of the membrane to be determined.

2.2.4 Dead End Filtration

For the dead end filtration experiments, a Sepa ST dead-end cell (Osmonics, CA., USA) was used. A schematic of the dead end filtration apparatus is shown in Figure 2.2. Membrane disc of 49 mm in diameter were cut and inspected for defects before being placed in the cell. The membrane disc were placed on top of a sintered stainless steel disc with the active surface (14 cm^2) facing the solvent before being sealed within the cell using a PTFE coated O-ring.

The cell was placed on a magnetic stirrer and a PTFE coated stirrer bar was placed in the cell and the solvent mixture was poured in. Pressure was supplied using nitrogen gas with stirring. 150 mL of solvent was used to pre-condition the membrane and to remove the conditioning agent. The conditioning procedure consists of permeating solvent until a steady flux was achieved before MWCO determination tests were carried out. The flux was calculated using the equation below.

$$J = \frac{V}{A \cdot t} \qquad \left(L \cdot m^{-2} \cdot h^{-1}\right) \qquad \textbf{Equation 2.3}$$

Toluene was used as the solvent and a pressure of 30 bar was used. The solute mass balance (equation 2.4) was also evaluated to ensure that no solute was left on the inside of the cell or absorbed into the membrane, ie to check loss of material in the batch filtration experiment. In the majority of cases the mass balance (MB) of each solute was within 90 – 100%.

$$MB_i\ (\%) = \frac{C_{P,i} \times V_P + C_{R,i} \times V_R}{C_{F,i} \times V_F} \times 100 \qquad \textbf{Equation 2.4}$$

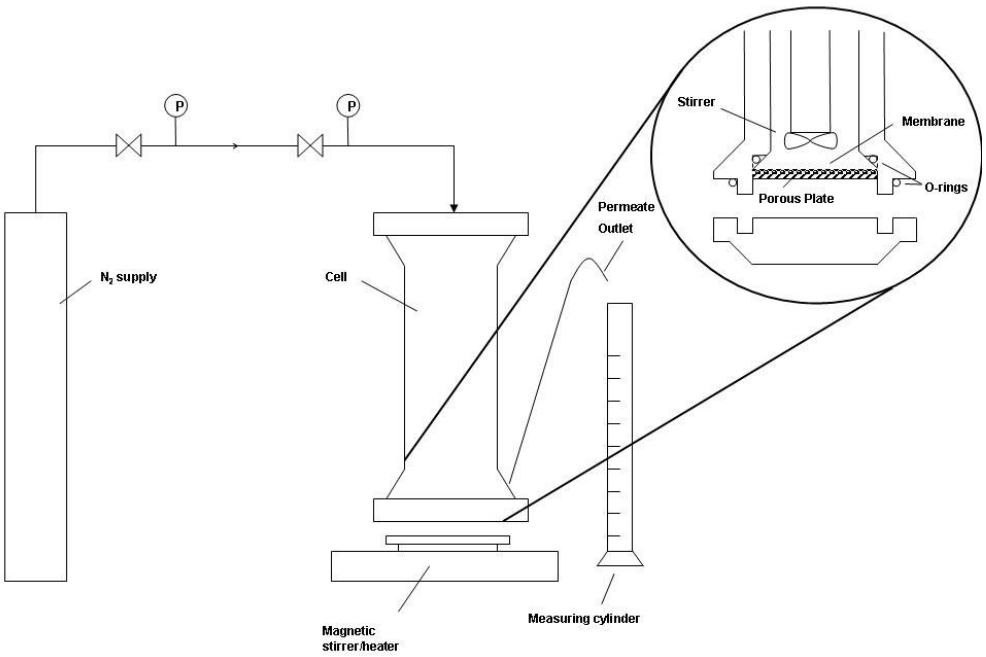

Figure 2.2 Schematic of experimental pressure cell used in the testing of membranes in dead end filtration.

2.2.5 Cross Flow Filtration

A cross flow filtration apparatus (Figure 2.3) was used in to determine the longer term performance of the membrane. The membrane discs of 49 mm in diameter and an active area of 14 cm^2 were placed into a custom made cross flow test cells (Figure 2.4) connected in series.

The cumulative pressure drop across the 4 cells was measured to be less than 0.5 bar. The feed solution was charged into a 5 L feed tank and re-circulate at a flow rate of 90 $L.h^{-1}$ using a diaphragm pump (Hydra-Cell, Wanner International). The pressure of 30 bar in the cells was regulated using a back pressure regulator located downstream of a pressure gauge and the temperature was kept at 30ºC using a heat exchanger. During operation, permeate samples were collected from individual sampling ports and feed sample were taken from the feed tank. Rejection and flux were calculated according to equation 2.2 and 2.3.

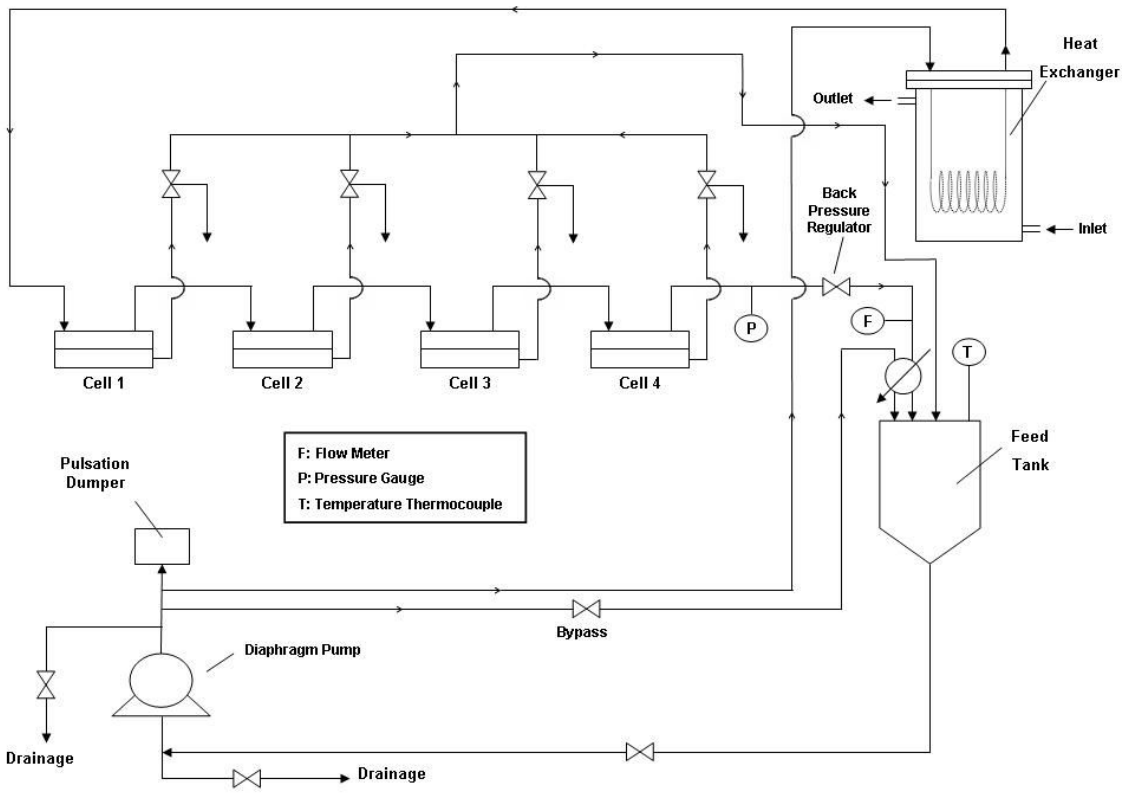

Figure 2.3 Schematic of cross flow filtration apparatus used in the testing of membranes in cross flow conditions

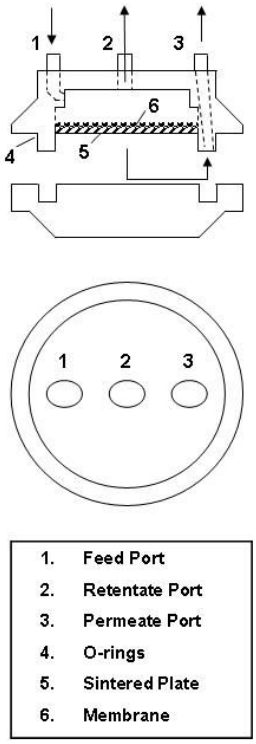

Figure 2.4 Schematic of a filtration cell used in the testing of membranes in cross flow conditions [106]

2.3 Membrane Performance

2.3.1 Dead End Filtration

A dead-end filtration was carried out to measure the membrane flux and MWCO. Figure 2.5 A shows the flux of toluene at 30 bar of STARMEM™ 122. The initial flux was 84 $L.m^{-2}.h^{-1}$ but this decreased to a steady state value of 63 $L.m^{-2}.h^{-1}$. This can be attributed to membrane compaction. In subsequent experiments, a minimum of 150 mL of pure solvent was permeated before the test solution was introduced to cell to obtain solute rejections. Also in Figure 2.5 A is shown a lower flux performance for STARMEM™ 122. Variation in the flux is attributed to slight temperature variations. Scarpello et al. [95] reported that a solvent flux increased substantially with increasing temperature over the range 20-40ºC. Batch variability in membrane production can also lead to different flux performances.

In Figure 2.5 A the flux of test solution is also represented. As expected the solvent flux with solute is slightly lower than the pure solvent flux due to concentration polarisation (Figure 1.8). The molecular weight cut beyond which 99.9% rejection occurs is also an important membrane performance parameter [165] as this indicates the point where effectively total exclusion of the species occurs demonstrating procedural and membrane integrity. Figure 2.5 B shows the MWCO curves. The MWCO curve for experiment 2 achieved 100% rejection for polysterene test solution and a MWCO of approximately 240 $g.mol^{-1}$ for STARMEM™ 122 which is in good

agreement with the value quoted by the manufacturer (220 g.mol^{-1}). [94] The MWCO curve for experiment 1 shows a plateau of rejection below 100% (~97%). This is a probable indication that a fraction of the collected permeate flux is composed of a 'leak flux' which can include a flow around the membrane seal, contacts between the O-ring and the membrane (see Figure 2.2) or thought defects in the membrane. [106]

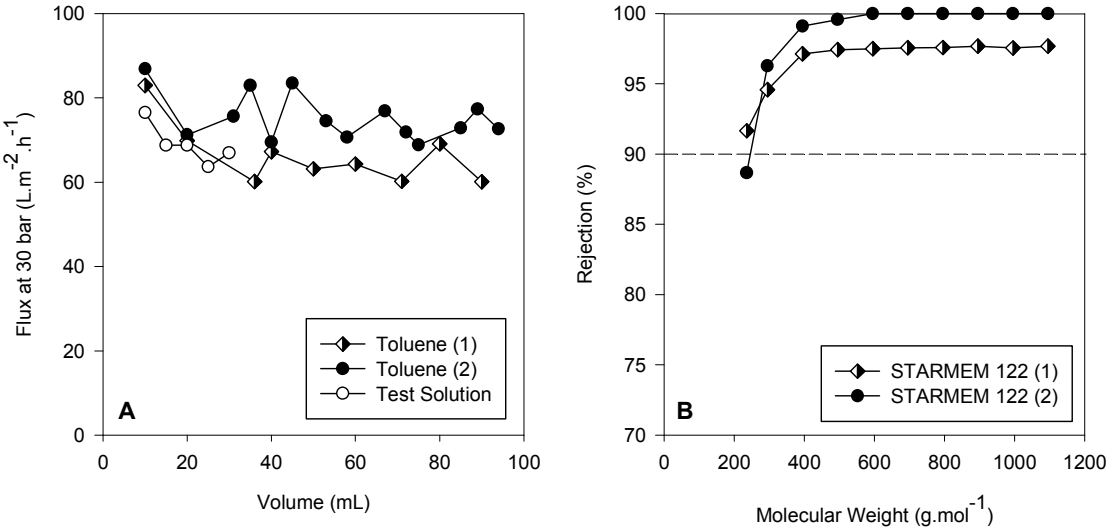

Figure 2.5 Pure solvent and test solution flux (A) and Molecular Weight Cut Off curve (B) for STARMEM™ 122 using toluene as solvent and a pressure of 30 bar

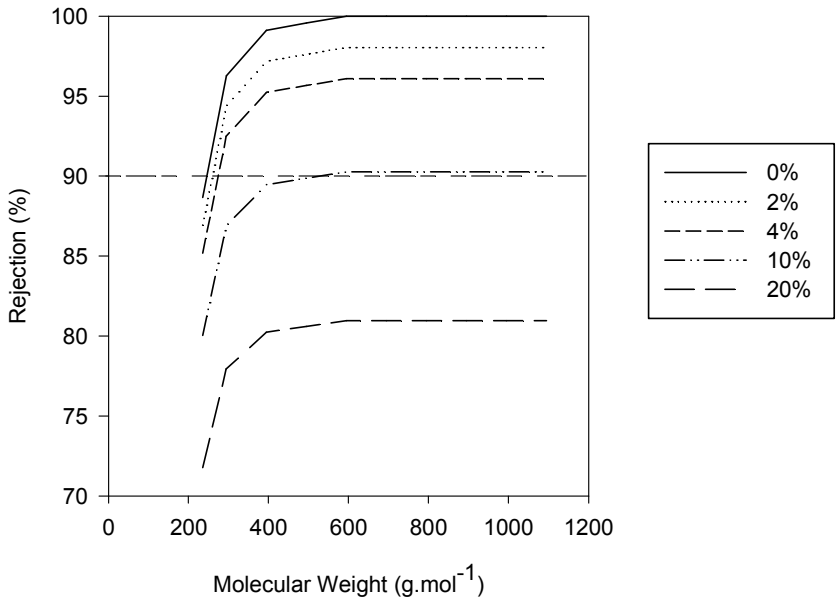

Figure 2.6 Vertical shift of MWCO curve due to different amounts of leak flux as a percentage of the total flux

Figure 2.6 shows the simulated vertical shift of the MWCO curve due to different amounts of leak flux as a percentage of the total flux. It is observed that even a small leak can result in the

plateau of the MWCO curve indicating a rejection of <99.9% for species of higher molecular weight.

Table 2.1 Mass Balance for dead end filtration using STARMEM™ 122 in toluene at 30 bar

Solute Molecular Weight ($gmol^{-1}$)	Mass Balance
236	95%
295	91%
395	93%
495	92%
595	93%
695	93%
795	91%
895	91%
995	92%
1095	92%

In batch filtration the system mass balance is also important in determining the validity of the MWCO curve. [106] The mass balance was calculated using equation 2.4. As shown in Table 2.1 the mass balance for each solute was calculated to be >90% indicating minimal loss of material in the experiment.

2.3.2 Cross-Flow Filtration

Cross flow experiments gave better hydrodynamics in the cell because the feed flow enter into the cell parallel to the surface of the membrane minimizing the effect of concentration polarization. The feed velocity inside of the cell is increased decreases the boundary layer resistance. Cross flow equipment also allows the membranes to be tested over an extended periods. [14] To investigate the longer term stability of STARMEM™ 122, the membrane was tested for > 20 hours in toluene at 30 bar at 30ºC. Figure 2.7 A shows the flux of STARMEM™ 122 in toluene tested in cross-flow filtration rig. The results for both experiments show that the flux is still declining after the first few hours and reaches steady state only after 20 hours. In the subsequent experiments, the membranes were tested for 24 hours before samples were taken to determine the MWCO of the membranes. This is to ensure that steady state had been achieved.

The decline in fluxes in experiment 1 and 2 could be due to membrane variability in the tested discs. Again the membrane in experiment 2 shows a plateau in the MWCO curve indicating a

possible leak or membrane defect. It is clear from the experiments that there is significant variability in commercially membranes.

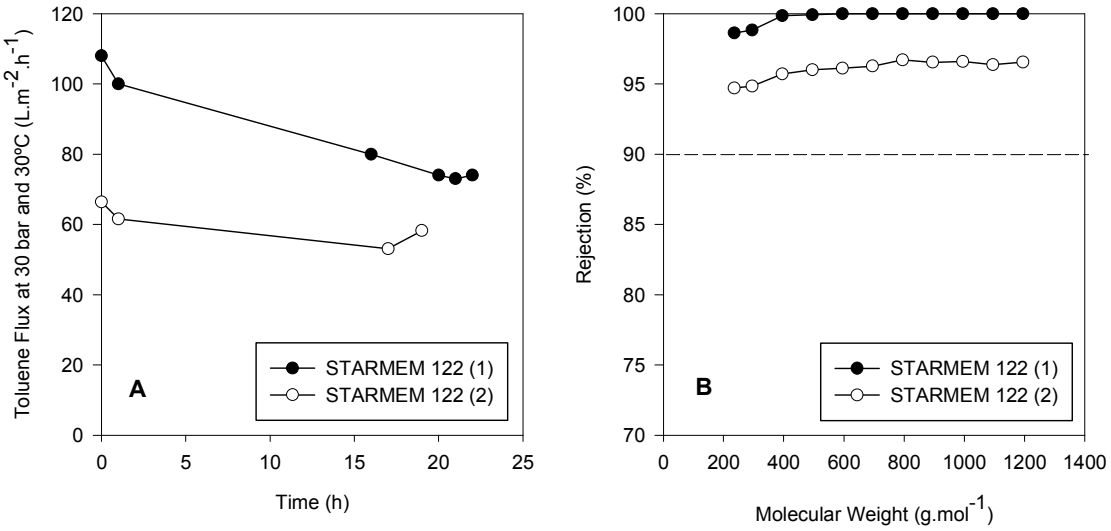

Figure 2.7 Pure solvent flux (A) and Molecular Weight Cut Off (B) of STARMEM™ 122 in toluene at 30ºC and 30 bar pressure.

2.4 Conclusions

A method to determine the MWCO is described in the previous section. [106] The tests carried out using a homologous series of styrene oligomers were found to be accurate in the determination of MWCO of the OSN membranes in a single filtration. The oligostyrenes cover a large range and were able to provide many points to give a comprehensive description of the membrane performance in the nanofiltration range.

Due to this large range, it was also possible determinate the molecular weight cut beyond which 99.9% rejection occur as this indicates the point where effectively total exclusion of the species occur demonstrating procedural and membrane integrity.

Membrane and equipment integrity can also be evaluated by observing the possible presence of a rejection curve plateau, indicating the presence of a leak flux. The oligostyrenes are also soluble in many organic solvents making this technique a useful tool for the cross comparison of membranes in different solvent systems. [106]

It is clear that using this method allows a rigorous and comprehensive understanding of membranes performance. The simplicity and effectiveness of this method makes it an attractive choice as a standard for nanofiltration tests in organic solvents. [106] Thus this technique will be used in the characterization of membranes in the following chapters.

3 P84

3.1 Introduction

P84 (BTDA-TDI/MDI, co-polyimide of 3,3'4,4'-benzophenone tetracarboxylic dianhydride and 80% methylphenylene-diamine + 20% toluene diamine), a most recent commercially available polyimide, has received significant attention for applications as a novel membrane material in ultrafiltration [4], nanofiltration [54], gas separation [116] or as a precursor in preparation of carbon molecular sieve membranes [166,167]. As membrane materials, polyimides have attached much attention for separation processes because of their excellent chemical resistance and thermal stability (high glass transition temperatures, T_g) [4,54,117,168]. P84 has a T_g= 315ºC [169]. It has been shown that P84 co-polyimide is a suitable membrane material for asymmetric membranes with good resistance to many organic solvents such like toluene, alcohols and ketones [4,54]. Their selectivity towards water is attributed to the preferential interaction between water molecules and the imide groups through hydrogen bonding.

Nanofiltration membranes have been fabricated from different polyimides including BTDA-TDI/MDI copolyimide (P84) [53,54,108,170]. Further developing membranes made of these polyimides could see the extend range of application of OSN.

Commercial polyimide (PI) OSN membranes have been show to give good performances in several organic solvents (e.g. toluene, methanol, ethyl acetate etc. [14]) but are however unstable in some amines [21] and have generally poor stability and performance in polar aprotic solvents such as methylene chloride (DCM), tetrahydrofuran (THF), dimethyl formamide (DMF) and n-methyl pyrrolidone (NMP) in which most of these membranes are soluble. Crosslinking has a huge effect on the physical, mechanical and thermal properties of the membranes. Most significantly, this causes the polymers to become insoluble [1]. This can give improved the membranes the solvent resistant characteristics.

A significant challenge in OSN in the ability to control the MWCO of membranes in the separation of high MW compounds enabling the fractionation of molecules in a membrane cascade system [155]. Some control of the MWCO for PI membranes was previously demonstrated by Ohya et al. [83] and Okazaki et al. [84] through the variation of formation parameters (evaporation times, additives, etc.). The effect of several parameters (non-solvent additives in the dope solution and heat treatment) on the physical structure of the membranes made from Lezing P84 was investigated by Qiao et al. [108] for use in pervaporation. Several authors [83,84,156] have previously attempted to change the MWCO of PI membranes by changing several formation parameters. However, the MWCO change reported and measured in these cases did not successfully report good control over the membrane separation

performance. Yanagishita et al. [113] suggests that the MWCO of PI membranes made from PI-2080 can be varied by changing the DMF:1,4-Dioxane ratio in the membranes. However the reduction of the ratio of co-solvent might result in a shorter demixing time and the formation of macrovoids in the membranes. Kim et al. [128] also demonstrated variation of the MWCO of Ultem 1000 polyetherimide in aqueous NF by changing the ratio of the same solvent/non-solvent composition in the dope. The authors do not comment on reasons of how this was achieved. Thus far, there are no studies of integrally skinned OSN membranes that relate the ratio of DMF:1,4-Dioxane and the MWCO of PI membranes. [171]

In this chapter the control over the MWCO of crosslinked and non-crosslinked membranes using a combination of membrane parameters and process conditions (pressure) is demonstrated. A study of membrane morphology was also performed using scanning electron microscopy (SEM).

3.2 Experimental

3.2.1 Chemicals

Lenzing P84 co-polyimide (Figure 3.1) was purchased from HP polymer GmbH and used without any further purification or treatment. The solvents used for the preparation of membranes were *N,N*-dimethylformamide (DMF) and 1,4-dioxane. Maleic acid (Fluka) was also used as additive in preparation of membranes. The stryrene oligomer mixture contained a mixture of PS580 and PS1050 (purchased from Polymer Labs, UK). Analytical grade toluene used as organic solvent was purchased from Fisher Scientific. The other organic solvents used like ethyl acetate, hexane, isopropanol methyl ethyl ketone and methanol were purchased from VWR (AnalaR).

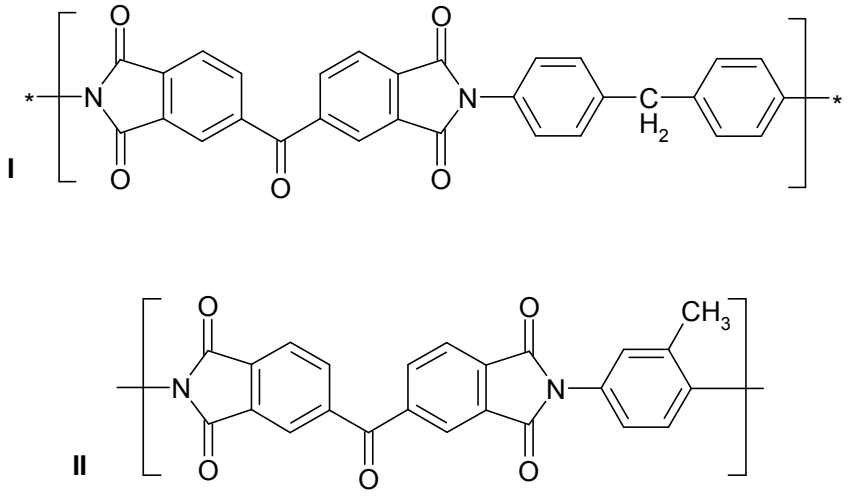

Figure 3.1 Chemical structure of Lenzing P84 (HP Polymer GmbH, Germany) (I) 20% and (II) 80% [4]

3.2.2 Membrane Preparation

Lenzing P84 and maleic acid (in some cases) were dissolved in DMF and 1,4-dioxane (different ratios of DMF:1,4-Dioxane) and stirred continuously overnight to obtain a homogeneous dope solution. The polymer solution was allowed to stand for a further 24 h to remove air bubbles at room temperature. The dope solution was used to cast films 200 μm thick on a backing support - polyester (Hollytex 3329, Ahlstrom) or polypropylene (Novatexx 2471) - using an adjustable casting knife on an automatic film applicator (Braive Instruments, UK). Immediately after casting the film was immersed, parallel to the surface, into a precipitation water bath at room temperature. The membranes were subsequently immersed in solvent exchange baths of isopropanol to remove water. The membrane was subsequently immersed into a solution of cross linker in isopropanol. Some of the membranes were then transferred from the isopropanol bath to a MEK/PEG 400 (40/60% v/v) bath. After the membranes were soaked in this bath, it was possible to handle the membranes in a "dry" state. Cracks were formed in the membranes if they were left to dry without the addition PEG as a conditioning agent. The ones that were not conditioned had to stay permanently immersed in solvent. A summary of the membrane preparation parameters is given in Table 3.1.

Table 3.1 Characteristics of P84 membranes

Membrane Designation	Polymer conc. (wt %)	Solvent composition[1]	Additive (2%)	Backing	Cross-Linking Agent
M1	22	1:3	___	PBT	___
M2	22	1:1	___	PBT	___
M3	22	3:1	___	PBT	___
M4	22	1:0	___	PBT	___
M5*	18	1:3	___	PP	HDA[2]
M6	22	1:1	Maleic Acid	PP	HDA
M7	22	2:1	Maleic Acid	PP	HDA
M8	22	3:1	Maleic Acid	PP	HDA

*Conditioned with MEK/PEG 400

[1] (DMF:1,4-Dioxane)

[2] 1,6 – Hexanediamine

3.2.3 Experimental Procedure

Soaking tests were conducted in order to evaluate membrane stability in different solvents. The membrane was cut to strips which were dried, weight and then immersed in different bottles containing toluene, ethyl acetate, n-hexane, isopropanol methyl ethyl ketone and methanol. The

weight loss was determined for each sample after 5 days. A detailed study in order to evaluate the percentage of crosslinked polymer was performed using FTIR-ATR spectra (section 3.2.5). Filtration experiments in order to characterize the membranes prepared were conducted according to the procedure outlined in section 2.2.5.

The experiments in order to prepare the ternary phase diagram were conducted according to the procedure outlined in section 3.2.6.

3.2.4 Scanning electron microscopy

Scanning electron micrographs were taken using Leo 1525 field emission scanning electron microscope (FESEM). The membrane samples were taken from isopropanol and subsequently snapped in liquid nitrogen. The samples were taken mounted onto the SEM stubs and sputtered using an Emitech K550 gold sputter coater. SEM conditions used were: 5 mm working distance, Inlens detector with an excitation voltage of 5 kV.

3.2.5 FTIR-ATR

Chemical changes within the membranes before and after crosslinking were monitored using a Perkin Elmer Spectrum One FT-IR spectrometer with a MIRacle™ attenuated total reflection (ATR - Pike Technologies) attachment. The membranes were washed repeatedly in isopropanol to remove any excess crosslinker and dried before analysis. Typical polyimide bands at 1780 (C = O), 1713 (C = O) and 1380 cm^{-1} (C – N) and amide bands at 1648 (C = O) and 1534 cm^{-1} (C – N) were identified to track changes to the polymer structure.

3.2.6 Ternary phase diagrams

In the preparation of ternary phase diagrams, a series of P84/DMF/1,4-dioxane dope solutions were prepared at different polymer concentrations. The solutions were stirred continuously in an oil bath at 25 ± 0.1^{o}C until total dissolution of the polymer gave a homogeneous dope solution. For each dope solution, the non-solvent (deionised water) was gradually added drop-wise until non-homogeneity (slight turbidity) was observed. The concentration (mass) of non-solvent added was determined gravimetrically.

3.3 Results and Discussion

3.3.1 Polymer Characteristics

Table 3.2 Soak test of P84 membrane in organic solvents (error ±1,83%)

Solvent	(%) Polymer Weight Change
Toluene	2,05
Ethyl Acetate	3,27
n-Hexane	-1,38
Isopropanol	2,96
Methyl Ethyl Ketone	-0,70
Methanol	0,00

Soaking tests give a comparison of the chemical resistance of the polymeric material. The results are summarized in Table 3.2. Table 3.2 shows that the polymer change is in most cases indicating polymer stability. Beerlage et al. [21] also reported no significant differences in porous structures upon immersion of polyimide membrane in isopropanol, n-hexane, ethyl acetate and toluene for long periods (600 days). The only exception in their results is methanol where the polymer showed a high degree of swelling caused by specific polymer-solute interactions. Thus P84 has a low degree of instability in a range of organic solvents. However, it is also unstable in solvents such like dioxane, methylene chloride or cyclohexanone. [21]

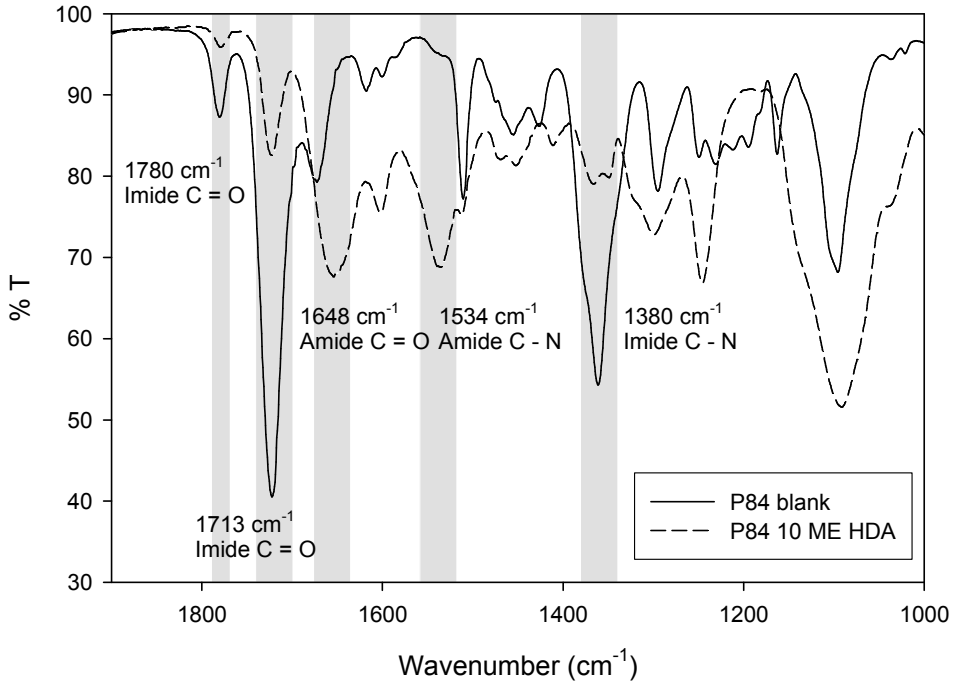

Figure 3.2 FTIR-ATR spectrum of P84 membrane crosslinked with HDA

Figure 3.2 shows FTIR-ATR for the original and crosslinked P84 membranes. The imide group is characterize by bands at around 1780 cm^{-1} (asymmetric stretch of C = O in the imide group), 1713 cm^{-1} (symmetric stretch of C = O in the imide group) and 1380 cm^{-1} (stretch of C – N in the imide group). [172] For the crosslinked membranes, the intensity of the imide C = O bonds are observed to be attenuated and replaced by amide C = O and C-N (amide groups) bonds indicating crosslinking according to the mechanism suggested by Tin et al. [136] (Figure 3.3).

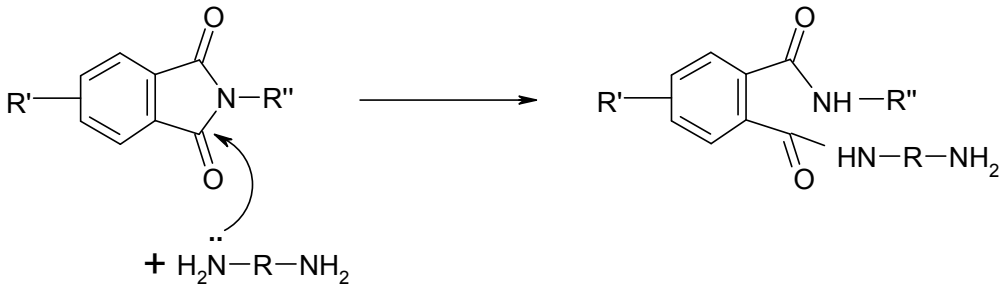

Figure 3.3 Schematic of the crosslinking reaction proposed by Tin et al. [136]

3.3.2 Membrane Performance in Cross-Flow Filtration

3.3.2.1 Non Chemically Modified Membranes

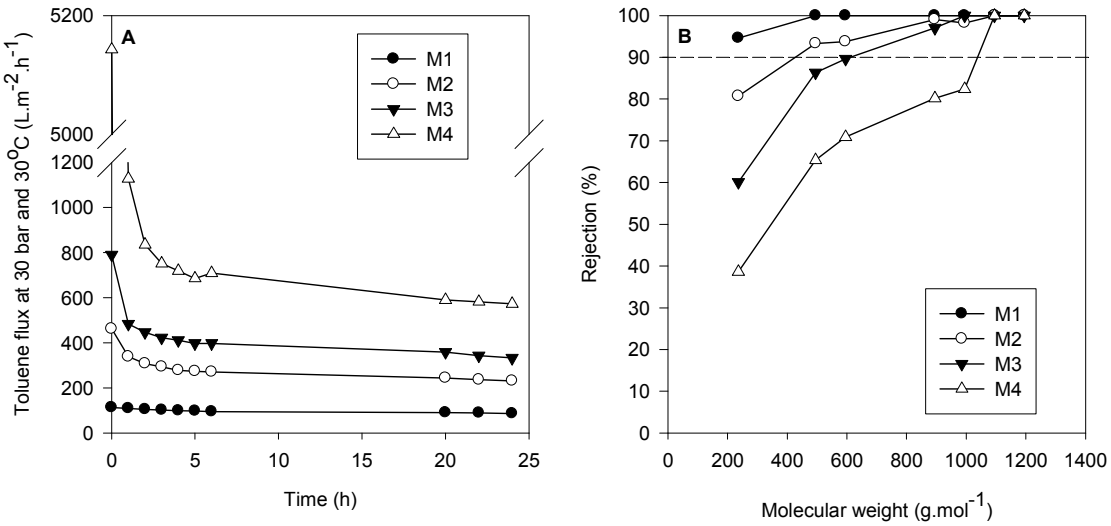

Figure 3.4 Toluene Flux profile (A) and MWCO curve in toluene (B) at 30 bar and 30ºC of membrane M1-M4 prepared at 22 wt% PI with different DMF:1,4-Dioxane ratios in the dope solution

Figure 3.4 (A) shows the toluene flux profile of membranes M1-M4 at 30 bar and 30ºC. Fluxes and compaction (equation 3.1) was observed to increase with DMF:1,4-Dioxane ratios, ie., increasing DMF concentration in the dope solution. In OSN, where the steady state separation

is only achieved after membrane compaction [70], increased macrovoids could result in longer pre-conditioning times [97]. Figure 3.4 (B) shows the MWCO curves for the corresponding membranes after steady state was achieved. These were determinated when no further flux decline was observed. The MWCO of the membranes was also been observed to increase with the DMF concentration in the dope solution. A MWCO of < 200, 420, 600 and 1000 $g.mol^{-1}$ was achieved for membranes M1-M4 respectively. This demonstrates the possibility of using the solvent composition as a possible handle for varying the MWCO of PI membranes in the NF range.

$$Compaction\ (\%) = \frac{J_i - J_f}{J_f} \times 100 \qquad \textbf{Equation 3.1}$$

SEM pictures of membranes M1-M4 are shown in Figure 3.6. Figure 3.6 A shows the cross section of the membranes. Figure 3.6 B shows a magnified cross section of the top separation surface of the membranes. A membrane separation layer thickness of 200 nm for polyimide OSN membranes had been previously estimated in the literature [96,97]. Figure 3.6 C shows a magnified cross-section of membranes. The membranes all show an asymmetric structure as it is shown in Figure 3.6 A. The most significant morphological change in M1 – M4 is the increase in macrovoid formation with higher DMF concentration in the dope solution. These features can account for the trend of higher compaction observed in membranes M1 – M4. Macrovoids can cause membrane collapse when pressure is applied because they make it unstable [1] leading to a decreasing in permeate flux. Membrane M1 do not present any macrovoids because the amount of 1,4-Dioxane was enough to increase the demixing time in a way that macrovoids did not occur in membrane formation during phase inversion in water. [128] Increased macrovoid formation with DMF concentration in the dope solution has also been observed by Kim et al. [128] for PEI membranes. This was attributed to the polymer solution system shifting from a delayed to an instantaneous demixing process at higher DMF (log K_{OW}: -1.01) concentrations due to the poorer affinity of 1,4-Dioxane (log K_{OW}: -0.27) for water. The diffusion coefficients for DMF and 1,4-Dioxane in water were calculated from modified Wilke-Chang equation [173] to be 1.11×10^{-9} and 1.05×10^{-9} $m^2\ s^{-1}$ respectively. In the equation the solute molar volume (V_i) at the boiling point was determined using a group contribution method as presented by Geankoplis [174].

$$D_{i,\infty} = 7{,}4 \times 10^{-8} (\phi \cdot M_{i,w})^{0,5} \frac{T}{\mu_0 \cdot V_i^{0,6}} \qquad \textbf{Equation 3.2}$$

The reduced demixing times may also be attributed to the faster diffusion coefficients for DMF compared to 1,4-dioxane in water. Instantaneous demixing leading to macrovoid formation occurs when the initial polymer composition lies close to the polymer precipitation curve [1,171]. Figure 3.5 shows the ternary diagram of P84 at different solvent compositions at 25°C. The

migration of the polymer precipitation curve at a higher DMF concentration towards the polymer/solvent axis corroborates this shift towards instantaneous demixing [59].

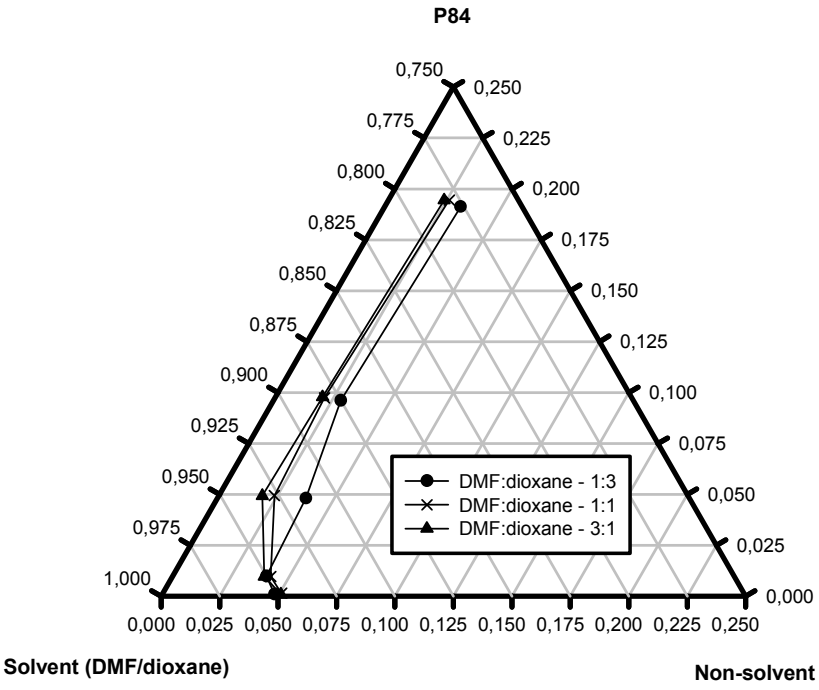

Figure 3.5 Ternary diagram of P84 at different DMF:1,4-Dioxane compositions at 25 ± 0.5 ^{o}C

The SEM pictures of the top layer - Figure 3.6 B - show that the predominant morphology within this length scale is that of a nodular structure. This morphological feature is frequently observed and reported in the top separation layer of ultrafiltration (UF) and nanofiltration (NF) membranes [28]. The formation mechanism and origins of nodules are however disputed and have been attributed to (i) aggregates or micelles [24,45,55] already present in the dope (ii) formation via liquid-liquid demixing during phase inversion [50,51,56] (iii) artefacts of sample preparation for SEM [57,58].

The size of the nodules appears to decrease from M1 – M4. A similar observation was reported by Wienk et al. [51] for polyethersulfone (PES) membranes where it was concluded that the size of nodules decreases if the initial composition of the dope solution is closer to the binodal composition. This is corroborated in this work by the shift of the cloud point curves towards the polymer-solvent axis (Figure 3.5) with increasing DMF concentration in the dope solution. [171]

In the formation of the nodular top layer, low polymer diffusion coefficients [175,176] compared to the solvent and non-solvent allow the assumption that little reorganisation of the polymer chains of the initial polymer solution could occur. As such, the demixing time controls the size of nodule formation with faster demixing leading to shorter coarsening [177] periods before vitrification and resulting in smaller nodule sizes.

The size of nodules has been previously reported to be independent of the MWCO of the membrane [51,178]. However, as no other significant morphological change could be observed in this layer, the different nodule sizes could be an indication of a physical parameter that induces a change in the separation performance of PI OSN membranes. Current transport models [143,179] used in OSN are unable to relate this morphological feature to OSN transport and further work is required to elucidate a transport mechanism coherent with the present observations.

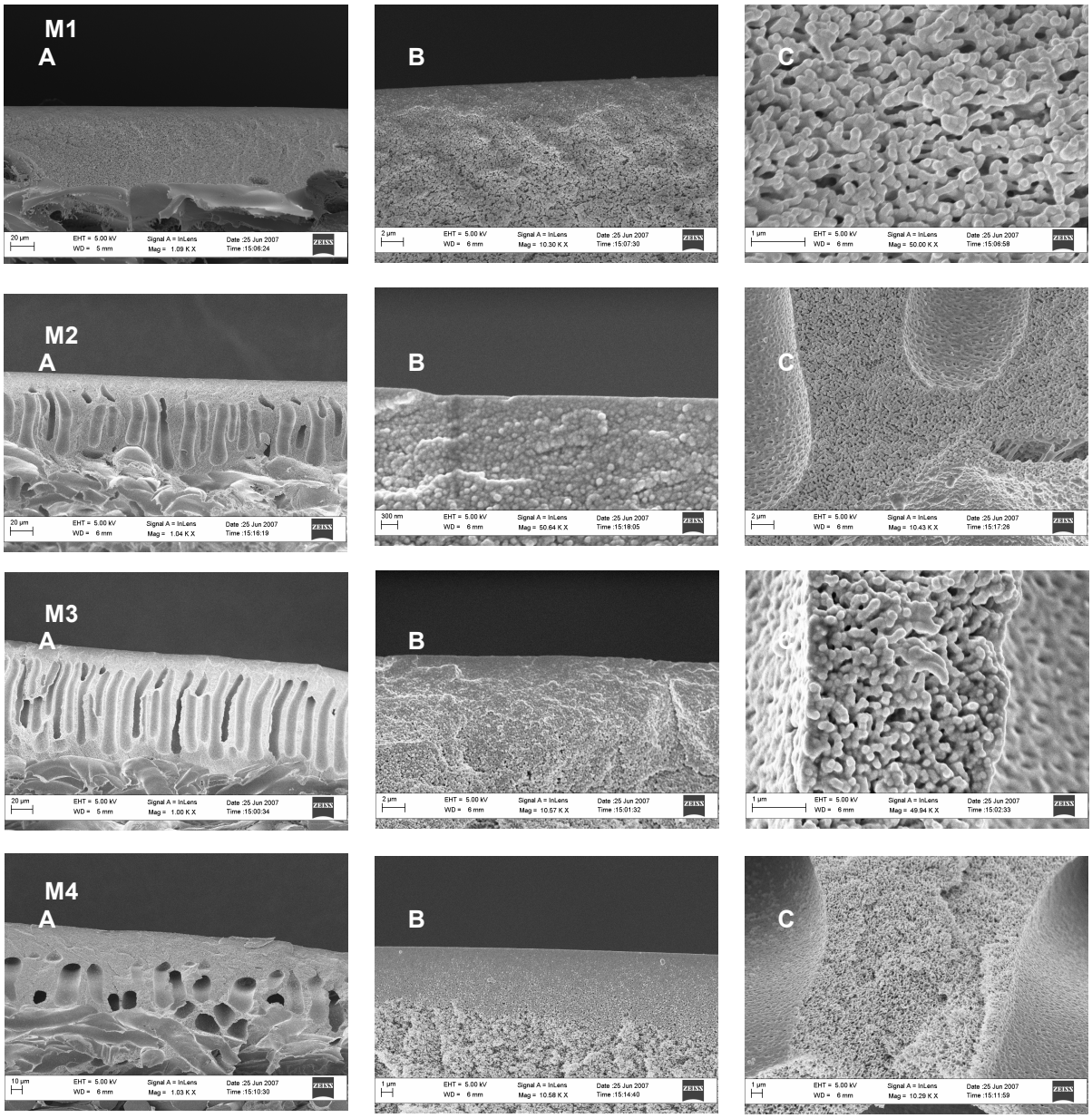

Figure 3.6 Morphological changes with shifting the ratio between DMF:1,4-Dioxane in the dope solution of membranes M1-M4 prepared from 22wt% PI. A. Cross section 1,000x, B. Top layer 10,000x (M1, M3, M4) and 50,000x (M2), C. Middle section 10,000x (M2 and M4) and 50,000x (M1 and M3)

The variation of the MWCO by altering the solvent composition in the dope presents a simple methodology in which to exploit a single polymer to achieve variable MWCO in OSN membranes. To further improve the chemical stability of these membranes, this technique was coupled with a previously reported crosslinking technique [12,171].

3.3.2.2 Chemically Modified Membranes

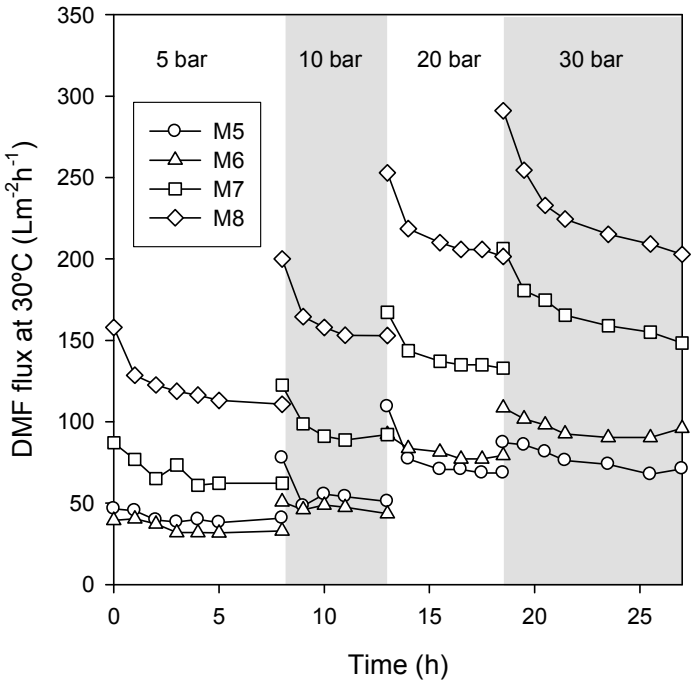

Figure 3.7 DMF flux profile with increase pressures at 30ºC for crosslinked membranes with different dope compositions.

Figure 3.7 represents the DMF flux profile at 30ºC of crosslinked membranes M5 (18wt%), M6-M8 (22wt%) with different dope compositions. The data shows that flux increases with pressure for these membranes. This behaviour corroborates with data demonstrated by others [70,95,180] for OSN membranes. The results also show that flux compaction (equation 4.1) increases with increasing DMF concentration in the dope solution. This may be explained by demixing times as suggested in section 3.3.2.1. Since no apparent change on the morphology occurs after crosslinking [12], membranes at high DMF concentration in the dope can expect to have increased amounts of macrovoids leading to increase compaction.

At 30 bar pressure the flux for M5, M6, M7 and M8 is, respectively, 71 $L.m^{-2}.h^{-1}$, 95 $L.m^{-2}.h^{-1}$, 148 $L.m^{-2}.h^{-1}$ and 202 $L.m^{-2}.h^{-1}$. Comparing the flux values for membranes M2 and M3 with membranes M6 and M8 is observed that the values for the crosslinked membranes are lower than the non-crosslinked analogues. This effect could be due to differences in solvent viscosity

but also be attributed to increased chain rigidity [181] in the crosslinked membranes. In addition, lower fluxes have been previously observed for crosslinked membranes over the non-crosslinked membranes for gas separation as the interstitial spaces between polymer chains are reduced through the inclusion of the crosslinker into the polymer matrix [137]. Increasing of polymer concentration also leads to a flux decreasing [182].

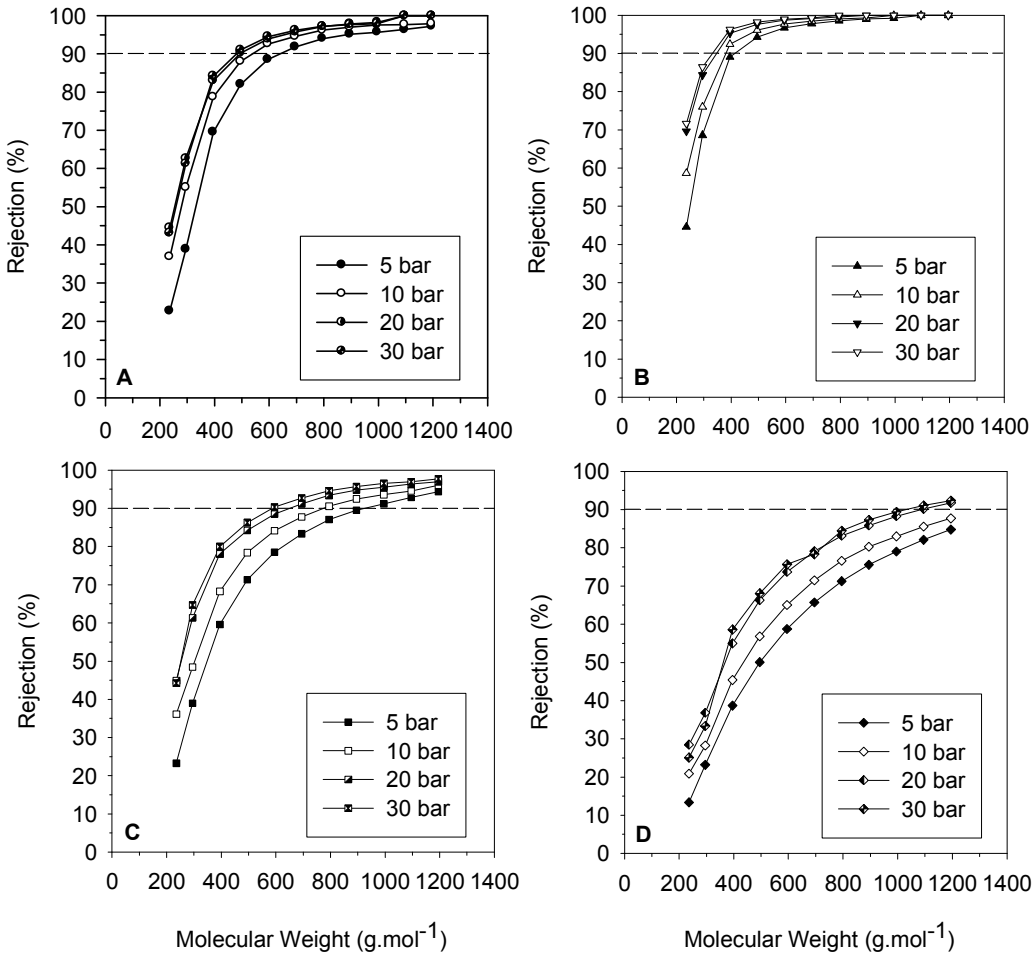

Figure 3.8 Membrane performance of crosslinked membranes with different dope compositions in DMF with increasing pressures. (A) M5, (B) M6, (C) M7 and (D) M8.

Figure 3.8 shows MWCO curves of crosslinked membranes with different dope compositions at 30ºC with increasing pressures in DMF. The MWCO of the membranes was observed to decrease with operating pressure. This has been attributed to the tightening/sealing of pores with increasing pressure [95]. The MWCO was also observed to increase with DMF concentration in the dope solution. The figure demonstrates the possible shift of the MWCO curve by varying the DMF:1,4-Dioxane ratio. In addition to the intrinsic membrane separation characteristics, the use of pressure can also allow further control over the MWCO. In Figure 3.8 (C) and (D) is shown a trend in the MWCO curve going up until UF range. Although the MWCO curves of both membranes do not achieve 100% in the nanofiltration range the MWCO does, 620 $g.mol^{-1}$ for M7 and 1000 $g.mol^{-1}$ for M8.[171]

The changing in MWCO by changing DMF:1,4-Dioxane ratio could imply that polymer characteristics in solution is critical in determining the final MWCO of the membrane and little or no re-organization of the initial polymer solution could occur during the immersion precipitation step [183].

According to Figure 3.7 as the ratio between DMF:1,4-Dioxane increases for DMF the flux increases and, apparently, the rejection decreases. This reduction in rejection with an increase in flux (permeance) was also observed by Bulut et al. [184] and See Toh et al. [53] for PI membranes.

3.4 Conclusions

Integrally skinned asymmetric membranes made of Lenzing P84 with different ratios of DMF:1,4-Dioxane were prepared and tested for extended periods in toluene for 24h. The resultant membranes showed different and controllable MWCOs in NF range.

Chemical crosslinking of integrally skinned asymmetric membranes made of Lenzing P84 was performed by immersion of the preformed membrane into a bath of aliphatic diamine. The resultant membrane showed good chemical stability across a range of organic solvents including DMF. Extended periods of testing in DMF show the membranes to be stable, whilst still affording good separation. Changing the dope composition and operating pressure also allowed for control of the MWCO curves.

The SEM pictures show that macrovoids formation increases when more DMF is used as the increase affinity to water promotes faster demixing. 1,4-Dioxane was used as a co-solvent to promote a delay in the demixing time which was also confirmed with the same results.

In conclusion, the results demonstrate that crosslinking can be coupled to changing dope composition in a tandem process to simultaneously control the MWCO and improve the chemical stability of PI membranes. In addition, pressure can be used as a process variable in the nanofiltration experiments in which to fine tune the required separation [7]. From a manufacturing perspective, this method allows different membranes of distinct separation performance to be fabricated using the same processing steps by just changing the dope compositions.

4 Matrimid 5218

4.1 Introduction

In the last decade Matrimid 5218, a BTDA-DAPI formed from 3,3',4,4'-benzophenone tetracarboxylic dianhydride (BTDA) and 5(6)-amino-1-(4'-aminophenyl)-1,3-trimethylindane (DAPI), was widely studied as a material for gas separation membranes [119]. Its use in OSN applications has thus far been limited [120] due to its poorer stability in organic solvents. This polyimide membrane showed good performances for the low temperature separation of low molecular weight organic materials from solvents by hyperfiltration. Benefits are improved energy costs and throughput of product when the membrane separation technique is used in the solvent dewaxing process of lube oil. Matrimid 5218 is a polyimide so that it has an excellent chemical resistance and thermal stability (high glass transition temperatures T_g = 302ºC [118]) [4].

Nanofiltration membranes have been fabricated from different polyimides including Matrimid 5218 [4,120]. The crosslinking strategy currently applied to Lenzing P84 could be extended to the other polyimides, such like Matrimid 5218, to improve solvent stability of these membranes. Tin et al. [136] has shown that Matrimid crosslinking reaction (crosslinking reaction conducted in a solution of methanol) is similar to the one that had been proposed for P84.

Similarly to P84, Matrimid has poor stability and performance in polar aprotic solvents such as methylene chloride (DCM), tetrahydrofuran (THF), dimethyl formamide (DMF) and n-methyl pyrrolidone (NMP) in which most of these membranes are soluble. Crosslinking is a possible mean to improve physical, mechanical and thermal properties of the membranes. Crosslinking also confers solvent resistant characteristics to the membranes.

The aim of this chapter is to develop a new polyimide membrane for OSN and to extend the crosslinking strategy already applied for P84 to other polyimide. In order to do that, different dope solutions composition were prepared and the membranes were characterized according to their solvent flux and MWCO curves.

4.2 Experimental

4.2.1 Chemicals

Matrimid 5218 (Figure 4.1) was purchased from Huntsman and used without any further purification or treatment. The solvents used for the preparation of membranes were *N,N*-dimethylformamide (DMF) and 1,4-dioxane and tetrahydrofuran (THF) and 1-methyl-2-pyrrolidinone (NMP). Maleic acid (Fluka) was also used as additive in preparation of membranes. The stryrene oligomer mixture contained a mixture of PS580 and PS1050 (purchased from Polymer Labs, UK). Analytical grade toluene used as organic solvent was purchased from Fisher Scientific. The other organic solvents used like ethyl acetate, hexane, isopropanol methyl ethyl ketone and methanol were purchased from VWR (AnalaR).

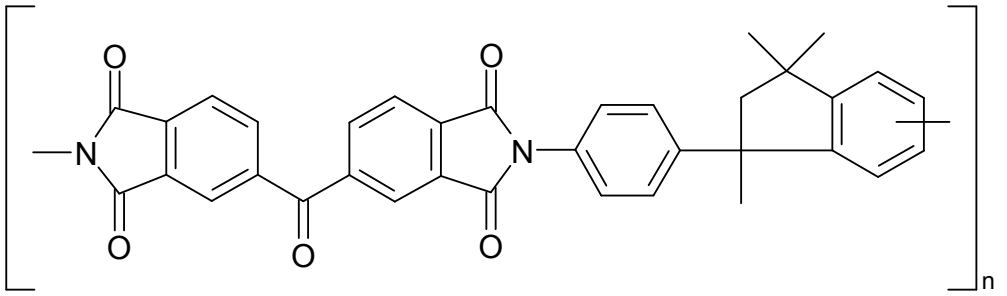

Figure 4.1 Chemical structure of Matrimid 5218 (Huntsman Advanced Materials GmbH, Switzerland) [4]

4.2.2 Membrane Preparation

Matrimid 5218 and Maleic acid were dissolved in DMF and 1,4-dioxane or NMP and THF and stirred continuously overnight to obtain a homogeneous dope solution (Table 4.1). The polymer solution was allowed to stand for a further 24 h to remove air bubbles at room temperature. The dope solution was used to cast films 200 µm thick on a backing support – polyester (Hollytex 3329, Ahlstrom) or polypropylene (Novatexx 2471) - using an adjustable casting knife on an automatic film applicator (Braive Instruments). Immediately after casting, the film was immersed, parallel to the surface, into a precipitation water bath at room temperature. The membranes were subsequently immersed in solvent exchange baths of isopropanol to remove water. The membrane was subsequently immersed into a solution of cross linker in isopropanol.

Table 4.1 Characteristics of Matrimid membranes

Membrane Designation	Polymer conc. (wt %)	Solvent composition	Additive (2%)	Backing	Cross-Linking Agent
M9	18	1:3[1]	Maleic Acid	PBT	___
M10	18	1:3[1]	Maleic Acid	PP	EDA[3]
M11	20	1:3[1]	Maleic Acid	PP	EDA
M12	26	1:2[2]	Maleic Acid	PBT	___

[1] (DMF:1,4-Dioxane)

[2] (THF:NMP)

[3] 1,2 – Ethylenediamine

4.2.3 Experimental Procedure

Soaking tests were conducted in order to evaluate membrane stability in different solvents. The Matrimid 5218 membrane and Matrimid 5218 crosslinked membrane were cut to strips which were dried, weight and then immersed in different bottles containing toluene, ethyl acetate, n-hexane, isopropanol methyl ethyl ketone and methanol. The weight loss was determined for each sample after 5 days. A detailed study in order to evaluate the percentage of crosslinked polymer was performed using FTIR-ATR spectra (section 3.2.5).

Filtration experiments in order to characterize the membranes prepared were conducted according to the procedure outlined in section 2.2.4 and 2.2.5.

4.3 Results and Discussion

4.3.1 Polymer Characteristics

Table 4.2 shows the results of soaking tests conducted to evaluate the chemical and physical stability of matrimid in several organic solvents. The results show an insignificant change in almost all cases. However methanol seems to be the worst solvent. This corroborates with Tin et al. [136] who reported a swelling of the polymer chains in methanol considering it an intermediate and unstable process. The data shows that crosslinked membranes increased their chemical stability in organic solvents which was already reported for several authors [12,15,16]. In addition to solvent stability, this also highlights the importance of processibility in the choice of solvents in further processing steps.

Table 4.2 Soak test of Matrimid membrane in organic solvents (error ±1,83%)

Solvent	(%) Polymer Weight Change	(%) Polymer Weight Change of Crosslinked membranes
Toluene	-2,07	5,31
Ethyl Acetate	3,68	2,54
Hexane	-1,79	3,00
Isopropanol	0,00	2,65
Methyl Ethyl Ketone	-8,67	-1,61
Methanol	-21,14	11,65

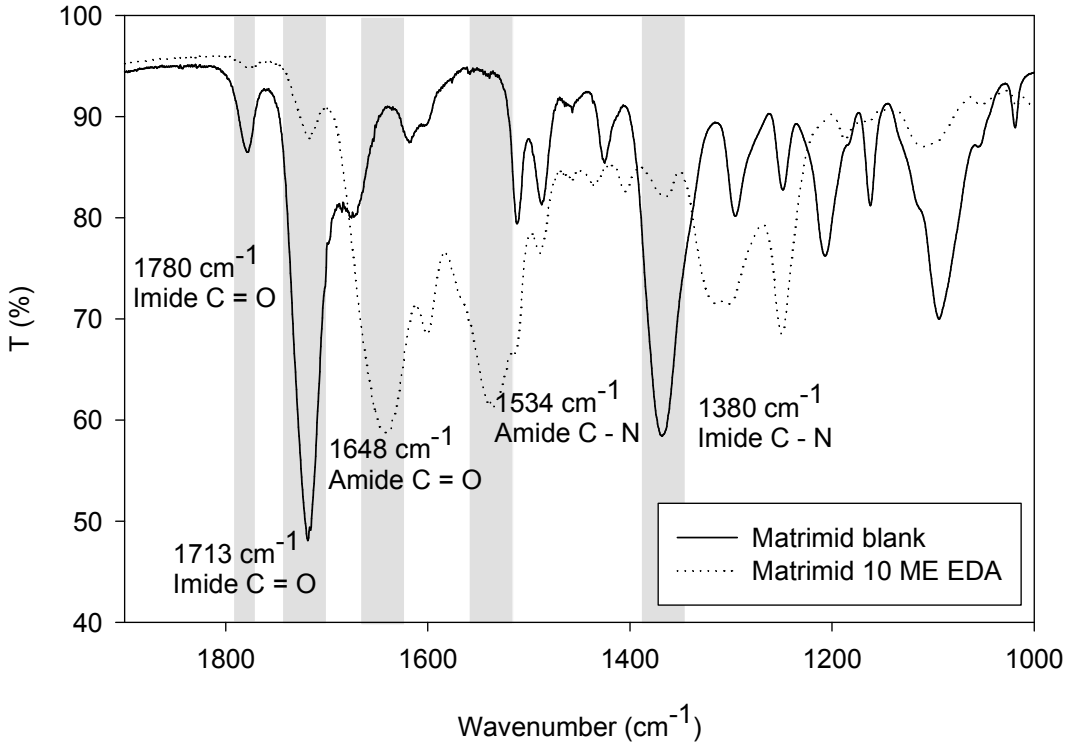

Figure 4.2 FTIR-ATR spectrum of Matrimid membrane crosslinked with EDA.

Figure 4.2 shows FTIR-ATR for the original and crosslinked matrimid membranes. The imide group is characterize by bands at around 1780 cm^{-1} (asymmetric stretch of C = O in the imide group), 1713 cm^{-1} (symmetric stretch of C = O in the imide group) and 1380 cm^{-1} (stretch of C – N in the imide group). [136] For the crosslinked membranes, the intensity of the imide C = O bonds are observed to be attenuated and replaced by amide C = O and C-N (amide groups) bonds indicating crosslinking according to the mechanism suggested by Tin et al. [136] (Figure 3.3).

4.3.2 Membrane Performance in Dead End Filtration

4.3.2.1 Non Chemically Modified Membranes

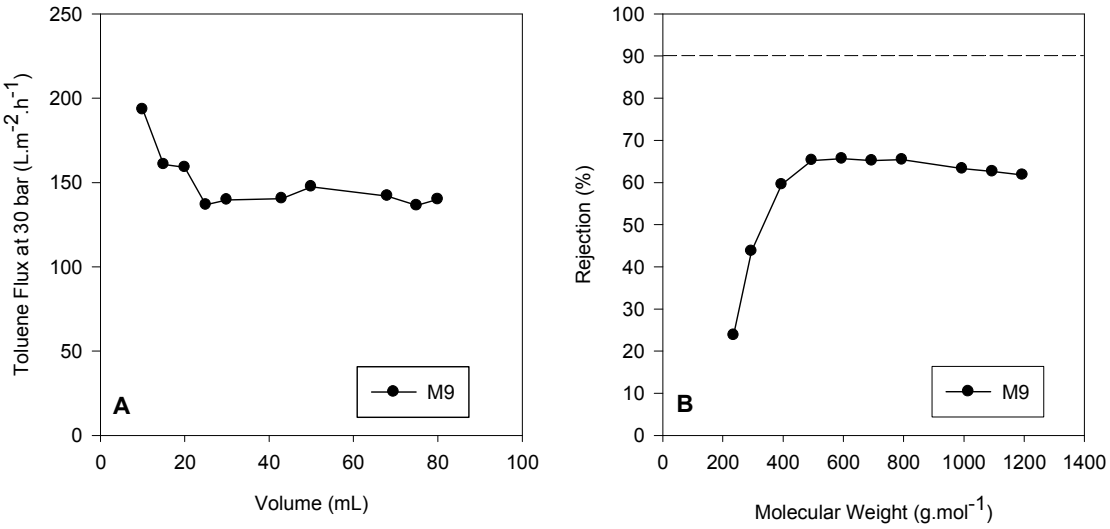

Figure 4.3 Toluene Flux profile (A) and MWCO curve in toluene (B) at 30 bar of membrane M9

Figure 4.3 shows the flux (A) and MWCO curve (B) for membrane M9 in toluene at 30 bar. A steady state flux of 140 $L.m^{-2}.h^{-1}$ was achieved after permeating 80 mL of pure solvent. The MWCO curve is observed to reach a plateau at 70%. This indicates that whilst some separation was achieved, the membrane was defective. A probable reason is the fact that PP backing material which might have dissolved/swelled inducing surface defects.

4.3.2.2 Chemically Modified Membranes

In Figure 4.4 is represented the flux (A) and MWCO curves (B) in DMF for membranes M10 and M11. The data shows that increasing the polymer concentration the flux decreases which corroborates with several authors [1,53,182,185]. Comparing the flux values for membranes M9 and M10 is observed a decreasing. This effect could be due to differences in solvent viscosity but also be attributed to increased chain rigidity [181] in the crosslinked membrane. In Figure 4.4 (B) is shown a trend to increase the MWCO until the UF range. This indicates that the membrane might possess separation charateristics in the UF range. In addition, for membrane M10 the curve do not achieved 70% in contrast with membrane M9 which is not only because of the difference in the solvents used but also a consequence of the flux decreasing. This reduction in rejection with an increase in flux was also observed by Bulut et al. [184] and See Toh et al. [53] for PI membranes.

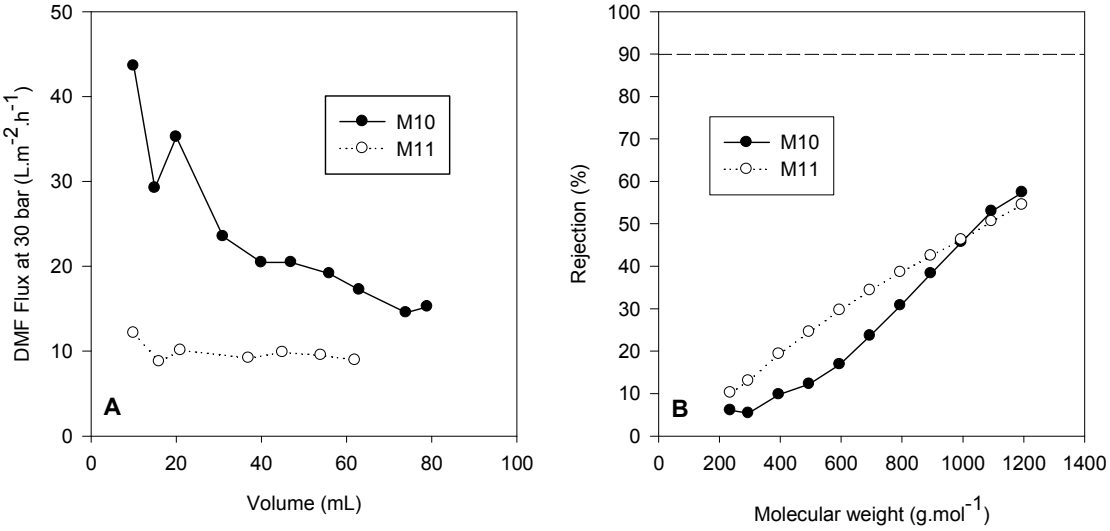

Figure 4.4 DMF Flux profile (A) and MWCO curves in DMF (B) at 30 bar of membrane M10 and M11

4.3.3 Membrane Performance in Cross Flow Filtration

4.3.3.1 Non Chemically Modified Membranes

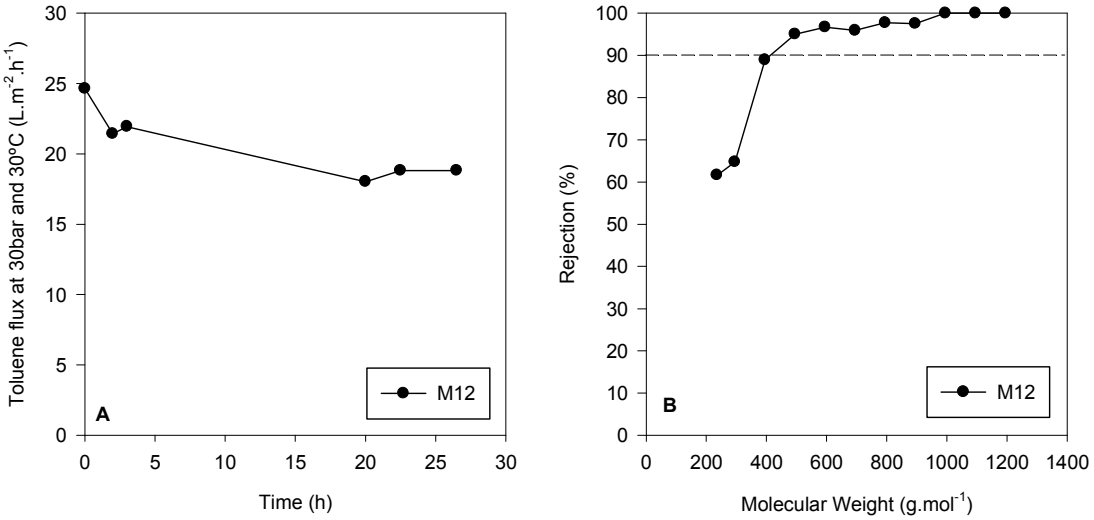

Figure 4.5 Toluene flux profile (A) and MWCO curve in toluene (B) at 30 bar and 30ºC of membrane M12

Figure 4.5 (A) shows the toluene profile of membrane M12 at 30 bar and 30ºC. Steady state was achieved after 22 hours. Good solvent flux was achieved with stable performance over 24 hours in toluene.

Figure 4.5 (A) shows the MWCO curve for membrane M12 in toluene. The MWCO was approximately 400 g.mol^{-1} with a rejection of >99% achieved after 900 g.mol^{-1}.

4.4 Conclusions

Integrally skinned asymmetric membranes made of Matrimid 5218 were prepared and tested in toluene to evaluate membrane performances. The resultant membranes showed different performances with changing solvent/non-solvent system. Better results where achieved with THF and NMP where the membrane showed a good rejection and a MWCO curve in the NF range.

Crosslinking these membranes was confirmed by FTIR-ATR and improved the membrane stability but this was achieved at the expense of flux. Crosslinking the polymer improved its stability in all of the solvents tested.

Further development of the membrane will focus on improvement of MWCO and flux performances.

5 Ultem 1000

5.1 Introduction

Ultem polymers were introduced in Europe during the early 1980's and belong to a high performance polymer family yielding good mechanical, thermal and electric properties [123]. Ultem 1000 has been used in many instances in gas separation [160,161,186], ultra [162] and nanofiltration membranes [128,163]. It has a T_g of 215ºC [161] and a structure. This polymer is manufactured from the polycendensation of bisphalic anhydride and 1,3-diaminobenzene and is known to be totally amorphous [123].

Nanofiltration membranes have been fabricated from different polyetherimides [128,162]. Ultem 1000 has been reported to possess a high MWCO in the NF range and also in the UF range (>1000 g mol^{-1}) [124]. Also the use of 1,4-dioxane as a co-solvent in this kind of membranes has been shown to reduce macrovoid formation [128].

The ester linkage between the chains have been reported [124] to offer better chain flexibility and hence improve processibility of the membrane and an imide ring opening reaction for ultem has also been previously demonstrated opening possibilities for crosslinking reactions to improve the chemical stability of the polymer [187].

Recent investigations on PEI biocompatibility have shown that this polymer do not exert any significant level of cytotoxicity or hemolysis and allow the attachment and growth of cells [157,158]. Therefore, it was anticipated that PEI is a candidate for biomedical applications for parts of intraocular lenses, biosensors, oxygenators or neuroprostheses [159]. Due to its considerable mechanical strength and thermal stability PEI is suitable for steam sterilization. PEI has very good membrane forming properties [125,161]. The functional groups are accessible for a wet chemistry modification to adapt the resulting membrane material to a specific application such as contact with blood or tissue cells. So that polyetherimide membranes could be an alternative for biohybrid organs.

Membranes have been manufactured for use in NF range but no reported applications of Ultem 1000 in OSN. The aim of this chapter is to develop a polyetherimide OSN membrane. Different dope solution compositions were prepared and the membranes were characterized according to their solvent flux and MWCO curves determined under dead end filtration at 30 bar. Crosslinking reaction was also induced to improve the membrane performance under harsh environments.

5.2 Experimental

5.2.1 Chemicals

Ultem 1000 (Figure 5.1) was purchased from General Electric and used without any further purification or treatment. The solvents used for the preparation of membranes were *N,N*-dimethylformamide (DMF) and 1,4-dioxane. Maleic acid (Fluka) was also used as additive in preparation of some membranes. The stryrene oligomer mixture contained a mixture of PS580 and PS1050 (purchased from Polymer Labs, UK). Analytical grade toluene used as organic solvent was purchased from Fisher Scientific. The other organic solvents used like ethyl acetate, hexane, isopropanol methyl ethyl ketone and methanol were purchased from VWR (AnalaR).

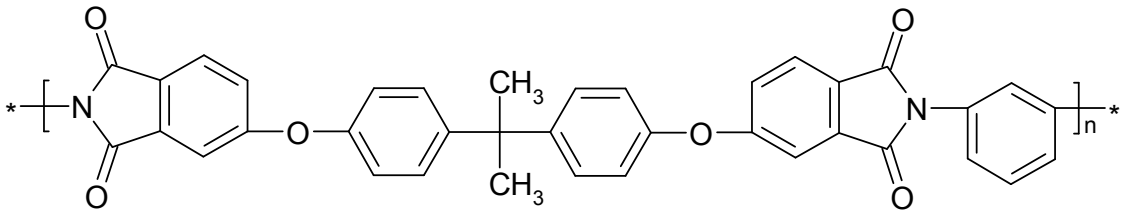

Figure 5.1 Structure of Ultem 1000 (General Electric Plastics, Ltd., UK) [188]

5.2.2 Membrane Preparation

Ultem 1000 and Maleic acid (in some cases) were dissolved in DMF and 1,4-dioxane and stirred continuously overnight at 60ºC to obtain a homogeneous dope solution. The polymer solution was allowed to stand for a further 24 h to remove air bubbles at room temperature. The dope solution was used to cast films 200 µm thick on a backing support - polyester (Hollytex 3329, Ahlstrom) or polypropylene (Novatexx 2471) - using an adjustable casting knife on an automatic film applicator (Braive Instruments). Immediately after casting the film was immersed, parallel to the surface, into a precipitation water bath at room temperature. The membranes were subsequently immersed in solvent exchange baths of isopropanol to remove water. The membrane was subsequently immersed into a solution of the cross linker in isopropanol.

Table 5.1 Characteristics of Ultem membranes

Membrane Designation	Polymer conc. (wt %)	Solvent composition[1]	Additive (2%)	Backing	Cross-Linking Agent
M13	18	1:3	Maleic Acid	PBT	___
M14	20	1:3	___	PBT	___
M15	24	1:3	Maleic Acid	PBT	___
M16	24	1:3	Maleic Acid	PP	PDA

[1] (DMF:1,4-Dioxane)

[2] 1,3 – Propylenediamine

5.2.3 Experimental Procedure

Soaking tests were conducted in order to evaluate membrane stability in different solvents. The Ultem 1000 membrane and Ultem 1000 crosslinked membrane were cut to strips which were dried, weight and then immersed in different bottles containing toluene, ethyl acetate, n-hexane, isopropanol methyl ethyl ketone and methanol. The weight loss was determined for each sample after 5 days. A detailed study in order to evaluate the percentage of crosslinked polymer was performed using FTIR-ATR spectra (section 3.2.5).

Filtration experiments in order to characterize the membranes prepared were conducted according to the procedure outlined in section 2.2.4.

5.3 Results and Discussion

5.3.1 Polymer Characteristics

Table 5.2 shows the results of soaking tests conducted to evaluate the chemical and physical stability of ultem in several organic solvents. The results show a change in almost all cases, especially for methanol. The data shows that crosslinked membranes increased their chemical stability in organic solvents. The strip immersed in MEK curled indicating poor solvent affinity. In addition to solvent stability, this also highlights the importance of processibility in the choice of solvents in further processing steps.

Table 5.2 Soak test of Ultem membrane in organic solvents (error ±1,83%)

Solvent	(%) Polymer Weight Change	(%) Polymer Weight Change of Crosslinked membranes
Toluene	-1.50	4.05
Ethyl Acetate	-5.29	-1.54
Hexane	-3.06	0.00
Isopropanol	-4.12	2.72
Methyl Ethyl Ketone	0.00	1.44
Methanol	-17.60	0.69

Figure 5.2 shows FTIR-ATR for the original and crosslinked ultem membranes. The imide group is characterize by bands at around 1780 cm^{-1} (asymmetric stretch of C = O in the imide group), 1713 cm^{-1} (symmetric stretch of C = O in the imide group) and 1380 cm^{-1} (stretch of C – N in the imide group). [136] For the crosslinked membranes, the intensity of the imide C = O bonds are observed to be attenuated and replaced by amide C = O and C-N (amide groups) bonds indicating crosslinking according to the mechanism suggested by Tin et al. [136] (Figure 3.3).

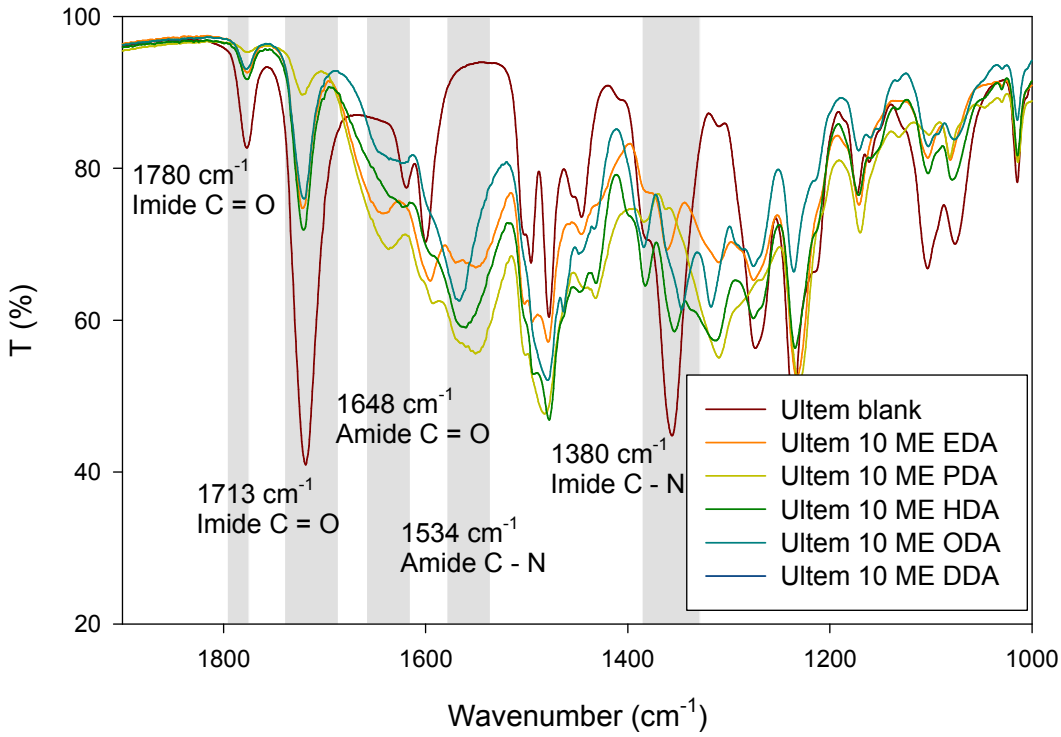

Figure 5.2 FTIR-ATR spectrum of Ultem membrane crosslinked with different crosslinkers 10 ME – EDA: ethylenediamine, PDA: 1,3-propylenediamine, HDA: 1,6-hexanediamine, ODA: 1,8-octanediamine, DDA: 1,12-dodecyldiamine.

The crosslinking results suggest that either the orientation of polymer chains in the membrane are non-uniform or that the electron poor regions (imide bonds) are lining up thus enabling crosslinking to occur. Also chain proximity might reduce crosslinking by hindering diffusion or larger species (ODA or DDA) or facilitate dissolution by allow smaller diamine (EDA or PDA) to freely permeate into the membrane.

The results show that PDA is the cross linker that induces the most changes in the bands that characterize cross-linking occurrences. Of the membranes tested, PDA crosslinked membrane was undissolved when immersed in DMF. This indicates that the chain lengths should be crucial in extending this technology to other polyimides.

5.3.2 Membrane Performance in Dead End Filtration

5.3.2.1 Non Chemically Modified Membranes

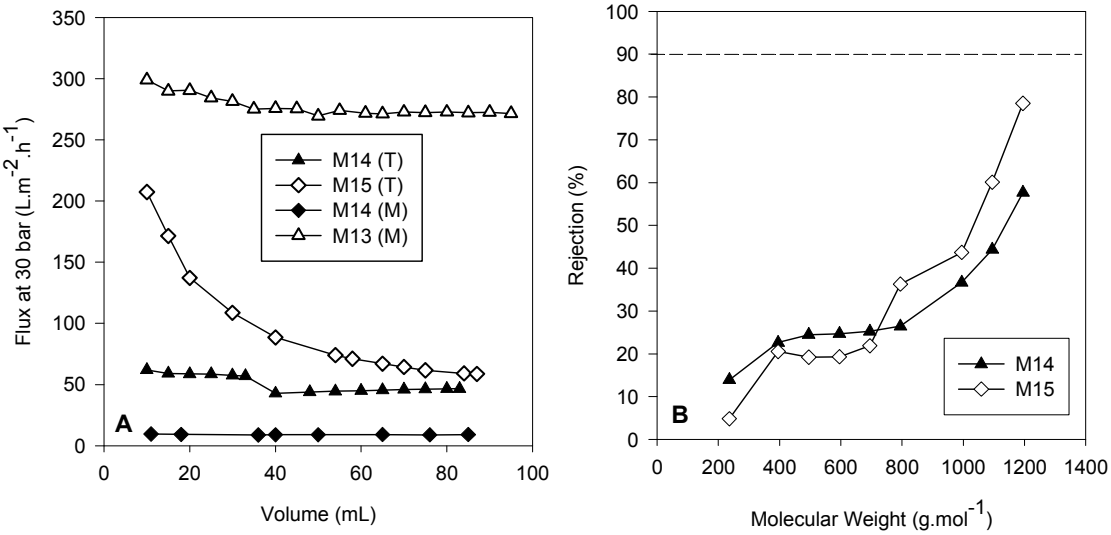

Figure 5.3 Toluene Flux (T) profile for membranes M13 and M14 and Methanol Flux (M) profile for membranes M13 and M12 (A) and MWCO curve in toluene for membranes M13 and M14 at 30 bar

Figure 5.3 shows the toluene flux for membranes M14 and M15 and methanol flux for membranes M14 and M13 (A) and MWCO curve for membranes M14 and M15 in toluene at 30 bar. Steady state was achieved after permeating 80 mL. The flux is lower for ultem membrane M14 for both solvents. This may be explained by the non-existence of maleic acid in dope solution which as been shown to decrease macrovoid formation [52]. The macrovoids were reported as a cause of membrane collapse when pressure is applied leading to a decrease in flux. [1] The observed MWCO of membranes was > 1000 $g.mol^{-1}$. No rejection of polysterene standard was observed for the all the membranes tested in methanol (MeOH). This could be due to dissolution of the polymer in methanol.

5.3.3 Membrane Performance in Cross-Flow Filtration

5.3.3.1 Chemically Modified Membranes

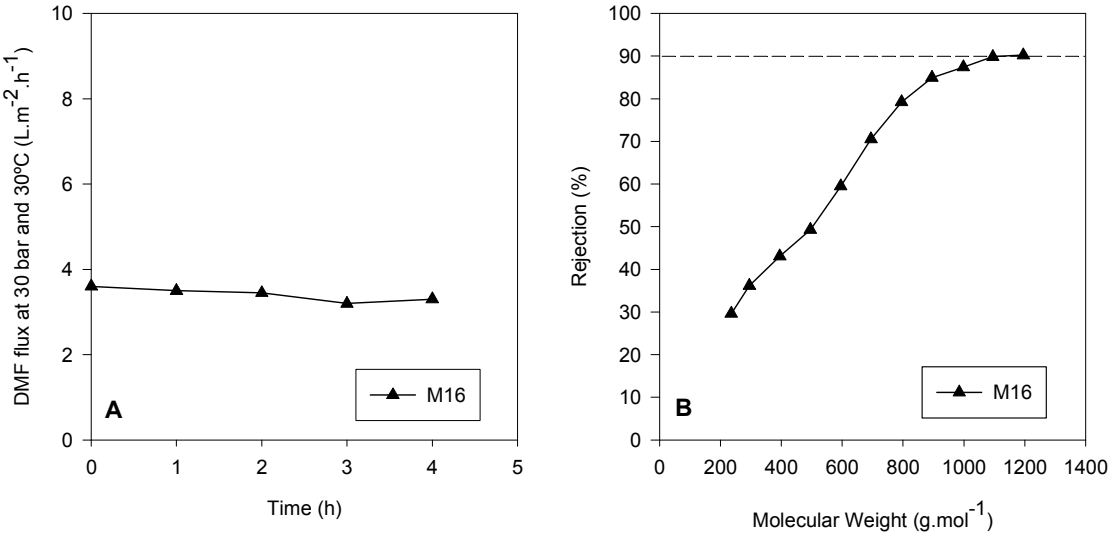

Figure 5.4 DMF Flux profile (A) and MWCO curve in DMF (B) at 30ºC and 30 bar of membrane M16

In Figure 5.4 is represented the flux (A) and MWCO curve (B) in DMF for membrane M16. The steady state was achieved after 4 hours with a very low flux. Comparing the flux values for ultem membranes M15 and M16 is observed a decreasing. This effect could be due to differences in solvent viscosity but also be attributed to increased chain rigidity in the crosslinked membrane [181]. Crosslinking was observed to improve the MWCO curve. The MWCO of membrane M16 is 1100 $g.mol^{-1}$.

The membrane demonstrated good stability under cross flow conditions. However, further work is required in order to optimize the flux for use in DMF.

5.4 Conclusions

Integrally skinned asymmetric membranes made of Ultem 1000 were prepared and tested in toluene to evaluate membrane performances. The resultant membranes showed a satisfactory flux however the rejection did not achieved 90%. Soak tests showed that the membrane was unstable in several solvents making it unstable for use without further treatment.

Crosslinking this membranes improved the stability with a MWCO about 1000 $g.mol^{-1}$. Membrane stability and FTIR-ATR confirms the crosslinking reaction. Crosslinking the polymer showed to improve its stability in all of the solvents tested.

Further development of the membrane will focus on improvement of MWCO and flux performances.

6 Nanofiltration Membrane Cascade Design

6.1 Introduction

Nanofiltration operations are becoming increasingly favoured over traditional processes especially for the treatment of industrial process effluents. Frank et al. [189] used a two step NF process to remove colour from an effluent stream and recycled the process water. This was installed to produce effluent of suitable quality for disposal via municipal wastewater treatment plants and was deemed economically viable. However, recovering of high-value products from industrial effluent not only reduces the environmental burden of the effluent, but also increases the overall yield of the manufacturing process.

Membrane cascades have been applied to several different separation problems [190-192] using different membranes, e.g. ultrafiltration (UF), nanofiltration (NF) and reverse osmosis (RO). The configuration for each of these membrane cascades was highly dependent on the purpose of the separation. [193]

In this chapter is briefly demonstrates the practical use of NF modelling in the design and optimization of an industrial membrane process. The development of polyimide OSN membranes with variable MWCO in the previous chapter is the basis for establishing if membrane fraction via a cascade system [155] is viable.

6.2 Process

The simulated process studied in the sections below is schematically represented in Figure 6.1. The process involves the separation of two compounds (500 $g.mol^{-1}$ and 1000 $g.mol^{-1}$). The solvent and solute are introduced in a mixing tank. The process stream allows two filtrations using different membranes as shown in Figure 6.1. The retentate from stage 1 enters as the feed to stage 2. The residue is collected in stream R.

Equation 6.1 and 6.2 demonstrates the mass balance made to the system with two stages of separation and equation 6.3 and 6.4 the fraction of compound i in each steam. Equation 6.5 and 6.6 gives the solute rejection in each membrane.

$$F_1 = P_1 + F_2 \qquad \textbf{Equation 6.1}$$

$$F_2 = P_2 + R \qquad \textbf{Equation 6.2}$$

$$x_{F1,i} \cdot F_1 = x_{P1,i} \cdot P_1 + x_{F2,i} \cdot F_2 \qquad \textbf{Equation 6.3}$$

$$x_{F2,i} \cdot F_2 = x_{P2,i} \cdot P_2 + x_{R,i} \cdot R \qquad \textbf{Equation 6.4}$$

$$R_{m1,i} = 1 - \frac{x_{P1,i}}{x_{F2,i}} \qquad \textbf{Equation 6.5}$$

$$R_{m2,i} = 1 - \frac{x_{R,i}}{x_{P2,i}} \qquad \textbf{Equation 6.6}$$

The purity of each compound in each steam can be calculated from the equation below:

$$Purity = \frac{x_{j,i}}{\sum_{i=1}^{n} x_{j,i}} \qquad \textbf{Equation 6.7}$$

The numerator corresponds to the fraction of the compound i in steam j and the denominator is the sum of all compounds (i=1, … ,n) in stream j.

The objective of using these two systems is to evaluate if the separation of the mixture is physically and economically viable to obtain a stream of compound A (500 $g.mol^{-1}$) with a high purity.

The membrane characteristics such like MWCO, flux, operative pressure and rejection for each compound are shown in Table 6.1. Membranes are assumed to have an area of 0,5 m^2. The membranes are used in the first and second stage of the process to recover MW compound with a higher and lower MW, respectively. A mixture of equal percentages of MW 500 $gmol^{-1}$ and MW 1000 $gmol^{-1}$ ($X_{F1,500}$ = 0,5 and $X_{F1,1000}$ = 0,5) is considered and a flux of 400 $L.h^{-1}$ in steam F1 is assumed. Solving the system represented in equation 6.1 and 6.2 and considering that P1 and P2 are the experimental fluxes of each membrane is possible to determinate feed 2 (F2) and the residue stream (R).

In Table 6.2 is shown the purity of permeate streams, P1 and P2, and the residue stream for both systems.

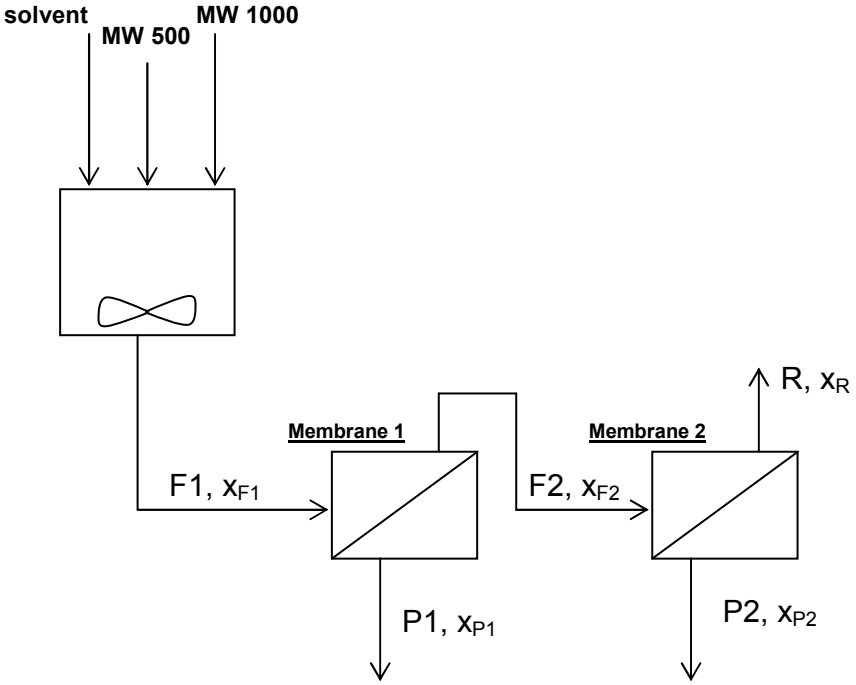

Figure 6.1 Schematic of membrane cascade system with two stages of separation (membrane 1 and membrane 2). Feed 1 (F1), Feed 2 (F2), Permeate 1 (P1), Permeate 2(P2) and Residue (R).

Table 6.1 Membrane characteristics applied in system 1 and 2.

System	***Membrane***		***Membrane Characteristics***				
			MWCO ($g.mol^{-1}$)	**Flux ($L.m^{-2}.h^{-1}$)**	**Operative Pressure (bar)**	**Rejection**	
						MW 500	***MW 1000***
1	1	M8	1000	205	20	0,7	0,9
	2	M5	500	50	10	0,9	0,97
2	1	M8	> 1200	110	5	0,54	0,79
	2	M6	350	80	20	0,97	1,00

Table 6.2 Streams purity for system 1 and 2.

System	***Stream Purity***					
	MW 500			**MW 1000**		
	Permeate 1	*Permeate 2*	*Residue*	*Permeate 1*	*Permeate 2*	*Residue*
1	0,74	0,76	0,48	0,26	0,24	0,52
2	0,67	1,00	0,48	0,33	0,00	0,52

For system one the purity in each stream does not achieve 90%. The higher purity is achieved for MW 500 $g.mol^{-1}$ compound in both membranes. Is evident that MW of 1000 $gmol^{-1}$ compound is practical totally rejected by both membranes which explains the low fraction and purities of it in permeate streams and high purity in residue stream. This is also shown by rejection results in Table 6.1 almost reaching 100% for this compound. Although the rejection presents good results the purities for the compounds in the permeate streams are not the desired so, the system may not be the appropriate one for the desired separation.

In system two the purity for MW 500 $g.mol^{-1}$ compound is decreased in the first permeate but improved in the second permeate stream achieving 100%. Similarly to system one the higher purity in both streams is for MW 500 $g.mol^{-1}$ compound. The compound with a MW 1000 $g.mol^{-1}$ has a higher purity in the residue owing to it partial or total exclusion for M8 and M6, respectively. The poor separation of solutes in this simple model indicates that in order for good separation and efficient use of membranes, membranes with a sharpe separation must be further develop.

6.3 Conclusions

The present chapter allowed showing the possibility to develop a membrane cascade system with the developed membranes from section 3.2.2. The resulting systems showed different performances. Results from system two revealed a high purity for compound with a MW 500 $g.mol^{-1}$ however at the expense of wasting too much solvent.

It was possible to extend developed polyimide membranes application in the OSN range in the separation of high MW compounds (500 $g.mol^{-1}$ and 1000 $g.mol^{-1}$) enabling the fractionation of molecules in a membrane cascade type system [155] but there is still more work to be done in the field to improve membrane fabrication for the process to be feasible.

7 Conclusion and Future Work

In this work we have demonstrated the formation of OSN membranes using polyimides. Improve chemical stability has been achieved through crosslinking of the various polyimides using a chemical crosslinking strategy. Further, the variation of the dope solution and pressure has enabled control over the MWCO thereby extrending the potencial application of OSN for P84 membranes. The ease of preparation trought variation of the dope composition makes this route of membrane tailoring highly suitable for scale up.

Matrimid 5218 and Ultem 1000 have shown good stability in harsh environments when crosslinked. However this was achieved at the expense of flux. The MWCO curves of investigated crosslinked matrimid membranes showed a trend to go up into UF range opening a new opportunity in this field. Crosslinked Ultem 1000 membrane has shown a MWCO in the NF range.

In conclusion, a better understanding of flux and the factors that influence it in these particular membranes would lead to a wider range of options for these novel membranes. The MWCO of these membranes also need to be improved. Many opportunities exist for the extension of these PI and PEI in the organic solvent nanofiltration or ultrafiltration range.

8 References

1. Mulder, M., *Basic Principles of Membrane Technology*, 2nd ed., Kluwer Academic Publishers, Netherlands, 1996.
2. Mulder, M.H.V., *Energy Requirements in Membrane Separation Processes* in: Crespo, J.G. and Böddeker, *Membrane Processes in Separation and Purification*, NATO ASI Series, K.W., Kluwer Academic Publishers, 1994.
3. Mulder, M.H.V., *The use of membrane processes in environmental problems, an introduction* in: Crespo, J.G. and Böddeker, *Membrane Processes in Separation and Purification*, NATO ASI Series, K.W., Kluwer Academic Publishers, 1994.
4. White, L.S., Polyimide membranes for hyperfiltration recovery of aromatic solvents, US 6,180,008, 2001.
5. Linder, C., Nemas, M., Perry, M. and Katraro, Silicon derived solvent stable membranes, US 5,265,734, 1993.
6. Van der Bruggen, B., Schaep, J., Wilms, D. and Vandecasteele, C., Comparison of models to describe the maximal retention of organic molecules in nanofiltration, *Sep.Sci.Tech.*, 35 (2000) 169.
7. Peeva, L.G., Gibbins, E., Luthra, S.S., White, L.S., Stateva, R.P. and Livingston, A.G., Effect of concentration polarisation and osmotic pressure on flux in organic solvent nanofiltration, *J.Membr.Sci.*, 236 (2004) 121.
8. Van der Bruggen, B. and Vandecasteele, C., Modelling of retentation of uncharged molecules with nanofiltration, *Water Research*, 36 (2002) 1360.
9. Bhanushali, D. and Bhattacharyya, D., Advances in solvent-resistant nanofiltration membranes - Experimental observations and applications, *Adv.Memb.Tech.*, 984 (2003) 159.
10. Geens, J., Boussu, K., Vandecasteele, C. and Bruggen, B., Modelling of solute transport in non-aqueous nanofiltration, *J.Membr.Sci.*, 281 (2006) 139.
11. Bhanushali, D., Kloos, S., Kurth, C. and Bhattacharyya, D., Performance of solvent-resistant membranes for non-aqueous systems: solvent permeation results and modeling, *J.Membr.Sci.*, 189 (2001) 1.
12. See Toh, Y.H., Lim, F.W. and Livingston, A.G., Polymeric membranes for nanofiltration in polar aprotic solvents, *J.Membr.Sci.*, 3 (2007) 301.
13. Bhanushali, D., Kloos, S. and Bhattacharyya, D., Solute transport in solvent-resistant nanofiltration membranes for non-aqueous systems: experimental results and the role of solute-solvent coupling, *J.Membr.Sci.*, 208 (2002) 343.
14. Silva, P., Han, S. and Livingston, A.G., Solvent transport in organic solvent nanofiltration membranes, *J.Membr.Sci.*, 262 (2005) 49.
15. Kita, H., Inada, T., Tanaka, K. and Okamoto, K., Effect of photocrosslinking on permeability and permselectivity of gases through benzophenone - containing polyimide, *J.Membr.Sci.*, 87 (1994) 139.
16. Hayes, R.A., Polyimide gas separation membranes, US 4,717,393, 1988.
17. Baker, R.W., *Membrane Technology and Applications*, 2nd ed., John Wiley & Sons Ltd., England, 2004.
18. Gunther R., Engineering for high pressure reverse osmosis, *J.Membr.Sci.*, 121 (1996) 95.
19. Ho, W.S.W. and Sirkar, K.K., *Membrane Handook*, Van Nostrand Reinhold, New York, 1992.
20. J.L.Maubois, G.Mocquot and L.Vassal, Preparation of cheese using ultrafiltration, 4,205,090, 1980.
21. Beerlage, M.A.M., Polyimide ultrafiltration membranes for non-aqueous systems,PhD Thesis, University of Twente Enschede, 1994.
22. Kolega, M., Grohmann, G.S., Chiew, R.F. and Day, A.W., Disinfection and clarification of treated sewage by advanced microfiltration, *Wat.Sci.Tech.*, 23 (1991) 1609.
23. Ferry, J.D., Ultrafilter membranes and ultrafiltration, *Chem.Rev.*, 18 (1936) 373.
24. Kesting, R.E., Concerning the microstructure of dry-RO membranes, *J.Appl.Polym.Sci.*, 17 (1973) 1771.

25. Strathmann, H., *Membranes and Membrane Separation Processes* in: *ULLMANN'S - Processes and Process Engineering*, Wiley - VCH Verlag GmbH & Co. KGaA, Federal Republic of Germany, 2004.
26. Strathmann, H., Koch, K., Amar, P. and Baker, R.W., The formation mechanism of asymmetric membranes, *Desalination*, 16 (1975) 179.
27. Lee, H.J., Jung, B., Kang, Y.S. and Lee, H., Phase separation of polymer casting solution by nonsolvent vapor, *J.Membr.Sci.*, 245 (2004) 103.
28. Witte, P., Dijkstra, P.J., Berg, J.W.A. and Feijen, J., Phase separation processes in polymer solutions in relation to membrane formation, *J.Membr.Sci.*, 117 (1996) 1.
29. Reuvers, A.J., Berg, J.W.A. and Smolders, C.A., Formation of membranes by means of immersion precipitation: Part I. A model to describe mass transfer during immersion precipitation, *J.Membr.Sci.*, 34 (1987) 45.
30. Strathmann, H., Scheible, P. and Baker, R.W., A rationale for the preparation of Loeb-Sourirajan - type cellulose acetate membranes, *J.Appl.Polym.Sci.*, 15 (1971) 811.
31. Wijmans, J.G., Baaij, J.P.B. and Smolders, C.A., The mechanism of formation of microporous or skinned membranes produced by immersion precipitation, *J.Membr.Sci.*, 14 (1983) 263.
32. Sariban, A. and Binder, K., Spinodal decomposition of polymer mixtures - A Monte-Carlo Simulation, *Macromolecules*, 24 (1991) 578.
33. Koros, W.J. and Pinnau, I., *Membrane Formation for Gas Separation Processes* in: D.R.Paul and Y.P.Yampol'skii, *Polymeric Gas Separation Membranes*, CRC Press, Boca Raton, FL, 1994.
34. Pinnau, I. and Koros, W.J., A qualitative skin layer formation mechanism for membranes made by dry/wet phase inversion, *J.Polym.Sci., Polym.Phys.*, 31 (1993) 419.
35. Altena, F.W. and Smolders, C.A., Calculation of liquid-liquid phase separation in a ternary system of a polymer in a mixture of solvent and non-solvent, *Macromolecules*, 15 (1982) 1491.
36. Yilmaz, L. and McHugh, A.J., Analysis of nonsolvent-solvent-polymer phase diagrams and their relevance to membrane formation modelling, *J.Appl.Polym.Sci.*, 31 (1986) 997.
37. Mulder, M., A rationale for the preparation of asymmetric pervaporation membranes, *J.Appl.Polym.Sci.*, 30 (1985) 2805.
38. Kim, J.E.Y., Lee, H.K., Baik, K.J. and Kim, S.C., Liquid-liquid phase separation in Polysulfone/Solvent/Water systems, *J.Appl.Polym.Sci.*, 65 (1997) 2643.
39. Cohen, C., Tanny, G.B. and Prager, S., Diffusion controlled formation of porous structures in ternary polymer systems, *J.Polym.Sci., Polym.Phys.*, 17 (1979) 477.
40. Cheng, L.P., Soh, Y.S., Dwan, A.H. and Gryte, C.C., An improved model for mass-transfer during the formation of polymeric membranes by the immersion-precipitation process, *J.Polym.Sci., Polym.Phys.*, 32 (1994) 1413.
41. Kim, Y.D., Kim, J.Y., Lee, H.K. and Kim, S.C., A new modeling of asymmetric membrane formation in rapid mass transfer system, *J.Membr.Sci.*, 190 (2001) 69.
42. Kimmerle, K. and Strathmann, H., Analysis of the structure-determining process of phase inversion membranes, *Desalination*, 79 (1990) 283.
43. Broens, L., Koenhen, D.M. and Smolders, C.A., On the mechanism of formation of asymmetric ultra and hyper-filtration membranes, *Desalination*, 22 (1977) 205.
44. Reuvers, A.J. and Smolders, C.A., Formation of membranes by means of immersion precipitation: Part II. The mechanism of formation of membranes prepared from the system cellulose acetate-acetone-water, *J.Membr.Sci.*, 34 (1987) 67.
45. Panar, M., Hoehn, H.H. and Hebert, R.R., The nature of asymetry in reverse osmosis membranes, *Macromolecules*, 6 (1973) 777.
46. Kamide, K. and Manabe, S.I., Role of microphase separation phenomena in the formation of porous polymeric membranes, *ACS Symp.Ser.*, 269 (1985) 197.
47. Kunst, B., Skevin, D. and Dezelic, G., A light-scattering and membrane formation study on concentrated cellulose acetate solutions, *J.Appl.Polym.Sci.*, 20 (1976) 1339.
48. Kunst, B. and Vajnaht, Z., On the structure of concentrated cellulose acetate solutions, *J.Appl.Polym.Sci.*, 21 (1977) 2505.
49. Ray, R.J., Krantz, W.B. and Sani, R.L., Linear stability theory model for finger formation in asymmetric membranes, *J.Membr.Sci.*, 23 (1985) 155.

50. Boom, R.M., Wienk, I.M., Boomgaard, Th. and Smolders, C.A., Microstructures in phase inversion membranes. Part 2: The role of a polymeric additive, *J.Membr.Sci.*, 73 (1992) 277.
51. Wienk, I.M., Boomgaard, Th. and Smolders, C.A., The formation of nodular structures in the top layer of ultrafiltration membranes, *J.Appl.Polym.Sci.*, 53 (1994) 1011.
52. Wienk, I.M., Boom, R.M., Beerlage, M.A.M., Bulte, A.M.W., Smolders, C.A. and Strathmann, H., Recent advances in the formation of phase inversion membranes made from amorphous or semi-crystalline polymers, *J.Membr.Sci.*, 113 (1996) 361.
53. See Toh, Y.H., Ferreira, F.C. and Livingston, A.G., The influence of membrane formation parameters on the functional performance of organic solvent nanofiltration membranes, *J.Membr.Sci.*, 299 (2007) 236.
54. White, L.S., Transport properties of a polyimide solvent resistant nanofiltration membrane, *J.Membr.Sci.*, 205 (2002) 191.
55. Kesting, R.E., The four tiers os strucutre in integrally skinned phase inversion membranes and their relevance to the various separation regimes, *J.Appl.Polym.Sci.*, 41 (1990) 2739.
56. Smolders, C.A., Reuvers, A.J., Boom, R.M. and Wienk, I.M., Microstructures in phase inversion membranes. Part 1: Formation of macrovoids, *J.Membr.Sci.*, 73 (1992) 259.
57. Kamusewitz, H., Tiedemann, M.S., Keller, M. and Paul, D., Characterization of polymeric membranes by means of scanning force microscope (SFM) in comparison to results of scanning electron microscopy (SEM), *Surface Science*, 377-379 (2007) 1076.
58. Tiedemann, M.S. and Paul, D., Improved preparation of membrane surfaces for fields-emission scanning electron microscopy, *J.Membr.Sci.*, 187 (2001) 85.
59. Strathmann, H. and Koch, K., The formation mechanism of phase inversion membranes, *Desalination*, 21 (1977) 241.
60. Lee, K.W., Seo, B.K., Nam, S.T. and Han, M.J., Trade-off between thermodynamic enhancement and kinetic hindrance during phase inversion in the preparation of polysulfone membranes, *Desalination*, 159 (2003) 289.
61. Musale, D.A., Kumar, A. and Pleizier, G., Formation and characterization of poly(acrylonitrile)/Chitosan composite ultrafiltration membranes, *J.Membr.Sci.*, 154 (1999) 163.
62. Deshmukh, S.P. and Li, K., Effect of ethanol composition in water coagulation bath on morphology of PVDF hollow fibre membranes, *J.Membr.Sci.*, 150 (1998) 75.
63. Kobayashi, T., Ono, M., Shibata, M. and Fujii, N., Cutoff performance of Escherichia coli by charged and noncharged polyacrylonitrile ultrafiltration membranes, *J.Membr.Sci.*, 140 (1998) 1.
64. Li, L., Xiao, Z., Tan, S., Pu, L. and Zhang, Z., Composite PDMS membrane with high flux for the separation of organics from water by pervaporation, *J.Membr.Sci.*, 243 (2004) 177.
65. Song, C., Wang, T., Wang, X., Qiu, J., and Cao, Y., Preparation and gas separation properties of poly(furfuryl alcohol)-based C/CMS composite membranes, *Sep.Purif.Tech.*, In press.
66. Rao, A.P., Joshi, S.V., Trivedi, J.J., Devmurari, C.V. and Shah, V.J., Structure-performance correlation of polyamide thin film composite membranes: effect of coating conditions on film formation, *J.Membr.Sci.*, 211 (2003) 13.
67. Bruggen, B., Jansen, J.C., Figoli, A., Geens, J., Boussu, K. and Drioli, E., Characteristics and performance of a "universal" membrane suitable for gas separation, pervaporation and nanofiltration applications, *J.Phys.Chem.B*, 110 (2006) 13799.
68. Vankelecom I.F.J., Smet, K.D., Gevers, L.E.M., Livingston, A.G., Nair, D., Aerts, S., Kuypers, S. and Jacobs, P.A., Physio-chemical interpretation of the SRNF transport mechanism for solvents through dense silicone membranes, *J.Membr.Sci.*, 231 (2004) 99.
69. Pasternak, M., Membrane process fro treating a mixture containing dewaxed oil and dewaxing solvent, US 5,093,002, 1992.
70. Whu, J.A., Baltzis, B.C. and Sirkar, K.K., Nanofiltration studies of larger organic microsolutes in methanol solutions, *J.Membr.Sci.*, 170 (2000) 159.
71. See Toh, Y.H., *Organic Solvent Nanofiltration: Applications and Novel Membrane Development* in: Imperial College London, *Chemical Engineering Departamental Symposium*, 2007.

72. Gevers, L.E.M., Meyen, G., Smet, K.D., Velde, P., Prez, F., Vankelecom I.F.J. and Jacobs, P.A., Physico-chemical interpretation of the SRNF transport mechanism for solutes through dense silicone membranes, *J.Membr.Sci.*, 274 (2006) 173.
73. Cadotte, J., Interfacially synthesized reverse osmosis membrane, US 4,277,344, 1981.
74. Arthur, S.D., Multilayer reverse osmosis membrane of polyamide-urea, US 5,019,264, 1991.
75. Stafie, N., Stamatialis, D.F. and Wessling, M., Insight into the transport of hexane-solute systems through tailor made composite membranes, *J.Membr.Sci.*, 228 (2004) 103.
76. Nogami, N., Chowdhury, G. and Matsuura, T., Preparation and performance testing of sulfonated poly(phenylene oxide) based composite membranes for nanofiltration, *J.Appl.Polym.Sci.*, 91 (2004) 2624.
77. Wang, Y.C., Li, C.L., Chang, P.F., Fan, S.C., Lee, K.R. and Lai, J.Y., Separation of water-acetic acid mixture by pervaporation through plasma-treated asymmetric poly(4-methyl-1-pentene) membrane and dip-coated with polyacrylic acid, *J.Membr.Sci.*, 208 (2002) 3.
78. Wang, D.M., Lin, F.C., Chiang, J.C. and Lai, J.Y., Control of the porosity of asymmetric TPX membranes, *J.Membr.Sci.*, 141 (1998) 1.
79. Daisley, G.R., Dastgir, M.G., Ferreira, F.C., Peeva, L.G. and Livingston, A.G., Application of thin film composite membranes to the membrane aromatic recovery system, *J.Membr.Sci.*, 268 (2006) 20.
80. Russell, S.P. and Weinkauf, D.H., Vapor sorption in plasma polymerized vinyl acetate and methyl methacrylate thin films, *Polymer*, 42 (2001) 2827.
81. Zhang, C., Wyatt, J. and Weinkauf, D.H., Carbon dioxide sorption in conventional and plasma polymerized methyl methacrylate thin films, *Polymer*, 45 (2004) 7665.
82. Chan, C.M., Ko, T.M. and Hiraoka, H., Polymer surface modification by plasmas and photons, *Surf.Sci.Rep.*, 24 (1996) 1.
83. Ohya, H., Okazaki, I., Aihara, M., Tanisho, S. and Negishi, Y., Study on molecular weight cut-off performance of asymmetric aromatic polyimide membrane, *J.Membr.Sci.*, 123 (1997) 143.
84. Okazaki, I., Ohya, H., Semenova, S.I., Aihara, M. and Negishi, Y., Study on molecular weight cut-off performance of asymmetric aromatic polyimide membrane "Effect of the additive agents", *J.Membr.Sci.*, 141 (1998) 277.
85. Sterescu, D.M., Bolhuis-Versteeg, L., Vegt, N.F.A., Stamatialis, D.F. and Wessling, M., Novel gas separation membranes containing covalently bonded fullerenes, *Macromolecular Rapid Communications*, 25 (2004) 1674.
86. Jimenez, D.B.M., Narbaitz, R.M., Matsuura, T., Chowdhury, G., Pleizier, G. and Santerre, J.P., Influence of processing conditions on the properties of ultrafiltration membranes, *J.Membr.Sci.*, 231 (2004) 209.
87. Whu J.A., Modelling of nanofiltration - assisted organic synthesis, *J.Membr.Sci.*, 163 (1999) 319.
88. Scott K., *Handbook of Industrial Membranes*, 1st ed., 1995.
89. Vankelecom, I.F.J., Polymeric membranes in catalytic reactors, *Chem.Rev.*, 102 (2002) 3779.
90. Koch Membrane Systems, Inc, http://www.kochmembrane.com/index.html, 2006.
91. Bruggen, B., Influence of organic solvents on the performance of polymeric nanofiltration membranes, *Sep.Sci.Tech.*, 37 (2002) 783.
92. Machado, D., Hasson, D. and Semiat, R., Effect of solvent properties on permeate flow through nanofiltration membranes. Part I: Investigation of parameters affecting solvent flux, *J.Membr.Sci.*, 163 (1999) 93.
93. Machado, D., Hasson, D. and Semiat, R., Effect of solvent properties on permeate flow through nanofiltration membranes. Part II: Transport Model, *J.Membr.Sci.*, 166 (2000) 63.
94. W.R.Grace & Co. - Conn., http://www.grace.com/, 2006.
95. Scarpello, J.T., Nair, D., Santos, L.M.F., White, L.S. and Livingston, A.G., The separation of homogeneous organometallic catalysts using solvent resistant nanofiltration, *J.Membr.Sci.*, 203 (2002) 71.
96. White, L.S. and Nitsch, A.R., Solvent recovery from lube oil filtrates with a polyimide membrane, *J.Membr.Sci.*, 179 (2000) 267.

97. Gibbins, E., D'Antonio, M., Nair, D., White, L.S., Santos, L.M.F., Vankelecom, I.F.J. and Livingston, A.G., Observations on solvent flux and solute rejection across solvent resistant nanofiltration membranes, *Desalination*, 147 (2002) 307.
98. Nair, D., Luthra, S.S., Scarpello J.T., White, L.S., Santos, L.M.F. and Livingston, A.G., Homogeneous catalyst separation and re-use through nanofiltration of organic solvents, *Desalination*, 147 (2002) 301.
99. Nair, D., Scarpello, J.T., Vankelecom, I.F.J., Santos, L.M.F., White, L.S., Kloetzing, R.J., Welton, T. and Livingston, A.G., Increased catalytic productivity for nanofiltration-coupled Heck reactions using highly stable catalyst systems, *Green Chemistry*, 4 (2002) 319.
100. Cuperus, F.P. and Smolders, C.A., Characterization of UF Membranes - Membrane characteristics and characterization techniques, *Advances in Colloid and Interface Science*, 34 (1991) 135.
101. Barzin, J., Madaeni, S.S., Mirzadeh, H. and Mehrabzadeh, M., Effect of Polyvinylpyrrolidone on morphology and performance of hemodialysis membranes prepared from polyether sulfone, *J.Appl.Polym.Sci.*, 92 (2004) 3804.
102. Razdan, U., Joshi, S.V. and Shah, V.J., Novel membrane processes for separation of organics, *Curr.Sci.India*, 85 (2003) 761.
103. Boussu, K., Zhang, Y., Cocquyt, J., Meeren, P., Volodin, A., Haesendonck, C.V., Martens, J.A. and Bruggen, B., Characterization of polymeric nanofiltration membranes for systematic analysis of membrane performance, *J.Membr.Sci.*, 278 (2006) 418.
104. Tarleton, E.S., Robinson, J.P., Millington, C.R. and Nijmeijer, A., Non-aqueous nanofiltration: solute rejection in low-polarity binary systems, *J.Membr.Sci.*, 252 (2005) 123.
105. Yang, X.J., Livingston, A.G. and Santos, L.M.F., Experimental observations of nanofiltration with organic solvents, *J.Membr.Sci.*, 190 (2001) 45.
106. See Toh, Y.H., Loh, X.X., K.Li, Bismarck, A. and Livingston, A.G., In search of a standard method for the caracterisation of organic solvent nanofiltration membranes, *J.Membr.Sci.*, 291 (2007) 120.
107. Shuey, H.F. and Wan, W., Asymmetric polyimide reverse osmosis membrane, method for preparation of same and use thereof for organic liquid separations, US 4,532,041, 1985.
108. Qiao, X., Chung, T.S. and Pramoda, K.P., Fabrication and characterization of BTDA-TDI/MDI (P84) co-polyimide membranes for the pervaporation dehydration of isopropanol, *J.Membr.Sci.*, 264 (2005) 176.
109. Ohya, H., Kudryavtsev, V.V. and Semenova, S.I., *Polyimide Membranes - Applications, Fabrications and Properties*, Gordon and Breach Publishers, 1996.
110. Koros, W.J., Fleming, G.K., Jordan, S.M., Kim, T.H. and Hoehn, H.H., Polymeric membrane materials for solution-diffusion based permeation separations, *Prog.Polym.Sci.*, 13 (1988) 339.
111. Tanihara, N., Tanaka, K., Kita, H. and Okamoto, K., Vapor-permeation separation of water-ethanol mixtures by asymmetric polyimide hollowfiber membrane modules, *J.Chem.Eng.Jpn.*, 25 (1992) 388.
112. Okamoto, K., Tanihara, N., Watanabe, H., Tanaka, K., Kita, H., Nakamura, A., Kusuki, Y. and Nakagawa, K., Vapor permeation and pervaporation separation of water–ethanol mixtures through polyimide membranes, *J.Membr.Sci.*, 68 (1992) 53.
113. Yanagishita, H., Maejima, C., Kitamoto, D. and Nakane, T., Preparation of asymmetric polyimide membrane for water/ethanol separation in pervaporation by phase inversion process, *J.Membr.Sci.*, 86 (1994) 231.
114. Kim, J.H., Lee, K.H. and Kim, S.Y., Pervaporation separation of water from ethanol through polyimide composite membranes, *J.Membr.Sci.*, 169 (2000) 81.
115. Yanagishita, H., Kitamoto, D., Haraya, K., Nakane, T., Okada, T., Mastyda, H., Idemoto, I. and Koura, N., Separation performance of polyimide composite membrane prepared by dip coating process , *J.Membr.Sci.*, 188 (2001) 165.
116. Barsema, J.N., Kapantaidakis, G.C., Vegt, N.F.A., Koops, G.H. and Wessling, M., Preparation and characterization of highly selective dense and hollow fiber asymmetric membranes based on BTDA-TDI/MDI co-polyimide, *J.Membr.Sci.*, 216 (2003) 195.
117. Iwama, A. and Kanuse, Y., New polyimide ultrafiltration membranes for organic use, *J.Membr.Sci.*, 11 (1982) 297.

118. Vu, Q. and Koros, W.J., High pressure CO2/CH4 separation using carbon molecular sieve hollow fiber membranes, *Ind.Eng.Chem.Res.*, 41 (2002) 367.
119. Bos, A., Punt, I.G.M., Wessling, M. and Strathmann, H., Plasticization-resistant glassy polyimide membranes for CO2/CH4 separations, *Sep.Purif.Tech.*, 14 (1998) 27.
120. White, L.S., Wang, I.F. and Minhas, B.S., Polyimide membrane for separation of solvents from lube oil, US 5,264,166, 1993.
121. Eastmond, G.C., Paprotny, J. and Webster, I., Isomeric poly(ether imide)s: synthesis, thermal properties and permeabilities, *Polymer*, 34 (1993) 2865.
122. Chen, H.L., You, J.W. and Porter, R.S., Intermolecular interaction and conformation in poly(ether ether ketone)/poly(ether imide) blends- an infrared spectroscopic investigation, *J.Polym.Res.*, 3 (1996) 151.
123. Krause, E., Yang, G.M. and Sessler, G.M., Charge Dynamics and Morphology of Ultem 1000 and Ultem 5000 PEI Grade Films, *Polymer International*, 46 (1998) 59.
124. Xu, Z.K., Shen, L.Q., Yang, Q., Liu, F., Wang, S.Y. and Xu, Y.Y., Ultrafiltration hollow fiber membranes from poly(ether imide): preparation, morphologies and properties, *J.Membr.Sci.*, 223 (2003) 105.
125. Peinemann, K.V., Maggioni, J.F. and Nunes, S.P., Poly(ether imide) membranes obtained from solution in cosolvent mixtures, *Polymer*, 39 (1998) 3411.
126. Peinemann, K.V., Verfahren zur Herstellung einer integral-asymmetrischen Membran, DE 3420373, 1985.
127. Tao, C.T. and Young, T.H., Polyetherimide membrane formation by the cononsolvent system and its biocompatibility of MG63 cell line, *J.Membr.Sci.*, 269 (2006) 66.
128. Kim, I.C., Yoon, H.G. and Lee, K.H., Formation of integrally skinned asymmetric polyetherimide nanofiltration membranes by phase inversion process, *J.Appl.Polym.Sci.*, 84 (2002) 1300.
129. Rautenbach, R. and Albrecht, R., *Membrane Processes*, Wiley, Chichester, 1989.
130. Uragami, T., Tamura, M. and Sugihara, M., Synthesis and Permeability of Special Polymer Membranes, *J.Membr.Sci.*, 4 (1979) 305.
131. Reddy, K.K., Kawakatsu, T., Snape, J.B. and Nakajima, M., Membrane concentration and separation of L-aspartic acid and L-phenylalanine derivatives in organic solvents, *Sep.Sci.Tech.*, 31 (1996) 1161.
132. Visvanathan, C., Removal of THMP by nanofiltration: effects of interfering parameters, *Water Research*, 32 (2007) 3527.
133. See Toh, Y. H., Green asymmetric molecule manufacture using organic solvent nanofiltration and homogeneous catalyst recycle, Department of Chemical Engineering and Chemical Technology, Imperial College - London, London SW7 2BY, UK, 2005.
134. Tsuru, T., Miyawaki, M., Kondo, H., Yoshioka, T. and Asaeda, M., Inorganic porous membranes for nanofiltration of nonaqueous solutions, *Sep.Purif.Tech.*, 32 (2003) 105.
135. Kim, J.H., Koros, W.J. and Paul, D.R., Effects of CO2 exposure and physical aging on the gas permeability of thin 6FDA-based polyimide membranes - Part 2: With crosslinking, *J.Membr.Sci.*, 282 (2006) 32.
136. Tin, P.S., Chung, T.S., Liu, Y., Wang, R., Liu, S.L. and Pramoda, K.P., Effects of cross-linking modification on gas separation performance of matrimid membranes, *J.Membr.Sci.*, 225 (2003) 77.
137. Chung, T.S., Shao, L. and Tin, P.S., Surface modification of polyimide membranes by diamines for H-2 and CO2 separation, *Macromolecular Rapid Communications*, 27 (2006) 998.
138. Scaiano, J.C., Becknell, A.F. and Small, R.D., Photochemistry of A Benzophenone containing Bisimide: A Model for Inherently Photosensitive Polyimides, *Journal of Photochemistry and Photobiology*, Chemistry, 44 (1988) 99.
139. Liu, Y., Wang, R. and Chung, T.S., Chemical cross-linking modification of polyimide membranes for gas separation, *J.Membr.Sci.*, 189 (2001) 231.
140. Lin, A.A., Sastri, V.R., Tesoro, G., Reiser, A. and Eachus, R., On the cross-linking mechanism of Benzophenone - containing polyimides, *Macromolecules*, 21 (1998) 1165.
141. Bickela, C.S. and Koros, W.J., Improvement of CO2/CH4 separation characteristics of polyimides by chemical crosslinking, *J.Membr.Sci.*, 155 (1999) 145.
142. Park, H.B., Lee, C.H., Sohn, J.Y., Lee, Y.M., Freeman, B.D. and Kim, H.J., Effect of crosslinked chain length in sulfonated polyimide membranes on water sorption, proton conduction, and methanol permeation properties, *J.Membr.Sci.*, 285 (2006) 432.

143. Wijmans, J.G. and Baker, R.W., The solution-diffusion model: a review, *J.Membr.Sci.*, 107 (1995) 1.
144. Koops G.H., Separation of linear hydrocarbons and carboxylic acids from ethanol and hexane solutions by reverse osmosis, *J.Membr.Sci.*, 189 (2001) 241.
145. Bhattacharya, S. and Hwang, S.T., Concentration polarization, separation factor, Peclet number in membrane processes, *J.Membr.Sci.*, 132 (1997) 73.
146. Sourirajan, S. and Matsuura, T., *Reverse Osmosis/Ultrafiltration Process Principles*, National Research Council, Ottawa, Canada, 1985.
147. Nakao, S.I., Models of membrane transport phenomena and their applications for ultrafiltration data, *J.Chem.Eng.Jpn.*, 15 (1982) 200.
148. Sahimi, M., *Flow and Transport in Porous Media and Fractured Rock: from classical methods to modern approaches*, Wiley-VCH Verlag GmbH, 1995.
149. Robinson, J.P., Tarleton, E.S., Millington, C.R. and Nijmeijer, A., Solvent flux through dense polymeric nanofiltration membranes, *J.Membr.Sci.*, 230 (2004) 29.
150. Sinnott, R.K., Coulson, J.M. and Richardson, J.F., *Chemical Engineering: Particle Technology and Separation Processes*, Butterworth-Heinemann, 2002.
151. Svarovsky, L., *Solid-Liquid Separation*, 4th ed., Butterworth-Heinemann, 2001.
152. Foley, G., A review of factors affecting filter cake properties in dead-end microfiltration of microbial suspensions, *J.Membr.Sci.*, 274 (2006) 38.
153. Lonsdale H.K., Transport properties of cellulose acetate membranes to selected solutes, *J.Appl.Polym.Sci.*, 9 (1965) 1341.
154. Williams M.E., Separation of organic pollutants by reverse osmosis and nanofiltration membranes: mathematical models and experimental verification, *Ind.Eng.Chem.Res.*, 38 (1999) 3683.
155. Lin, J.C.T. and Livingston, A.G., Nanofiltration membrane cascade for continous solvent exchange, *Chem.Eng.Sci.*, 62 (2007) 2728.
156. Okazaki, I., Ohya, H., Semenova, S.I., Kikuchi, S., Aihara, M. and Negishi, Y., Nanotechnological method to control the molecular weight cut-off and/or pore diameter of organic-inorganic composite membrane, *J.Membr.Sci.*, 141 (1998) 65.
157. Imai Y., Watanabe A., Masuhara E. and Imai Y., Structure-biocompatibility relationship of condensation polymers, *J.Biomed.Mater.Res.*, 17 (1983) 905.
158. Richardson R.R.Jr, Miller J.A. and Reichert W.M., Polyimide as biomaterials: Prelinary biocompatibility testing, *Biomaterials*, 14 (1993) 627.
159. Stiglitz T. and Meyer J.U., Implantable microsystems. Polyimide based neurotheses for interfacing nerves, *Med.Device Technol.*, 10 (1999) 28.
160. Pinnau, H.I. and Wind, B.J., Process for increasing the selectivity os asymmetric membranes, US 5,007,944, 1991.
161. Kneifel, K. and Peinemann, K.V., Preparation of hollow fiber membranes from polyetherimide for gas separation, *J.Membr.Sci.*, 65 (1992) 295.
162. Kim, I.C. and Lee, K.H., Effect of poly(etylene glycol) 200 on the formation of a polyetherimide asymmetric membrane and its performance in aqueous solvent mixture permeation, *J.Membr.Sci.*, 230 (2004) 183.
163. Kim, I.C., Lee, H.K. and Tak, T.M., Preparation and characterization of integrally skinned uncharged polyetherimide asymmetric nanofiltration membrane, *J.Membr.Sci.*, 183 (2001) 235.
164. Tkacik, G. and Michaels, S., A rejection profile test for ultrafiltration membranes and devices, *Bio-Technology*, 9 (1991) 941.
165. Mulherkar, p. and Reis, R., Flex test: a fluorescent dextran test for UF membrane characterization, *J.Membr.Sci.*, 236 (2004) 171.
166. Barsema, J.N., Vegt, N.F.A., Koops, G.H. and Wessling, M., Carbon molecular sieve membranes prepared from porous fiber precursor, *J.Membr.Sci.*, 205 (2002) 239.
167. Tin, P.S., Chung, T.S. and Hill, A.J., Advanced fabrication of carbon molecular sieve membranes by nonsolvent pretreatment of precursor polymers, *Ind.Eng.Chem.Res.*, 43 (2004) 6476.
168. Strathmann, H., Asymmetric polyimide membranes for filtration of non-aqueous solutions, *Desalination*, 26 (1978) 85.
169. Widjojo, N., Chung, T.S. and Krantz, W.B., A morphological and structural study of Ultem/P84 copolyimide dual-layer hollow fiber membranes with delamination-free morphology, *J.Membr.Sci.*, 294 (2007) 132.

170. Ren, J., Li, Z. and Wong, F.S., Membrane structure control of BTDA-TDI/MDI (P84) co-polyimide asymmetric membranes by wet-phase inversion process, *J.Membr.Sci.*, (2004) 305.
171. See Toh, Y.H., Silva, M. and Livingston, A.G., Membrane tailoring for applications in Organic Solvent Nanofiltration, *J.Membr.Sci.*, (2007) *Submitted*
172. P.S.Tin, T.S.Chung, Y.Liu, R.Wang, S.L.Liu and K.P.Pramoda, Effects of cross-linking modification on gas separation performance of Matrimid membranes, *J.Membr.Sci.*, 225 (2003) 77.
173. Reid, R.C., Prausnitz, J.M. and Poling, B.E., *The properties of gases and liquids*, McGraw Hill Book Company, 1987.
174. Geankoplis, C.J., *Transport processes and unit operations*, Allyn and Bacon Inc., 1983.
175. Tkacik, G. and Zeman, L., Component mobility analysis in the membrane-forming system water/n-methyl-2-pyrrolidone/polyethersulfone, *J.Membr.Sci.*, 31 (1987) 273.
176. Zeman, L. and Tkacik, G., Thermodynamic analysis in the membrane-forming system water/n-methyl-2-pyrrolidone/polyethersulfone, *J.Membr.Sci.*, 32 (1988) 119.
177. Cahn, J.W., Phase separation by spinodal decomposition in isotropic systems, *J.Chem.Phy.*, 42 (1965) 93.
178. Dietz, P., Hansma, P.K., Inacker, O., Lehmann, H.D. and Herrmann, K.H., Surface pore structures of micro- and ultrafiltration membranes imaged with atomic force microscope, *J.Membr.Sci.*, 65 (1992) 101.
179. Bowen, W.R. and Welfoot, J.S., Modelling the performance of membrane nanofiltration-critical assessment and model development, *Chem.Eng.Sci.*, 57 (2002) 1121.
180. Kong, Y., Shi, D., Yu, H., Wang, Y., Yang, J. and Zhang, Y., Separation performance of polyimide nanofiltration membranes for solvent recovery from dewaxed lube oil filtrates, *Desalination*, 191 (2006) 254.
181. Desrocher, D.J., Membranes for the recovery of a homogeneous catalyst,PhD Thesis, Georgia Institute of Technology, 2004.
182. See Toh, Y.H., Ferreira, F.C. and Livingston, A.G., The influence of membrane formation on functional performance of organic solvent nanofiltration membranes, *Desalination*, 199 (2002) 242.
183. Joly, C., Cerf, D., Chappey, C., Langevin, D. and Muller, D., Solvent effect on the conformation in solution of two polyimides, *Polymer International*, 44 (1997) 497.
184. Bulut, M., Gevers, L.E.M., Paul, J.S., Vankelecom, N.F.J. and Jacobs, P.A., Direct development of high-performance membranes via high-throughput and combinatorial strategies, *J.Comb.Chem.*, 8 (2006) 168.
185. Ismail, A.F. and Hassan, A.R., Formation and characterization of asymmetric nanofiltration membrane: effect of shear rate and polymer concentration, *J.Membr.Sci.*, 270 (2006) 57.
186. Browall, W.R., Ultrathin Polyetherimide Membrane and Gas Separation Process, US 4,156,597, 1979.
187. Seifert, B., Mihanetzis, G., Groth, T., Albrecht, W., Richau, K., Missirlis, Y., Paul, D. and Sengbusch, G., Polyetherimide: a new membrane - forming polymer for biomedical applications, *Artificial Organs*, 26 (2002) 189.
188. Liaw, D.J., Liaw, B.Y. and Yu, C.W., Systhesis and characterization of new organosoluble polyimides based on flexible diamine, *Polymer*, 42 (2001) 5175.
189. Frank, M.J.W., Westerink, J.B. and Schokker, A., Recycling of industrial waste water by using a two step nanofiltration process for the removal of colour, *Desalination*, 145 (2002) 69.
190. McCandless, F.P., Stage extent of separation in ideal countercurrent recycle membrane cascades, *J.Membr.Sci.*, 154 (1999) 15.
191. Ghosh, R., Novel cascade ultrafiltration configuration for continuous, high-resolution protein–protein fractionation: a simulation study, *J.Membr.Sci.*, 226 (2003) 85.
192. Voros, N., Maroulis, Z.B. and Marinos-Kouris, D., Optimization of reverse osmosis networks for seawater desalination, *Comp.Chem.Eng.*, 20 (Supply 1) (1996) S345.
193. Oatley, D.L., Cassey, B., Jones, P. and Bowen, W.R., Modelling the performance of membrane Nanofiltration – recovery of a high value product from a process waste stream, *Chem.Eng.Sci.*, 60 (2005) 1953.